

LOUGHBOROUGH
UNIVERSITY OF TECHNOLOGY
LIBRARY

AUTHOR/FILING TITLE

ANSARI, V

ACCESSION/COPY NO.

003346/02

VOL. NO.

CLASS MARK

copy

22

15 Oct 1981

-1 JUL 1981

LOAN 1 WITH + 2
UNLESS RECALLED

10 JUL 1982

Date due:

19 DEC 1981

-1 JUL 1983

25 JUL 1981

LOAN 1 WITH + 2
UNLESS RECALLED

-1 JUL 1983

-1 JUL 1983

-6 JUL 1984

05 OCT 81

07 OCT 83

000 3346 02



STRUCTURE AND PROPERTIES
RELATIONSHIPS IN POLY(VINYL CHLORIDE)

by

KALEEM ELAHI ANSARI, M.Sc.

A Master's Thesis

Submitted in partial fulfilment of the
requirements for the award of
Master of Philosophy
of the
Loughborough University of Technology

September 1979.

Supervisor: M Gilbert, Ph.D.

Institute of Polymer Technology

© by Kaleem Elahi Ansari, 1979

Loughborough University of Technology Library	
Date	Dec 79
Class	
Acc. No	003346/02

I certify that this work has not been
submitted to this or any other insti-
tution for consideration of a degree.

To
Asifa
and
Nadeem

ACKNOWLEDGEMENTS

I wish to thank Dr Marianne Gilbert for her invaluable guidance and help during the study and in the preparation of this thesis.

I am grateful to my parents and brothers for their patience, encouragement and support during my absence from home.

Sincere thanks are due to Professor A W Birley for his encouragement and help.

My thanks are also due to Mrs J Smith for her patience and immaculate typing of the script.

SUMMARY

This work has been undertaken to study the relationships between structure and properties of commercial Poly(vinyl chloride) within the time scale of processing and thermal treatment.

Two commercial grade resins (mass and suspension) have been used for this study. PVC resins were dry blended in the T K Fielder dry blending machine. Tin stabiliser and calcium stearate lubricant were added to the PVC to obtain clear moulded sheets.

Compression mouldings were prepared from the powder blends at a wide range of temperatures (160°C to 220°C at intervals of 10°C).

The structural changes during the course of processing were examined by X-ray diffraction and differential thermal analysis.

Differential thermal analysis demonstrated the variation in structure produced by different mould temperatures. The broad melting endotherm present in the blended powder gradually decreased in area and moved to a higher temperature. An additional lower temperature endotherm appeared, increasing in size as the mould temperature increased. The crystallinity of the samples as measured by X-ray diffraction was found to decrease

with increased moulding temperature. These observations have been explained in terms of primary and secondary crystallinity in PVC. The mechanical properties were studied by using an Instron tensile testing machine and a Charpy impact testing machine. Tensile yield stress and impact strength increase with increasing mould temperature due to improved fusion of powder particles. Primary crystallinity does not therefore appear to affect properties under these processing conditions, but the development of secondary crystallinity may be of importance. The mass polymer fuses more readily, and shows ductile behaviour at a much lower temperature.

In order to produce samples with a wider variety of structures present, samples which had been moulded at 200°C were subjected to various annealing conditions. Again, thermal analysis demonstrated that annealing was effective in structure modification. Crystallinities as measured by X-ray diffraction were found to increase on annealing, the maximum crystallinity being produced when an annealing temperature of 110°C was used. The effect appeared to be greater for mass PVC than suspension PVC. Tensile yield stresses increased on annealing; again the maximum value was obtained for samples annealed at 110°C. A minimum value of elongation was obtained for the same samples.

CONTENTS

Page No.

CHAPTER 1: INTRODUCTION

1.1	History of Poly(vinyl chloride)	1
1.2	Polymerisation and Manufacture of Poly(vinyl chloride)	3

CHAPTER 2: LITERATURE REVIEW

2.1	Morphology of PVC Powder Particles	7
2.2	Chain Stereochemistry	11
2.3	Crystallinity	17
2.4	Compounding and Preparation of Blends	26
2.4.1	Introduction	26
2.4.2	Compounding	30
2.4.3	Compression Moulding ...	33
2.5	Effects of Processing and Thermal Treatment on Structure	35
2.6	Mechanical Properties	52

CHAPTER 3: EXPERIMENTAL TECHNIQUES

3.1	Plan of Procedure	66
3.2	Preparation of Blends	70
3.3	Preparation of Mouldings	74
3.4	Physical Characterisation	76
3.4.1	Particle Size Distribution	76
3.4.2	Density of PVC Powder Blends	78

	Page Nos
3.5 Thermal Techniques	80
3.5.1 Thermal Treatment	80
3.5.2 Differential Thermal Analysis (DTA)	82
3.5.3 Thermal Mechanical Analysis (TMA)	86
3.6 X-Ray Diffraction	87
3.7 Mechanical Properties	93
3.7.1 Tensile Properties ...	93
3.7.2 Impact Strength	97
 CHAPTER 4: EXPERIMENTAL RESULTS	
4.1 Physical Properties	99
4.1.1 Particle Size Distribu- tion	99
4.1.2 Density of Powder Blends	99
4.2 Thermal Properties	102
4.2.1 Differential Thermal Analysis (DTA)	102
4.2.2 Thermomechanical Analy- sis (TMA)	107
4.3 X-Ray Diffraction	125
4.4 Mechanical Properties	140
4.4.1 Tensile Properties ...	140
4.4.2 Impact Strength	170
 CHAPTER 5: DISCUSSION	
5.1 Effects of Processing and Heat Treatment on Structure	174
5.1.1 Introduction	174
5.1.2 Discussion of the Results	176

	Page Nos
5.2 Mechanical Properties	189
5.3 Structure and Properties Relationships	199
CHAPTER 6: CONCLUSIONS	202
REFERENCES	205

(

CHAPTER 1

INTRODUCTION

1.1 History of Poly (Vinyl Chloride) (1,2,3,4)

Poly (vinyl chloride) is an unstable polymer and had no commercial importance until the discovery of suitable stabilisers and other additives. Today poly (vinyl chloride), in terms of tonnage consumption, is one of the most important plastic materials available in the world.

Vinyl Chloride monomer is gaseous at room temperature (boiling temperature - 14°C) and manufactured in petrochemical industries. Ethylene is treated with chlorine in liquid phase to produce ethylene dichloride which after dehydrochlorination gives vinyl chloride. The preparation of the monomer was first reported by Regnault in 1835. The method used was to treat ethylene dichloride with an alcoholic solution of potassium hydroxide. Other vinyl monomers such as vinyl bromide were produced by Reboud in 1872 by the reaction of acetylene with hydrogen bromide. Klatte in 1912 discovered the similar reaction with hydrochloric acid for the production of vinyl chloride. Earlier than this, Baumann, 1872, was polymerising vinyl chloride by petrochemical reaction. Ostromislensky, 1912, extended the work in this field.

Poly (vinyl chloride) as a commercial product was introduced by Carbide and Carbon Chemical Corporation, Du

Pont and I.G. Farben in 1928. But Ellis in 1935, writes that "one disadvantage of poly (vinyl chloride) as a moulding resin is its tendency to decompose at the temperature required in the moulding operation. It was Semon who found that poly (vinyl chloride) if mixed with tritolyl phosphate and heated to 150°C can produce a homogeneous stable compound and this approach became of great commercial significance.

Very little work was carried out until the early 1930's, in fact it was World War II which speeded up the development of poly (vinyl chloride) production. When it was realised that PVC could be an effective substitute for rubber in some applications, especially cable insulation and sheeting. Thus poly (vinyl chloride) helped to ameliorate the rubber shortage and at the same time established itself as a material in its own right. Now the PVC industry has been so much developed that the output of PVC is about 40% of the total production of thermoplastics in the world.

1.2 Polymerisation and Manufacture of Poly (Vinyl Chloride)

The word "polymer" is of Greek origin and means literally a molecule that consists of many (poly) parts (meros). The units that build up a polymer are called monomers. The process itself is known as polymerisation. Although there are many different types of polymerisation known, two of them are prevalent because of their simplicity and efficiency. These two methods are addition polymerisation and condensation polymerisation.

In the former case individual monomers add to each other directly without change in composition and form a long chain, whereas in condensation polymerisation two or more monomers react with each other, often with elimination of water molecules and form a polymer chain.

Vinyl chloride polymers are manufactured by free radical polymerisation (addition polymerisation).

There are four different techniques of radical polymerisation:

- a) Emulsion
- b) Suspension
- c) Bulk or Mass
- d) Solution.

Poly (vinyl chloride) is manufactured on commercial scale by the first three methods.

Emulsion Polymerisation:

In emulsion polymerisation method the liquid monomer is emulsified in water containing a water soluble catalyst. The temperature is raised and maintained until polymerisation is complete. The kinetics of emulsion polymerisation are entirely different from those of mass and suspension. The range of particle sizes produced in emulsion polymerisation is much narrower than the range encountered in suspension. In fact, the particles produced in an emulsion latex frequently may be of the order 0.05 to 2 μm .

The main disadvantage of this method is often the difficulty of removing all impurities from the polymer. Another disadvantage is that the polymer is produced as latex and cannot be agglomerated simply by dilution. Most often the latex is used directly.

Suspension Polymerisation:

Suspension polymerisation techniques have been the backbone of the industry for many years. Suspension polymerisation is similar to the emulsion polymerisation in that both are heterogeneous systems involving a dispersion phase and a dispersion medium. In suspension polymerisation, however, dispersion is maintained by vigorous stirring and the use of suspending agents and protective colloids. The polymer is obtained in the form of beads. After washing and drying it may be used directly in moulding.

Since the polymer is in the bead form there are minimal problems in isolating the product compared to emulsion and another advantage is the purity of the polymer product, the product is far easier to purify than the emulsion.

The polymerisation process advantages are:

1. The reaction is more easily controlled. While the process may be considered as a myriad of miniature bulk polymerisation that takes place within the droplets, the heat build-up associated with bulk polymerisation of vinyl chloride does not occur since the heat of polymerisation from the large number of sources is easily dissipated through the aqueous medium.
2. The final product is easily filtered and dried.
3. The process is economical, since water is inexpensive and non-hazardous. Another important aspect of this economy is that the polymerisation can be carried to almost complete exhaustion of monomer before interrupting the process, whereas, in the case of bulk polymerisations, the polymer must be separated before the reaction is more than 50 per cent complete so the local heat build-up is avoided. From kinetic point of view, suspension polymerisation is identical to bulk polymerisation.

Suspension resin particles are irregular in shape and have a porous structure. The resin particles have a

skin around them which makes it inferior to mass PVC in some respects.

Mass or Bulk Polymerisation:

Mass polymerisation has several advantages over other techniques. The system is simple and requires no elaborate isolation or purification steps. The polymer is obtained pure and hence gives better clarity.

Mass polymerisation is carried out in two stages. The first or prepolymerisation stage is carried out in essentially liquid medium and is described as bead formation stage. In the next stage pre-polymerised product is diluted with equal amounts of monomer. During this phase of polymerisation the beads grow in size. The process has economics that are comparable to suspension polymerisation.

Mass PVC particles are regular in shape and porosity. They have no skin around them and hence can absorb additives and plasticizer more uniformly than suspension PVC.

CHAPTER 2

LITERATURE REVIEW2.1 Morphology of PVC Powder Particles

The size and size distribution, shape and nature of PVC resin particles are reflected in properties such as surface area, which largely determines the capacity of plasticizer absorption, bulk and packing densities and powder flow. Plasticizer absorption capacity tends to increase with the decrease in bulk and packing densities. Non-porous particles have rather higher bulk and packing densities than the porous particles. The type and size distribution of poly (vinyl chloride) resins also have profound effects on processing behaviour. Thus a polymer having relatively large and porous particles will yield^a drier, less sticky mixture with plasticizers than the polymer having small and non-porous particles.

The type and size of resin particles depends on the polymerisation techniques used. Commercially poly (vinyl chloride) is manufactured by three main processes, emulsion, suspension and mass.

The emulsion poly (vinyl chloride) resin particles are fine and dusty and have hollow centred spheres called "cenospheres". They are made up of a large number of very small particles whereas suspension PVC resin particles are irregular in shape and have a porous structure. The resin particles are enclosed in membrane which give them smoothness. Suspension poly (vinyl chlorides) are

preferred to emulsion poly (vinyl chlorides) because the former are cheaper and generally yield products of better colour and clarity.

Mass poly(vinyl chloride) resin particles are regular in shape and porosity. Each particle of mass poly (vinyl chloride) can uniformly absorb plasticizer. Mass poly (vinyl chloride) resin particles are purer than suspension because mass polymerisation does not require suspending agents which are necessary for suspension polymerisation and more over mass poly (vinyl chloride) resin particles have no skin around them. Therefore mass poly (vinyl chloride) is easier to process than suspension.

Despite the commercial interest and value of poly (vinyl chloride) the morphology of its particles is not well understood.

Several authors^(5,6,7,8,9,10) have reported the presence of three kinds of particles (the arrangement of these particles is shown in the figure 1) namely primary particles $100 \text{ \AA} - 200 \text{ \AA}$ in diameter, secondary particles with diameter ranging from 0.1 to 2 \mu m and the final resin particle having diameter in the range of 100 \mu m . The morphology of these individual particles is still under investigation.

It is believed that primary particles contain some individual molecules⁽¹¹⁾ but there is no direct evidence, so far, for the arrangement of these molecules.

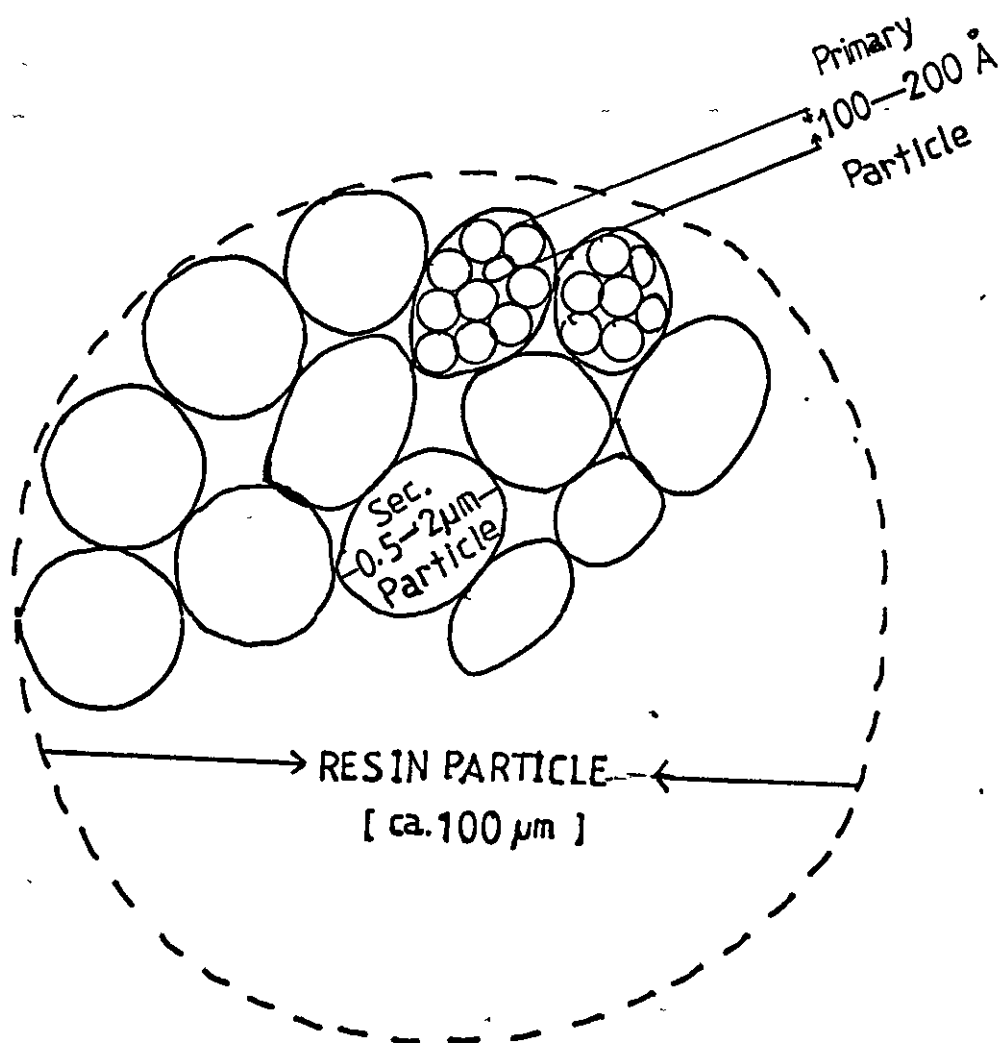


FIGURE 1

Schematic Illustration of PVC Structure

Primary particles agglomerate to give secondary particles and these secondary particles further agglomerate to give the final resin particle. The way in which these particles agglomerate determine the type of resin particles. Rudolf et al⁽¹²⁾ have observed five main types of resin particles in suspension poly (vinyl chloride) according to the manner in which the microparticles are packed.

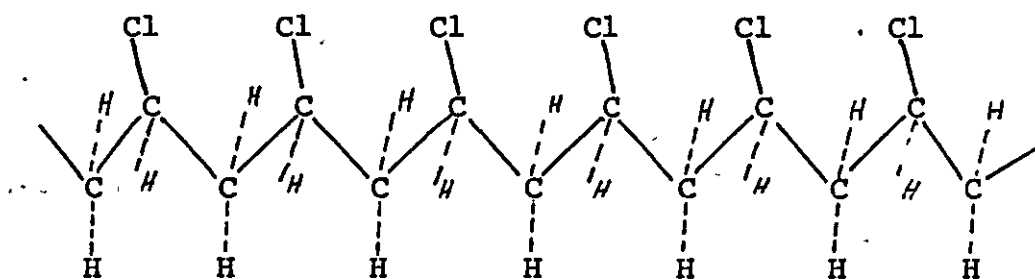
Several investigators^(6,12,13,14,15) have tried to find the internal structure of these particles.

Hattori et al⁽⁶⁾ have studied the particle formation of suspension poly (vinyl chloride). A droplet was taken from polymerisation at several different conversions and dried to obtain granules. The epoxy embedding method was employed to obtain the exact value of particle diameter in the droplet. Approximately spherical 0.1 μm diameter particles were seen in the granule of 10 μm in diameter which are covered with a thin skin formation. These particles grow as the degree of conversion increase. They reached about 1 μm in diameter at about 40% conversion and after this step these particles aggregate to form resin particles of diameter 100 μm . They have also compared the surface structure of these particles with that of the bulk polymerised poly (vinyl chloride) granules using Scanning-Electron Microscopy. The 1 μm (secondary particles) structure of suspension poly (vinyl chloride) granules is not as distinct as that of bulk poly (vinyl chloride). This is because of the skin formation at the surface of the former.

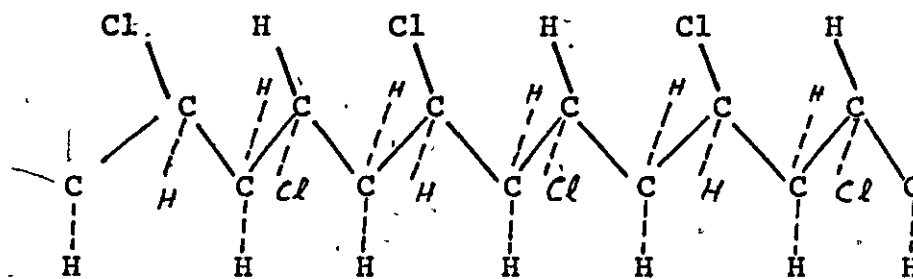
2.2 Chain Stereochemistry

A tactic polymer is defined as one in which there is an ordered structure with respect to at least one site of steric isomerism in each monomeric unit.

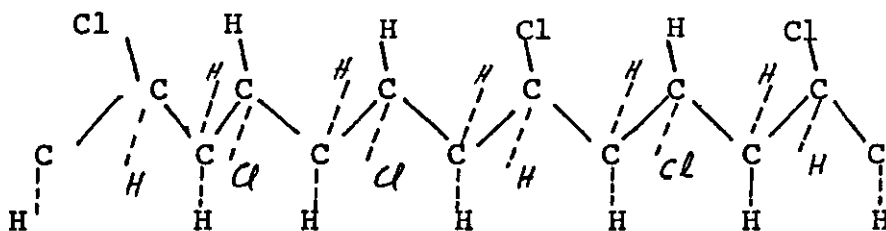
Poly (vinyl chloride) has a fundamental repeating unit $[\text{CH}_2 = \text{CH Cl}]_n$. There are two different arrangements for the chlorine atom in the ($-- \text{CH Cl}$) group of monomer unit $\text{CH}_2 = \text{CH Cl}$, which results into three different forms of polymer chain. These three forms are termed as isotactic, syndiotactic and atactic.



ISOTACTIC



SYNDIOTACTIC



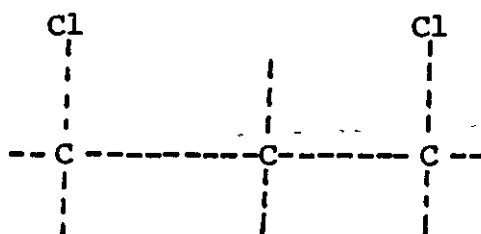
ATACTIC

In the isotactic form all chlorine atoms are found on the same side of the main chain whereas in syndiotactic sequences chlorine atoms are found in alternate positions. The atactic form can simply be regarded as the random distribution of syndiotactic and isotactic forms.

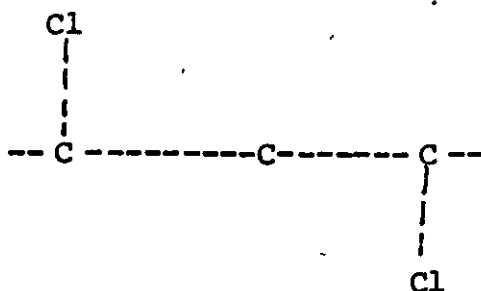
Tacticity can be measured by Nuclear Magnetic Resonance and Infra Red techniques. The values obtained by N.M.R. are more reliable than that of I.R.⁽¹⁶⁾. The Proton N.M.R. spectrum of poly (vinyl chloride) is usually interpreted in terms of triads and diads of monomer unit, but due to complexity arising from the overlapping of proton chemical shifts, C^{13} N.M.R. technique is preferred. C^{13} N.M.R. gives clear resolution of resonance bands corresponding to syndiotactic, isotactic and atactic triads of a monomer which makes it possible to measure tacticity more accurately.

The generation of triad sequence involves two monomer additions and hence Bovey⁽¹⁷⁾ has described the

nomenclature of two possible configurations of successive asymmetric carbon atoms as meso m, and racemic r, and this system can be extended to sequences of any length.

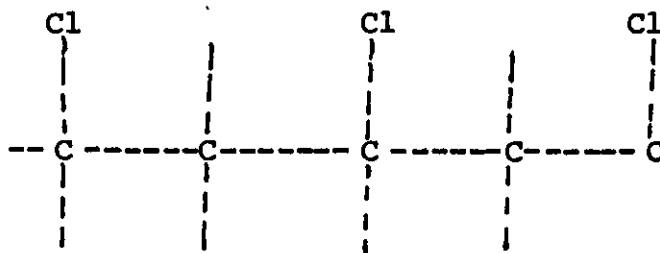


meso m

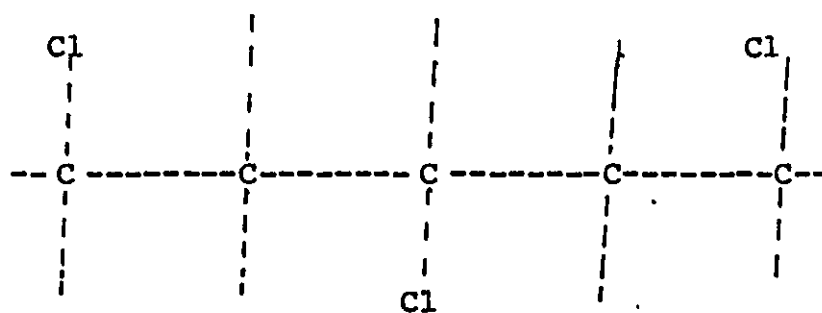
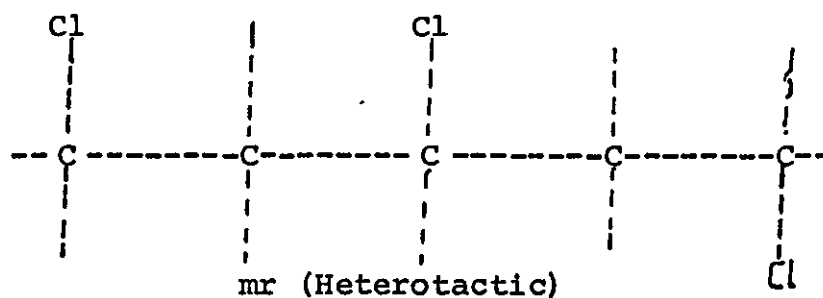


racemic r

A triad having mm arrangement is isotactic, mr arrangement heterotactic and rr arrangement will be syndiotactic.



mm (Isotactic)



rr (Syndiotactic)

In order to measure tacticity from N.M.R. spectrum the following formulae are used.

$$\text{Iso} = I + \frac{H}{2}$$

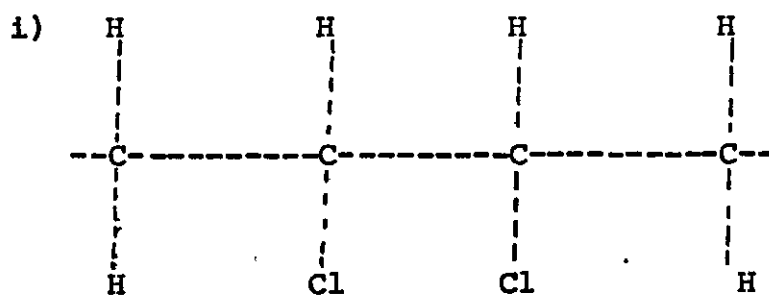
$$\text{Synd} = S + \frac{H}{2}$$

where I, S and H are iso, syndio and heterotactic triad concentration.

Syndiotacticity α , is defined as the fraction of syndiotactic sequences in the polymer chain. For 100% syndiotactic material α will be equal to 1.0. Polymer

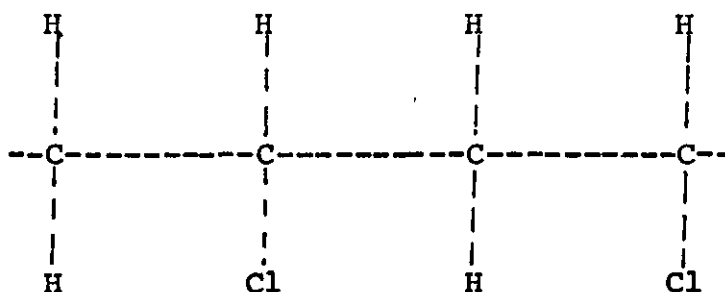
with α , value less than 0.5 do not occur because of the way in which tacticity is measured, as described above. Commercial grade poly (vinyl chlorides) have α value around 0.55. Several workers have measured syndiotacticity of poly (vinyl chloride) as a function of polymerisation temperature and found that α can be controlled by polymerisation temperature. Fordham⁽¹⁸⁾ has shown theoretically that in radical polymerisation of vinyl chloride syndiotactic placement is favoured over isotactic placement as the temperature is decreased. This has been shown to be true experimentally by several workers^(19,20,21)

There can be several possible steric forms depending on the placement of successive monomer units. If we consider $(-CHCl)$ as head and $(-CH_2)$ as tail in poly (vinyl chloride) monomer $(CH_2 = CHCl)$, then placement of successive monomers can be shown as follows.



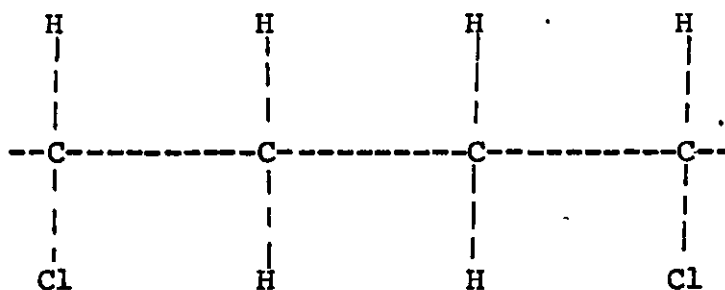
(Head-to-head)

ii)



(Head-to-tail)

iii)



(Tail-to-tail)

In addition to this there may be some irregularities in the above mentioned arrangements. Head-to-tail addition is significantly favoured over the other possibilities in poly (vinyl chloride) but it does not mean that the other steric forms are absent.

2.3 Crystallinity

Crystallinity is the measure of the ordered structure in a compound. This ordered structure is obtained from the periodic arrangement of the molecules in the space and can be explained in terms of thermodynamics. The most stable state of any assembly of molecules is that which has the lowest accessible free energy. All crystals are characterised by almost perfect order in their molecular arrangement. They are found to develop sharp external boundaries (crystal faces) inclined to one another at angles characteristic of the particular crystal.

For some substances intermediate states exist between the amorphous and crystalline state. They are named as semi-crystalline states. Physical investigation of the structure of some solid polymers has revealed the presence of microheterogenities. X-ray evidence has shown that the molecules in small volume elements have a geometric regularity of arrangement similar to that found in many crystals of low symmetry. These regions are called 'crystallites'. They are separated from each other by a material which gives a diffused X-ray pattern. For poly (vinyl chloride) the crystallites are estimated to be small, being less than 100 \AA in size.

A precise knowledge of the molecular arrangement in polymer crystallites has been obtained almost exclu-

sively from X-ray diffraction measurements. In its most complete form this method can give the symmetry and dimensions of the unit cell. Even when it has not been possible to carry out such a detailed elucidation of the structure, values have been obtained for the repeat distances along the molecular chains from which the mutual orientation of neighbouring monomer units may be deduced.

After the unit cell dimensions have been determined, the next step is to fix the position of the atoms in the unit cell. On account of the complication of the molecular structure, this has to be carried out by a process of trial and error. A structure is postulated which is consistent with normal bond lengths and angles, and also with the unit cell dimensions. The expected intensities of the particular spots which appear on the X-ray photograph are then calculated. Detailed alterations to the postulated structure are made until a close fit is obtained between the predicted and observed intensities.

Natta and Corradini⁽²²⁾ performed X-ray measurements with oriented fibres of commercial poly (vinyl chloride). The X-ray diagram reveals the equatorial reflections with interplanar spacings, $d = 5.39, 4.78, 3.74$, and 2.94 Angstrom. These reflections can be interpreted by an orthorhombic cell with axes $a = 10.6$, $b = 5.4$ and $c = 5.1$ Å.

The experimental values of lattice spaces and intensities are in agreement with the theoretical values and hence they confirm the proposed orthorhombic structure for PVC.

TABLE 1

Miller Indices	d(experimental)	d(theoretical)
200	5.39	5.4
010	—	5.3
110	4.78	4.79
210	3.74	3.76
310	2.94	2.95

Single crystals of poly (vinyl chloride) have been prepared by several workers. (23,24,25) The crystals were found to be lamellar in nature and of the order of 50 - 100 Å. X-ray and electron diffraction patterns of single crystals have confirmed the orthorhombic structure proposed by Natta and Corradini.

Smith and Wilkes (23) obtained single crystals from 2% chlorobenzene solution of highly syndiotactic low molecular weight poly (vinyl chloride) polymerised in the presence of butyraldehyde. These crystals were rectangular in shape and approximately 100 Å thick which represents the length of the folds.

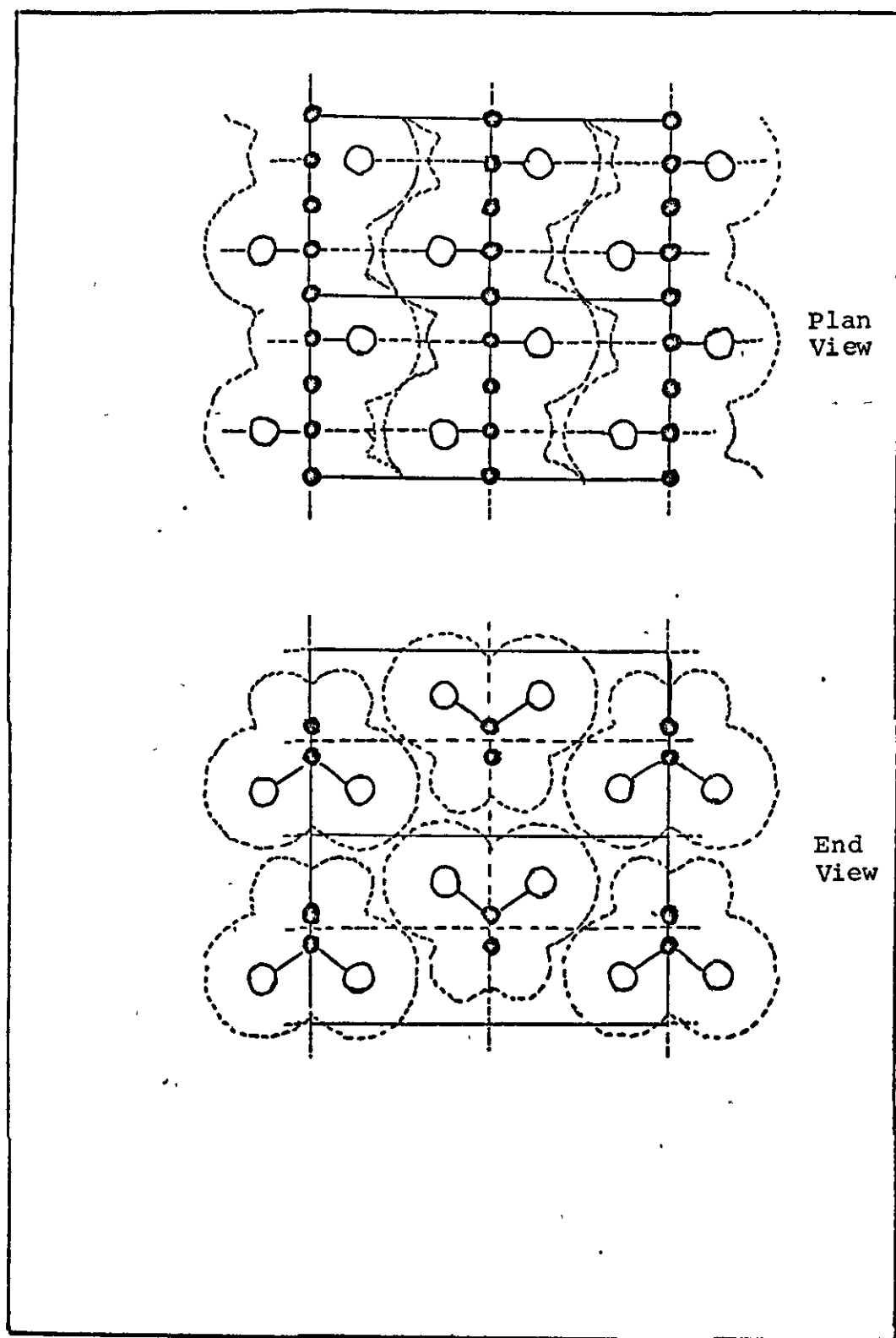


FIGURE 2 PVC Crystal Lattice according to Natta and Corradini⁽²²⁾

Nkajama and Hyashi⁽²⁴⁾ produced single crystals by slowly cooling 0.1% chlorobenzene solution. In their study, they used both syndiotactic and commercial grade poly (vinyl chloride) of high molecular weight. They also found the crystals to be lamellar and 50 - 100 Å thick in size. The X-ray diagram showed that the crystals were orthorhombic.

The lamellar structure of poly (vinyl chloride) crystallites have been observed by other workers^(15,26,27) as well. On the other hand Neilson and Jabarin⁽²⁸⁾ and Gezovich and Geil⁽⁵⁾ believe in a nodular structure of the crystallites. Bort et al⁽²⁹⁾ found by the use of electron microscopy, a structure composed of both lamellar and elongated particles. Recently Keller et al⁽³⁰⁾, in their thermo-reversible gelation studies of commercial grade poly (vinyl chloride) using X-ray diffraction techniques, suggested that at a moderate temperature both lamellar and micellar structures co-exist, but beyond certain annealing temperatures (130°C - in poly vinyl chloride) latter crystals disappear.

The existence of crystals in rigid poly (vinyl chloride) is thus well established, but there is a controversy in the literature about its exact form - whether the structural elements consist of elongated nodular particles, or of crystal lamellar.

From differential scanning calorimetry, investigations of various commercial grade poly (vinyl chloride), Jujin et al⁽³¹⁾ have the opinion that poly (vinyl chloride)

has two types of crystallinity. These are referred to as primary and secondary crystallinity. The former is created during polymerisation and has an orthorhombic structure, whereas secondary crystallinity is developed during annealing. This type of crystallinity has nematic structure and is of less perfect nature, as indicated by its lower melting temperature.

Poly (vinyl chloride) has two stereomeric (isotactic and syndiotactic) forms of the monomer which gives rise to different conformations of the chain. A part of the chain which is syndiotactic can have a planar zig-zag conformation and in this case chlorine atoms are found at alternate positions of the main chain. This spatial arrangement is energetically favourable over other possible conformations. Isotactic parts of the chain cannot have planar zig-zag conformations because of the steric hindrance and hence they have some other conformation. Only planar zig-zag parts of the chain can crystallise and that is the probable reason for low crystallinity of commercial poly (vinyl chloride) which has a syndiotacticity $\alpha = 0.55$. Some authors consider poly (vinyl chloride) as a co-polymer consisting of a syndiotactic, crystallisable part and an isotactic non-crystallisable part. Flory⁽³²⁾ has developed a theory for the crystallisation of partly crystallisable co-polymers. He showed, on thermodynamics ground that the size of the crystallites should have a minimum length, therefore the parts of the chain which

form crystallites should also have minimum length which is called minimum sequence length.

By applying the Flory theory of crystallisation of co-polymers, with the assumption that only the syndiotactic sequences can crystallise, Helwege and co-workers⁽³³⁾ have estimated the minimum number of syndiotactic sequences capable of crystallisation to be 12. However Talamini and Vidotto⁽²¹⁾ and Pöhl and Hummel⁽³⁴⁾ estimated the minimum number to be 5. Gray⁽³⁵⁾ has plotted calculated crystallinity against syndiotacticity and found that the minimum number to be 5-6.

Degrees of crystallinity can be measured by various techniques such as wide angle X-ray diffraction, small angle X-ray diffraction, small angle X-ray scattering, Infra Red spectroscopy and density measurements. Crystallinity evaluation varies somewhat from one author to another. Several workers^(21,35,36,37,38,39,40) have reported the value of crystallinity for commercial grade poly (vinyl chloride) in the range of 0-15%. Stafford et al⁽⁴⁰⁾ deny the existence of crystallinity in commercial poly (vinyl chloride) where other workers cannot neglect the crystallinity values based on various methods of separation amorphous and crystalline contribution to X-ray diffraction patterns.

Several investigators^(21,35,36,41-43) have found a direct correlation between the syndiotacticity and the degree of crystallinity. Syndiotacticity increases with the decrease in polymerisation temperature. D'Amato and Strella⁽⁴⁴⁾ have used X-ray techniques to

measure the degree of crystallinity of syndiotactic and commercial poly (vinyl chloride). Their results indicate a degree of crystallinity of about 10% for commercial poly (vinyl chloride) and about 23% for poly (vinyl chloride) polymerised at -60°C (highly syndiotactic). Gray⁽³⁵⁾ has reported a value of 11.9% for commercial poly (vinyl chloride) and 27.5% for syndiotactic poly (vinyl chloride), annealed at 160°C .

A very highly syndiotactic poly (vinyl chloride) can be prepared by urea canal complex methods outlined by White⁽⁴⁵⁾. In this method initiation is being carried out by high energy radiation and the vinyl chloride monomer are stacked in the channel of the complex such that the spatial arrangement protects against termination and branching. Polymers produced in this way are of low molecular weight, contain a syndiotacticity of 80% and a degree of crystallinity of 60%. Maddams et al⁽⁴⁷⁾ have also studied a highly syndiotactic poly (vinyl chloride) prepared by the same method. They used X-ray diffraction methods to measure crystallinity. They reported a value of 63% crystallinity in original samples and 78% after annealing at 180°C .

Horsley⁽⁴⁶⁾ and Lebedev et al⁽⁴⁸⁾ have studied the effect of plasticizer on degree of crystallinity and found that increase in order is at a maximum at approximately 10% of plasticizer concentration.

Witenhafer⁽⁴⁹⁾ has shown that poly (vinyl chloride) crystallinity can be measured by infra red spectroscopy

using a compensation technique. Nakajima⁽³⁶⁾ and Behrens⁽⁵⁰⁾ have calculated crystallinity by density measurement methods. Their values appear to be overestimated when compared with those obtained by X-ray diffraction methods.

2.4 Compounding and Processing of Blends

2.4.1 Introduction

At room temperature Poly (vinyl chloride) is inherently stable. Increase in temperature to above 100°C causes decomposition. As decomposition proceeds, the substantially colourless polymer usually becomes yellowish, then brown, and finally black. Therefore a stabilizer is an essential ingredient to make PVC a useful plastic material. The rate of decomposition and colour development are temperature dependent, increasing with increase in the latter. There are considerable differences in performance between different commercial resins, and it is thus common to speak of the "heat stability" of a particular resin and to compare the "heat stabilities" of different resins. Likewise, stabilizers differ in their ability to reduce decomposition and it is common practice to compare "heat stabilities" of different compositions.

Mechanisms of degradation are several, complex and not yet fully explained, but effective stabilizers are available.

Rigid PVC compounds will normally consist of the resin, the stabilizer, lubricant and modifier. Some rigid compounds may also contain a small amount of

plasticizer. It is an important general rule in formulation and compounding, that the interaction of all the components present should be borne in mind. Stabilizers can be classified into fairly well defined groups.

Group I comprises lead salts and soaps. They are the oldest general purpose stabilizers, conferring particularly good electrical properties and hence widely used in PVC compounds for electrical insulation. They are also comparatively cheap. Their limitations and disadvantages include toxicity, opacity in compounds, and susceptibility to staining in contact with sulphur bearing materials or the atmosphere.

Group II consists of salts and soaps of other metals, mainly calcium, cadmium, barium and zinc. Mostly they are used in mixtures for a complementary action and in some cases there are synergistic effects.

Group III consists of organo-tin compounds, some of which are the most effective and powerful stabilizers available. However, the organo-tin stabilizers are also the most expensive to use. They can confer the highest degree of heat stability and clarity. Few of them are approved for applications involving contact with food.

Group IV contain miscellaneous compounds of which the most important are epoxide oils and esters. They have plasticizing as well as stabilizing action.

Group V includes synergistic mixtures, usually of stabilizers of Group II with those of Group IV. Such mixtures can be very effective. Selected compositions, e.g. certain Ca/Zn systems in some cases with epoxy compounds and phosphites - combined good clarity with no toxicity, and are used in food contact applications.

All the above mentioned stabilizers are primarily heat stabilizers, although some of them have also light stabilizing action. The effectiveness of a stabilizer, or stabilizer system, can be affected by the other constituents of the compound. This should be borne in mind when selecting a stabilizer. Other main factors in choice are the processing conditions and variables, e.g. temperature, and the required properties of the compound, e.g. clarity, electrical properties, non-toxicity. Amounts of stabilizer added vary with their nature, but generally fall within the limits of 0.5 to 8 pph (parts per hundred).

Lubricants, although used at relatively low concentrations, are essential additives for poly (vinyl chloride) plastics. A lubricant is added to PVC compounds to reduce the frictional effects and sticking of

the plastic to the metal surfaces of the processing equipment. It is also added to reduce the frictional heat effect between resin particles during fusion, and between the resin molecules after fusion. Their effect between resin particles prior to fusion, and between metal and polymer melt surfaces after fusion, can be considered external, whereas their influence between resin molecules after fusion, are internal with reference to polymer melt.

Compounds used as lubricants include polyethylene, fatty acids, metal soaps, oil and waxes, fatty alcohols, esters and amides. The amount ranges from a fraction to a few pph.

Many other materials are frequently added for various reasons and effects, and these are also important in individual areas or applications. The most common of such ingredients include colourants, fillers, blowing agents and antistatic agents. Minor specialist additives may also be employed, for example, odourants to impart special odour, or deodorants, to combat a smell. A comprehensive discussion of compounding and formulation of PVC is available in the literature, notably in the monographs by Penn⁽¹⁾, Matthews⁽²⁾ and Nass⁽³⁾.

2.4.2 Compounding

Compounding PVC essentially involves adding to the base PVC resin, the components that will allow it to be processed into a finished product with desired properties. The families of materials that will be chosen will probably fall into one of the following classifications, which have already been discussed in the preceding section 2.4.1:

- a) Stabilizer
- b) Lubricant
- c) Plasticizer
- d) Impact modifier
- e) Fillers
- f) Colourants
- g) Miscellaneous.

Adding to the PVC resin the proper type and amount of additives (as outlined above) results in a compounded mixture that can subsequently be processed into a satisfactory finished product. Compounding can be defined as the mixing to homogeneity of PVC resin with the other components required for processing and performance.

It is normal to premix the ingredients in all processes except "dry blending". In fact dry blending should not be confused with pre-blending, which is just gentle physical mixing of ingredients. Various pre-mixing machines have been used for mixing of PVC compositions. The most common types are, tumble mixers, paddle mixers, ribbon blenders, air mixers and sigma blade mixers.

Little or no frictional heat is developed in these mixers, hence heating and cooling jackets are necessary for plasticized blends. It is time consuming process which gives gentle physical mixing of ingredients.

Further compounding is carried on, after PVC composition has been mixed properly by any of the methods described above. The common machines used are roll mills, Banbury mixer, and compounding extenders.

Poly (vinyl chloride) dry blending is one of the most important methods of mixing rigid PVC powder blends. The basic principle of dry blending is that all ingredients are mixed in a single operation to produce a completely dry, free flowing powder. This type of blender can prepare batches, including mixing and cooling, with relatively short cycles

(10 - 20 minutes) and achieve excellent dispersion.

In general a dry blending mixer consists of a mixing chamber fitted with a pitched-blade rotor or mixing impeller. An adjustable baffle blade is mounted vertically that acts as a deflector and its function is to direct the flow of material away from the wall to optimize the mixing action.

Due to the high speed of the mixer, frictional heat is developed and raises the temperature of the blend. When the required temperature is reached, the blend is discharged into a cooling chamber through a pneumatic valve. The cooling mixer is a jacketed bowl of large diameter and low height equipped with a rotor that operates at relatively low speeds.

Dry-blends can be fed directly to an extruder for fabrication into wire insulation, hoses or other final forms. In fact this technique of direct dry-blend extrusion is ever increasing. Porosity and surface roughness are the main difficulties, but valved extrusion⁽⁹³⁾ and vented extrusion⁽⁹⁴⁾ have helped in this direction. *Dry blends are used as feed-stock for twin screw extrusion process while pellet/granules are used as feed stock for single screw extrusion and moulding*

2.4.3 Compression Moulding

Compression moulding is not commercially a widely used technique for rigid PVC because it is a time consuming process. PVC is processed by the application of heat, shear and pressure or the combination of any of these parameters. Compression moulding involves the minimum shear forces, therefore high processing temperatures are required in this technique which is also not favourable from the commercial point of view. However the process is used in a few applications where other production methods are not suitable.

Practically every kind of plastics processing can be applied to PVC in one form or another. The various different routes by means of which PVC can be converted to finished products, are shown in figure 3⁽⁹⁵⁾. Shear rate encountered in PVC processing, varies from one method to another:

Compression moulding	$1 - 10 \text{ sec}^{-1}$
Milling and calendering	$10 - 10^2 \text{ sec}^{-1}$
Extrusion	$10^2 - 10^3 \text{ sec}^{-1}$
Injection moulding	$10^3 - 10^4 \text{ sec}^{-1}$

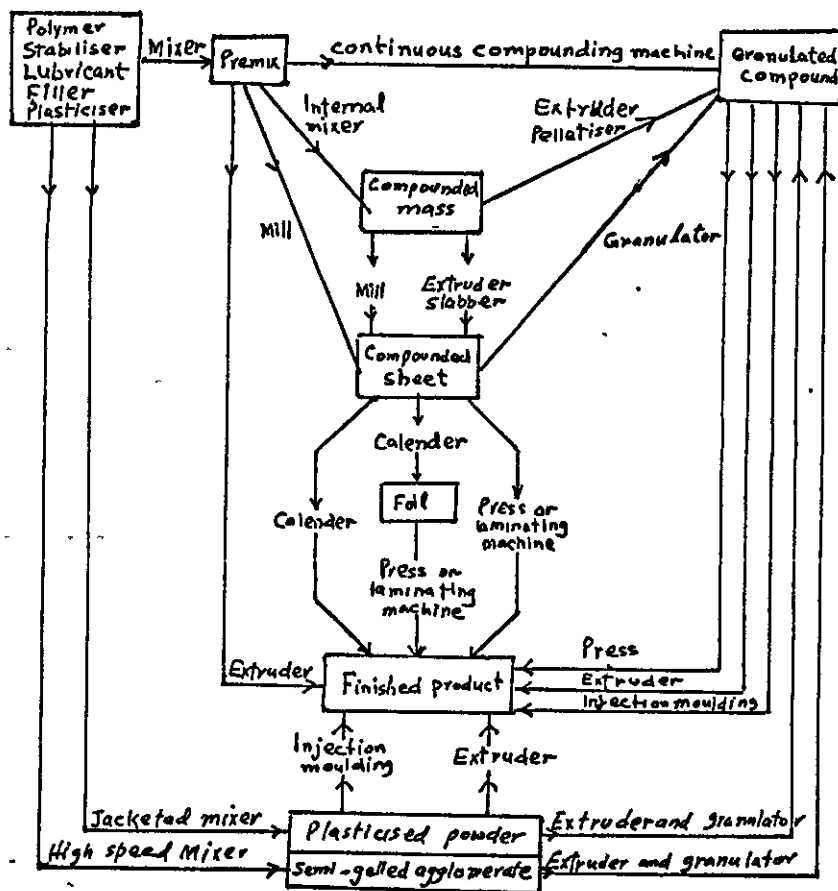


FIGURE 3

ROUTES OF CONVERSION OF PVC RESINS TO FINISHED PRODUCTS⁽⁹⁵⁾.

2.5 Effects of Processing and Thermal Treatment on Structure

A pure ^{crystalline} substance has a sharp melting point. When the amorphous phase contains an additional chemical substance, or diluent, melting takes place over a range of temperatures and a plot of the amount melted versus temperature is a solubility curve for the crystalline substance in the diluent. On account of the rather unusual nature of polymer crystallites, which contain regularly arranged segments rather than whole molecules and have consequently no sharp physical boundaries separating them from the amorphous phase, it is not immediately obvious whether they will show behaviour similar to that of ordinary crystalline substances.

There are at least two physical reasons why, even with the greatest refinement of experimental techniques, a homo-polymer of finite molecular weight would not melt at a single sharp temperature. The perfect arrangement of molecular segments in a crystallite would be disrupted by the presence of chain end groups. For this reason the end groups tend to remain in the amorphous phase where their concentration progressively increases as more and more polymer becomes incorporated into the crystalline phase. Thus the end groups may be thought of as an inevitable diluent which lowers the freezing point as crystallisation proceeds. The concentration, and hence the effect of these end groups, decreases as

the molecular weight increases and would just disappear at the imaginary limit of infinite molecular weight.

Secondly, it has long been known that for very small crystals, the interfacial energy between the crystal and its surroundings is an appreciable fraction of its total free energy. Hence very small crystals are found to melt at a lower temperature than macroscopic ones. In the case of polymer crystallites the lack of clear physical boundaries somewhat, the parallel chains in a crystallite are more closely packed than in the amorphous state and the chain emerging from the ends of a crystallite must therefore continue in a semi-ordered, slightly diverging array for a few chain units because there is insufficient cross sectional area for them to do anything else. There must be an excess of free energy associated with the semi-ordered region at each end of a crystallite. It will be independent of the crystallite length and hence of greater relative significance to a short crystallite than to a long one. Thus, in complete analogy with the effect of the interfacial energy, the smallest crystallite, however perfect their internal arrangement, will be expected to melt at a lower temperature than the larger ones.

The thermodynamic consequences of these two effects in producing a dispersion of the melting point are included in a comprehensive theoretical study of melting by Flory⁽⁵¹⁾. He has given a statistical thermodynamic

treatment of partial crystallinity based on a development of the lattice model which had already enabled the thermodynamic properties of concentrated solutions of polymer to be interpreted successfully. The crystalline polymer is represented in this theory by a fringed micelle model. The effect of molecular weight and added diluent are dealt with, and the results are extended to co-polymers.

Flory has assumed that contributions to the entropy associated with the subdivision of the crystalline material into numerous small crystallites, and with the random orientation of these crystallites, may be neglected. Moreover, this assumption would not be upset if the crystalline material were later found to have a more highly organised arrangement. If, however, chain folding were proved to play an important part in crystallisation from the melt some alteration would be required to the statistical description of the process by which the polymer and diluent are added to the pseudo-lattice of the theory. Chain folding in a polymer cannot occur to such an extent that all polymer molecules are either completely formed into crystallites, or not crystallised at all. If this were so the polymer would have a sharp melting point instead of a melting range.

The equilibrium of crystalline polymers with the mixture of amorphous polymer and diluent at melting point, T_m can be represented mathematically:

$$\frac{V_1}{v_1} \left(\frac{1}{T_m} - \frac{1}{T_m^0} \right) = \frac{R V_u}{\Delta H_u} \left(1 - \frac{B V_1}{R T_m} v_1 \right)$$

where: V_1 = the molar volume of the diluent.

V_u = the molar volume of the repeat unit.

v_1 = mole fraction of the diluent.

T_m = melting point of polymer/diluent system.

T_m^0 = melting point of pure polymer.

H_u = heat of fusion.

BV_1 = Polymer - diluent interaction parameter.

Anagnostopoulous et al⁽⁵²⁾ and Nakajima et al⁽³⁶⁾ have used this theory to determine T_m , the melting point of pure polymer. The former obtained a value of 176°C for a commercial type poly (vinyl chloride) whereas Nakajima et al concluded that the polymers made at 15°C and -30°C have melting points of 285°C and 310°C respectively.

Reding et al⁽⁵³⁾ investigated the effect of polymerisation temperature on both glass transition temperature T_g and melting point. The latter was found by extrapolation from data on plasticized samples, as the temperature at a stiffness modulus of 10 p.s.i. He found that poly vinyl chloride polymerised at temperatures of 150°, 40°, -10°, and -80°C, have melting points of 155°C, 220°C, 265°C and more than 300°C respectively. Similarly T_g went from 68°C to 100°C.

The melting point of crystalline poly (vinyl chloride) increase with the increasing stereoregularity. From X-ray measurements of the degree of crystallinity as a function of temperature, Kockott⁽⁵⁴⁾ has shown that the melting of the crystallites takes place over a wide range of temperatures from 150°C to 220°C for a sample polymerised at -70°C. The melting of the commercial polymer was extrapolated to 150°C and that of completely syndiotactic polymer to 273°C.

Munstedt⁽⁵⁵⁾ has studied the flow and elastic behaviour of suspension poly (vinyl chloride). Unlike ~~the~~ polymers. Poly (vinyl chloride) shows non-Newtonian flow behaviour for low shear rates which can clearly be interpreted as "particle flow". The elastic behaviour, too, demonstrated by the elastic shear modulus, shows that the poly (vinyl chloride) melts, consists at least to a considerable extent of particles. However it is remarkable that the flow behaviour and the elastic behaviour alter clearly at 200 - 210°C, the flow curves alter their gradient at about 200 - 210°C.

Pezzin⁽⁵⁶⁾ achieved a similar result during the investigation of flow behaviour of suspension poly (vinyl chloride) and he attributes this shifting to the melting of crystallites in poly (vinyl chloride).

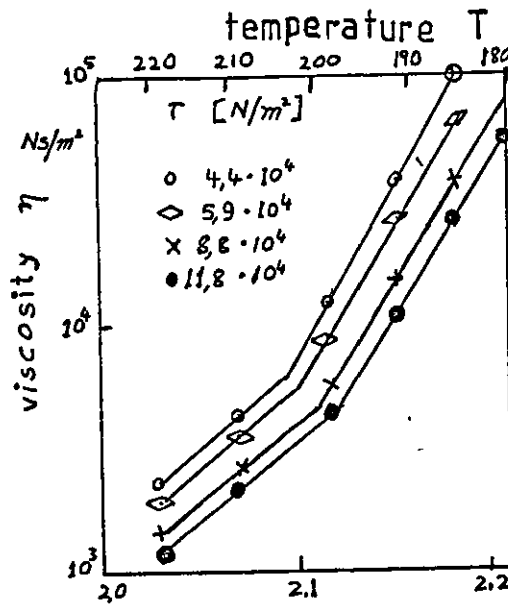


FIGURE 4

Viscosity of PVC as a function of temperature (measurements - Den Otter, quoted in Ref. 55)

H Hattori et al⁽⁶⁾, Shinagawa⁽⁷⁾, Singleton et al⁽⁸⁾ Faulker⁽⁹⁾ and Katchy⁽⁵⁷⁾ have studied the effects of processing on microstructure of poly (vinyl chloride). The particulate structure of poly (vinyl chloride) particles breaks down during processing under the combined effects of heat and shear. Hattori et al have also studied the breakdown of 1 μm particles only by heat. They concluded that heat can be effective in breaking down the 1 μm particles, but the potential for breakdown becomes more effective when heat is combined with shear.

In their study of fusion of particulate structure of PVC resin during powder extrusion, they observed that at low processing temperatures 160°C or 170°C, the inner structure seems not to have changed from the original

PVC granules. The 1 μm particle structure still remains, but at higher temperature these particles start breaking and finally the breakdown of the network is completed at 200°C. Shinagawa also reported the flow behaviour of PVC in the melt and correlated it with the degree of polymerisation. The flow behaviour of the melt can generally be divided into three types:

- a) Viscous flow:- polymers with low degrees of polymerisation show this type of flow in which particles vanish in a short time.
- b) Particle flow:- in this process of flow, particles exist even if it is mixed for long times. The type of behaviour is shown by the polymer having high degrees of polymerisation.
- c) Intermediate:- in this type of flow, polymers show an intermediate behaviour between (a) and (b), which shifts from the particle to viscous flow.

Katchy has examined the microstructure of commercial PVC moulded at different temperatures and found that particulate structure is largely retained, and this results in brittle failure, at low moulding temperatures. However as the moulding temperature is raised the primary particles are gradually broken down and corresponding changes in ductile failure occur. At significantly high moulding temperatures, only sub-primary particles are left as the microstructure.

Faulkner has investigated the processing characteristics of PVC using Brabender Plasticorder and found three distinct peaks in the temperature-torque curve. These peaks are regarded as the breakdown of resin, secondary and primary particles.

The first peak represents the breakdown of resin particles. The height and temperature of peak depends on the size and size distribution of resin particles.

The second peak is attributed to the fusion, behaviour of the compound. The position of this peak is not directly affected by the size and size distribution of resin particles.

The third peak represents the formation of true melt. The theoretical explanation of these three peaks found in a typical temperature torque, can be seen in the following figure:

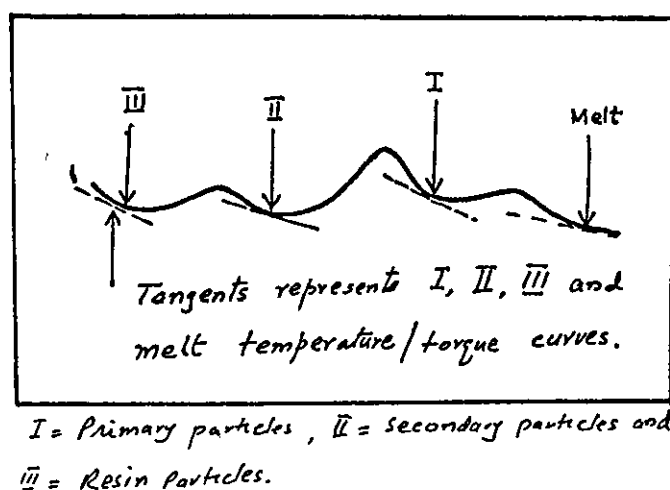


FIGURE 5

Schematic Representation of Temperature Curves
for PVC Compound (9)

These points will occur on the curve where the resin, secondary and primary particles predominate. Polymer melt will exist at a higher temperature, possibly after the third peak in the curve. The slope of the curve at these points will give the temperature-torque relationship for the resin, secondary and primary particles, and polymer melt. As each particle type is broken down, there is an increase in torque above the theoretically anticipated value of the next smaller particle (or melt in the case of the third peak). The torque-temperature relationship gradually reverts to that predicted by the next smaller particle, and this process continues until a true melt is obtained.

Several authors believe that PVC melt has some sort of structure which is not yet understood. Hattori et al have observed the fibril structure of the order of 300 \AA in the commercial grade PVC extruded at 210°C . Faulkner suggests a particle structure at the 10 nm level. He observed this structure by transmission electron microscopy in material taken from beyond the third peak.

Munstedt believes that non-destructible or irreversible particles exist in polymer melt, whereas Menz et al⁽¹³⁾ concludes from their studies on rigid PVC, that globules (0.1 to 2 μm particles) arising during polymerisation remain undestroyed up to high temperatures ($< 230^{\circ}\text{C}$). At most they are deformed for better filling of cavities.

Lyngaae-Jorgenson⁽¹¹⁾ has proposed a model which predicts the conditions under which the last trace of crystallinity disappears from PVC melt under continuous shear. This model is based on the postulate that the last crystallites in the PVC melt have the same structure as found in the dilute solution. In his earlier studies he found that in dilute solutions of commercial PVC, 10-15 molecules are held together by a crystalline nucleus:

$$\frac{1}{T_{\text{dyn}}} - \frac{1}{T_m} = \frac{\tau^2}{Q \cdot T_{\text{dyn}}^2}$$

where: Q = is a constant

T_{dyn} = melting temp in shear

T_m = static melting temperature

τ = shear stress.

Static melting temperatures can be estimated by Flory's equation.

Polymer structures are very dependent on the thermal history of the sample and thermal properties of a material are very sensitive to changes of the structure. This means that thermal properties are potentially useful methods of studying polymer structures.

A polymer is given a thermal history when it is either slowly or quickly cooled as a melt, or when it is heated again after having solidified. The effect of annealing and cooling rate on morphology, crystallinity, the melting point, are well established in the case of

many partly crystalline polymers. Any influence on crystallinity is generally only feasible by annealing above T_g . Annealing below T_g simply changes the free volume. The changes in properties with thermal history for an amorphous polymer close to its glass to rubber transition, can be interpreted in terms of "hole theory" of liquids as proposed by Eyring⁽⁶⁰⁾.

Hirai and Eyring⁽⁶¹⁾ developed the theory for polymers and Wunderlich et al⁽⁶²⁾ used the theory to interpret D.T.A. traces for polystyrene. In the "hole theory" it is proposed that polymer chain movement can take place by the jumping of segments into vacant "holes", and each segment leaving another hole for movement of a further segment and so on. In the liquid state the number of holes increases with temperature and expansion occurs, but on cooling there comes a point at which chain mobility is lost and segments cannot jump into holes. Then an equilibrium hole concentration is frozen in and the expansion coefficient is much reduced. The liquid has then reached the "glassy state" and a marked change of properties occurs. Wunderlich et al proposed this as a mechanism for the dependence of glass transition temperature on the rate of cooling. The effect of cooling and heating rate on hole concentration is

illustrated by figure 6⁽⁶³⁾. The concept of "holes" has now been replaced by free volume, where free volume can be roughly defined as that volume occupied by a material beyond the volume it would occupy if all its molecules were packed tightly as at absolute zero temperature.

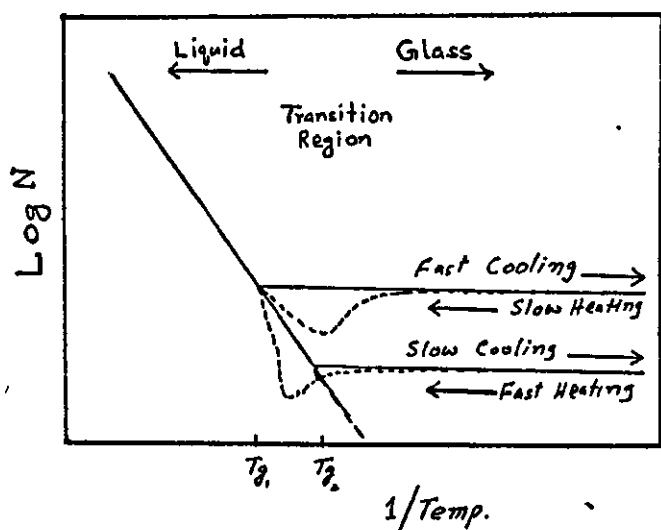


FIGURE 6 : Change of "hole concentration" with temperature.^[63]

Jujin et al⁽⁶⁴⁾ have studied in detail, the effect of thermal treatment on the structure of PVC. They have found that the magnitude of the annealing effect depends on the extent to which the primary crystallinity has been removed. The effect becomes larger when the amount of primary crystallinity left after preheating, decreases. An unreacted virgin powder does not show any effect at all.

Several workers⁽⁶⁴⁻⁶⁷⁾ have shown that annealing effects increase in intensity when annealing is prolonged. Endotherms observed in D.T.A. faces of PVC annealed samples, are considered to be due to the formation of crystallites which melt about 20°C above the annealing temperature. They all agree that the maximum effect of annealing is around 110°C.

The broad X-ray diffraction maxima and a very broad melting D.T.A. endotherm indicates that the crystallites in PVC are small and have a wide range of perfection. The orthorhombic structure of PVC is well established, but some times in X-ray diagrams of commercial PVC, a diffraction ring is found which cannot be ascribed to the orthorhombic crystal form. Mami and Nardi^(58,59) describe this reflection as being due to the so called mesomorphic or nematic structures which appear after annealing at 85° - 107°C of stretched fibres. The nematic structures consist of straight chains aligned in parallel with a distance, between the axes of 5.4 Å.

Jujin⁽⁶³⁾ believes that there are two types of crystallinity in PVC - these are referred to as primary and secondary crystallinity. Primary crystallinity is attained by the polymer during polymerisation or careful precipitation from its solution.

The primary crystallinity has the orthorhombic structure. He supported his argument by quoting Kockott's X-ray work on commercial PVC who showed that X-ray reflections disappear upon melting at 150°C. Jujin has found from his own calorimetric experimental work on various grades of PVC that this melting point is lower than that of partly syndiotactic PVC. He suggests that the introduction of atactic chain segments in the crystal lattice depresses the melting temperature.

Upon annealing secondary crystallinity is formed and this type of crystallinity has a nematic structure. The packing of the chains is less ideal compared with that in the orthorhombic lattice. This results in lower melting temperatures and a lower heat of fusion.

Lebedev et al⁽⁴⁸⁾ have found that annealing at 110°C produces reflections from orthorhombic and nematic structures at the same time, which means that the alignment of chains proceeds simultaneously with the formation of real orthorhombic crystallites.

Witenhafer⁽⁴⁹⁾ strongly believes that upon annealing above T_g , the imperfect crystallites in PVC form stable crystal structures which results in an increase in crystallinity.

Baker et al⁽⁴⁷⁾ have investigated the annealing

effect on highly syndiotactic PVC by X-ray diffraction and infra-red techniques. They have found that annealing causes increase in crystallinity and have suggested a mechanism for the increase in crystallinity on annealing. As the temperature is raised, some amorphous material is converted to a nematic phase, and this may crystallise during subsequent cooling.

In order to support this idea, they have compared the area beneath the three dimensional, 3d, two dimensional, 2d, and amorphous region reflections in X-ray diagrams. The result is shown in Table 2.

TABLE 2

Temperature	Area beneath the amorphous region	Area beneath 3 dimensional reflection (h,k,l) 240° - 260°	Area beneath 2 dimensional reflection (h,K,O), (h,O,O), 160° - 180°	Ratio 2d/3d
Ambient	36.6%	51.6%	11.8%	1:4.35
110°C	33.9%	52.0%	14.1%	1:3.68
180°C	28.8%	53.2%	18.0%	1:2.96

Table 2 clearly shows that, not only crystalline material forms at the expense of the amorphous material during the annealing process, but the two dimensional order

apparently increases more rapidly than the wholly crystalline phase.

The ratio of the two types of reflection after cooling from 180°C annealing temperature, is the highest, even higher than the one prior to annealing. This clearly shows that three dimensional order increases at the expense of two dimensional order.

TABLE

Temperature	Ratio of 2d/3d
Ambient	1:4.35
110°C	1:3.68
180°C	1:2.96
Cooled from 180°C	1:4.69

Gray⁽⁶⁴⁾ has studied in detail the effect of annealing below and above T_g on structural orders of various grades of PVC. Three vinyl chloride polymers were annealed at temperatures in the range 40°C - 160°C for times varying from 0.5 - 5 hours. Structural changes occurring in the polymer were examined by density measurements, differential thermal analysis, and X-ray diffraction.

X-ray results showed that annealing above T_g caused an increase in crystallinity. From the D.T.A.

traces it was concluded that annealing had caused the formation of crystallites which melt about 20°C above annealing temperature. Enthalpy changes corresponding to the fusion of these crystallites are found to pass through a maximum between T_g and T_m (melting temperature) in a manner typical of most crystallizing polymers.

There was no significant change in crystallinity upon annealing below T_g as was confirmed by X-ray measurements. Increase in density and an additional endothermic peak below T_g , have been assigned to the free volume changes.

Illers⁽⁶⁵⁾ has thoroughly investigated the annealing effect on the properties of PVC. He mainly used differential scanning calorimetric techniques to study property changes as a function of annealing times and temperatures. Illers found that after annealing samples at temperatures below T_g , endothermic peaks followed the T_g step on the D.S.C. trace, in fact this is due to overheating of the glassy lattice before an equilibrium hole structure is achieved. Illers also found that endothermic peaks occurring on D.S.C. traces after annealing above T_g are due to the melting of crystallites at temperatures 20 to 30°C above the annealing temperature.

2.6 Mechanical Properties

A phenomenological description of the mechanical properties of polymers appeared long before the first conception of the molecular nature of these bodies was formed. The discovery that polymer molecules are very large and are flexible if their structure is linear, led to a new stage in development of the "theory of mechanical properties of polymeric bodies". This theory also covers the relationship between mechanical properties and basic characteristics of macromolecules such as size and size distribution flexibility.

The theory of mechanical properties of polymeric bodies, was based on two main premises:

- i) Deformation of the polymer depends wholly on the behaviour of its macromolecules, reversible deformation being due to changes in conformations of the macromolecules, and irreversible deformations to their displacement.
- ii) Isotropic amorphous polymeric bodies are homogeneous bodies consisting of randomly arranged macromolecules, isotropic crystalline polymeric bodies being regarded as the result of ordering of small regions of these bodies into microcrystals.

It was considered that the macromolecules pass through several such crystalline regions and amorphous regions separating them. The anisotropy of polymeric bodies was attributed to straightening and orientation

of their macromolecules. The homogeneity of polymeric bodies was taken for granted.

The first polymeric bodies whose mechanical properties rapidly became an object of study, were amorphous synthetic rubbers, the structure of which corresponded more than those of other polymers to the basic premise of the theory. However as the sphere of polymeric objects expanded, various complications began to arise. It was especially difficult to reconcile such simplified ideas of the structure of a polymeric body with the mechanical properties observed in crystalline polymers. The discovery of super-molecular structures in amorphous and crystalline polymers, showed that the basic premises concerning the structure of polymeric bodies were no more than a first approximation which could serve only in the simplest cases. This marks the beginning of the second stage of development in the theory of relationships between the mechanical properties of polymeric bodies and their structures. At this stage the theory was based on the following premises:

- a) All polymeric bodies, whether isotropic or anisotropic liquid or solid, amorphous or crystalline, contain super-molecular formations of different degrees of complexity and of differing sizes. Their existence makes it possible to consider polymeric bodies homogeneous or even continuous in some cases.

- b) The deformation of a body and its mechanical properties are governed by the specific forms of its super-molecular formations and their properties, which in their turn depend both on their own characteristics and on macromolecular characteristics.

Thus, at this stage, polymeric bodies were in some cases regarded as continuous and homogeneous, and in others, as heterogeneous and rather even as microconstructions. Closest to the first group were polymer solutions and melts, and to the second group, crystalline polymers.

The second, modern stage in the theory of mechanical properties of polymeric bodies, features very rapid progress in both experimental and theoretical investigations, and in separation of the structural mechanics of polymers into an independent division of polymer mechanics.

The simplest type of supermolecular structure is the "Globular" type. Any polymer whose macromolecules are sufficiently flexible can be obtained in a globular structure which will be stable or unstable depending on the temperature. Polymeric amorphous bodies possessing globular structures, lose all characteristic features that can be traced to the flexibility of their macromolecules, they prove to be brittle, solid materials or very weak rubbers, provided their globules do not straighten during deformation, but if deformation involves a

structure transformation, the globular structure changing, for example, to a "fibrillar" one, the mechanical properties also improve substantially.

Thus, when considering the influence of the structure of polymeric bodies on their mechanical properties, two cases should always be distinguished, either the structure is preserved until the body fails completely, or structural transformations occur during the deformation.

Another characteristic type of supermolecular structure is the "Fibrillar" type. Polymeric bodies with fibrillar structures are always more deformable and stronger than polymeric bodies of the same composition and molecular build, but of globular structure. In the case of crystallizing polymers of fibrillar structure, a large number of more complex structural forms appear with corresponding complexes of properties.

The next type of supermolecular formation, is the "lamellar" type. As in the case of the fibrillar type sheets aggregate into a diversity of more complex structural forms. Polymers of sheet structure also possess a better complex of properties than do polymers of globular structure.

Finally, the most common type of supermolecular structure is "spherulite" types. The smaller the spherulite, the more uniformly are the mechanical stresses distributed, and the more the behaviour of

the polymeric body approaches that of a homogeneous body. This is why such bodies can withstand fairly high stresses before they fail, and develop a neck, i.e. change their spherulitic isotropic structure into an oriented anisotropic structure. For this reason, specimens of such bodies fail at larger ultimate elongations and under considerable stresses, but if the spherulites are large, interfaces appear between them, which maybe as large as cracks. Here, failure develops readily and the body suffers brittle rupture at small elongations and comparatively low stresses. Of importance in the origin of mechanical properties are not only the size of spherulites, but also their inner structure. This accounts for the numerous exceptions to this rule. Therefore, spherulite growth, which may occur during storage or usage of polymeric articles, has a significant effect on the stability of property values.

The basic characteristics of mechanical properties of solids are usually determined by tests resulting in various deformations-vs-stress dependencies, such as stress-strain diagrams.

When discussing stress-strain relationships, it must be agreed beforehand to which cross-sectional area of the specimen the force acting on that cross-section will be referred. Owing to the very high values of the strains actually obtained when elasto-

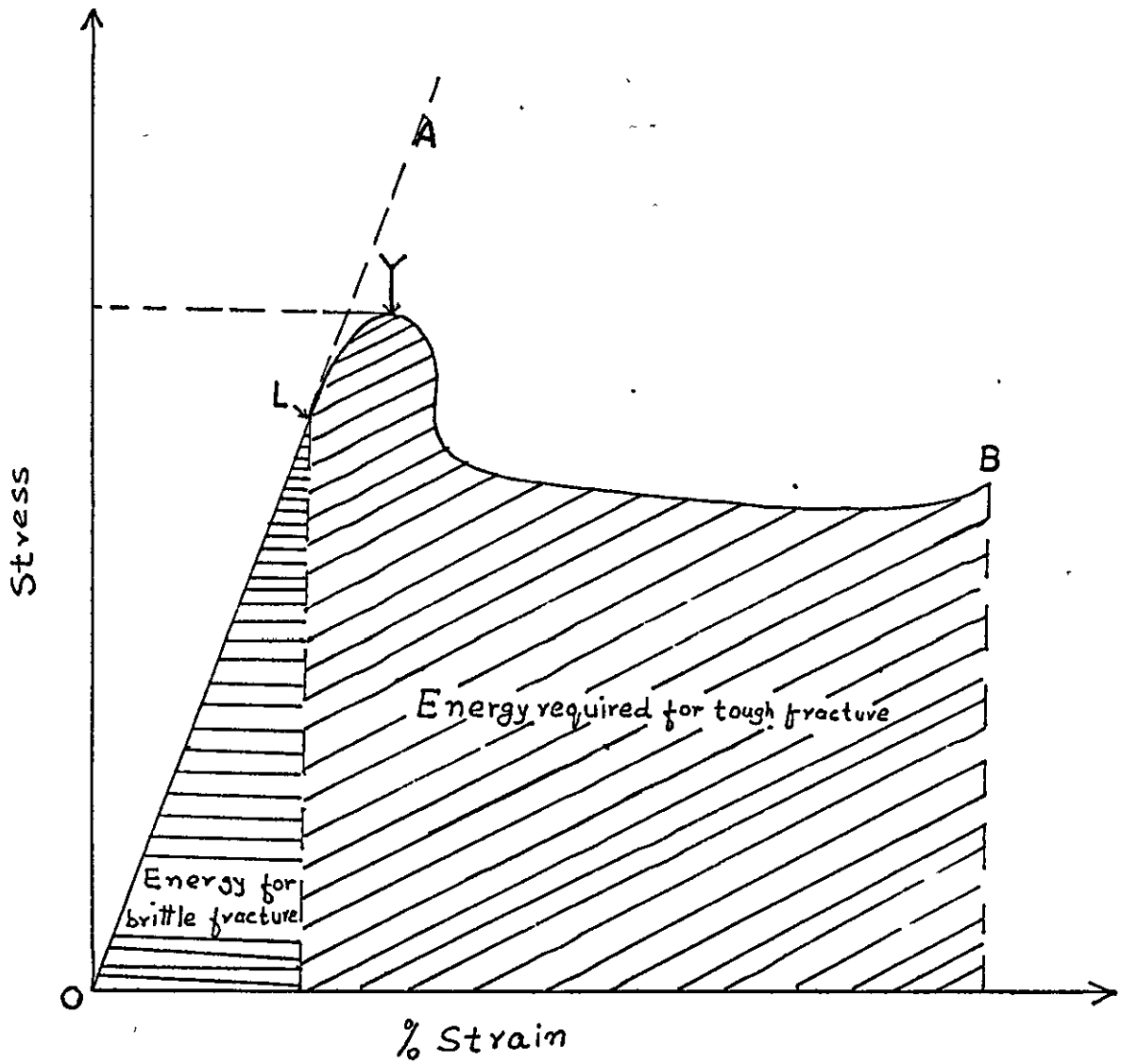


FIGURE 7 Idealised stress-strain curve. The slope of line OA is a measure of the true modulus

meric, crystalline, and glassy polymers are extended, the cross-sectional area of the strained specimen may vary severalfold. For this reason two values are ordinarily considered, namely, the actual stress and the nominal stress. The former is the quotient of the applied force divided by the actual cross-sectional area, and the latter, divided by the cross-sectional area of the original specimen.

By subjecting a specimen to a tensile force applied at a uniform rate and measuring the resulting deformation, a curve of the type shown in figure 7 is obtained. The shape of such a curve is dependent on the rate of testing and temperature at which the test has been carried out. Consequently, the testing conditions must be specified if a meaningful comparison of data is to be made and tests must be performed within as wide a range of temperatures as possible. In figure 7⁽⁶⁸⁾ the initial portion of the curve is linear and the tensile modulus 'E' is obtained from its slope. The point 'L' represents the stress beyond which a brittle material will fracture, and the area underneath the curve to this point is proportional to the energy required for brittle failure. If the material is tough, no fracture occurs, and the curve then passes through a maximum or inflection point 'Y', known as the yield point. Beyond this, the ultimate elongation is eventually reached and the polymer breaks

* Fig. 7 is an idealised curve and hence the slope of line OA gives the true value of modulus. In practice the slope of the linear portion is not truly constant and therefore such values relate only approximately to modulus.

at 'B'. The area under this part of the curve is the energy required for ductile failure to take place.

The term "tensile strength", though widely used, needs care because it can refer to three different phenomena which should be distinguished. In the above figure 7, tensile strength has been used to describe:

- i) σ_L = brittle strength - the maximum stress in brittle failure.
- ii) σ_Y = yield stress - the maximum stress at yield point.
- iii) σ_B = tensile strength at break - the maximum stress at the break point in ductile failure.

The values of modulus, tensile strength, and the elongation at break can be used to characterise the polymer material under test.

Several theories have been put forward to explain the yield and cold-drawing behaviour of polymers. According to Jackel⁽⁶⁹⁾, Marshall et al⁽⁷⁰⁾, and Muller⁽⁷¹⁾ a large amount of heat is generated during the stretching process and the major portion of it goes into the heating of the necked region and hence yielding and cold drawing occurs. Alternatively Vincent⁽⁷²⁾ explains the phenomenon by stating that stress in polymers lowers the softening temperature to about the

temperature at which the drawing occurs.

Some objectives have been put forward to the above theories. J S Lazurkin⁽⁷³⁾ has found that yielding and cold-drawing can occur even if the temperature during stretching is reduced by transferring it to surroundings and lowering the stretching speed. Robertson⁽⁷⁴⁾ and Sternstein et al⁽⁷⁵⁾ have found the yielding phenomenon in shear, and Whitney and Andrews⁽⁷⁶⁾ have observed this phenomenon in compression. Neither shear nor compression affect the softening temperature. Moreover there is no molecular mechanism to explain the lowering of softening temperature.

Lazurkin based his explanation therefore on the Eyring model. Such models have been proposed by other workers^(77,78,79). The effects of thermal motion and mechanical stresses during stretching combine to rupture intermolecular bonds and allow large scale configurational changes. Yielding occurs therefore when stresses or strains create increased segmental mobility. The magnitude of the force will be greatly dependent on the initial chain mobility of the sample to be deformed. The Lazurkin-Eyring model appears to explain the phenomenon most satisfactorily and has been used by several workers to explain the tensile behaviour of the polymers.

Another important mechanical property for plastics is the impact strength. The ability of a fabricated article to withstand shock is often a decisive factor in the replacement of a conventional material by a polymer. This impact resistance, or ability to withstand shock, may deviate appreciably from the results suggested by standard impact tests. The impact resistance of a plastic article depends not only on basic impact properties of the polymer, but also on the following factors:

- a) Design of the object.
- b) Conditions during fabrication.
- c) Environmental conditions.
- d) The nature of the blow.
- e) The frequency of the shock.

A rigid plastic is usually classified as brittle or ductile, according to the type of failure which results from a blow, but the usage is loose and does not precisely define the nature of the break.

1. Brittle failure:

Vincent⁽⁷²⁾ has defined brittle fracture as a failure in which there are no signs of permanent deformation. However, this may not be precise in that:

- a) there may be deformation which is not obvious to the naked eye,
- or
- b) the deformation may be recoverable so that the nature of the break has changed its appearance by the time the test samples are examined.

2. Ductile failure:

If the plastic undergoes deformation or yielding during failure, then the material will be adjudged to fail by a ductile fracture. The plastic is said to have good impact strength.

PVC is can be used variable material on which to study mechanical properties. The reproducibility of results is often poor. This is probably due to large number of influences on the properties, and careful standardisation of specimen preparation is required if meaningful results are to be obtained.

The greater structural regularity of the polymer molecules and the increased crystallinity of low temperature polymerised PVC, lead not only to a higher softening

but also to higher strength and greater resistance to creep. However the mechanical properties are strongly influenced by the processing conditions.

Malac⁽⁸⁰⁾ has studied the influence of processing conditions on sample properties. He examined the influence of pressing temperature and rate of cooling on tensile strength, impact strength and embrittlement properties of PVC. A slow rate of cooling gives an increase in tensile strength, a low impact strength and raises the embrittlement temperature from -15°C to $+15^{\circ}\text{C}$. This he attributed to the freezing-in of free volume in fast cooling.

Phillips et al⁽⁸¹⁾ found annealing above T_g causes a decrease in tensile strength and elongation, whereas yield stress increases. Retting⁽⁸²⁾ has examined tensile behaviour between speeds of 10^{-3} and 1 cm/sec. Samples were annealed below T_g . He found that modulus at low strain rates increases substantially with annealing time. At higher strains there was little effect of heat treatment. Illers⁽⁶⁶⁾ attributed changes in tensile behaviour to a decrease in free volume for samples heated below T_g , and crystallinity changes for those heated above T_g .

Influence of processing history and crystallinity on the mechanical properties, has been thoroughly investigated by Pezzin et al⁽⁸³⁾. They found that main transition α (glass transition) and the shear modulus above T_{α} depend on the thermal history and are strongly effected by crystallinity, whereas the dynamic mechanical

spectrum below T_{α} is not influenced by these parameters. They also found that room temperature tensile modulus and yield properties are very little affected by processing history and crystallinity, whereas the elongation at break and fracture energy increases with milling temperature.

Impact strength of crystalline PVC is lower than that of conventional PVC^(84,85). The impact strength of crystalline PVC can be improved by compounding the polymer with a suitable toughening additive, such as an ethylene-vinyl acetate copolymer. The notched impact strength of crystalline PVC can be increased by a factor of 3 (from 4 to 12 kgf cm/cm²) by adding 12% of ethylene vinyl acetate copolymer and by processing the compound at 200°C⁽⁸⁶⁾. Other toughening additives have ^{also} been found which increase the impact strength.

Static mechanical properties, creep and stress relaxation, have been studied by a number of authors in order to study structure and plasticization mechanisms. Aiken et al⁽⁸⁷⁾ carried out one of the earliest thorough investigations of creep behaviour in plasticized PVC. They pointed out that since plasticization can give rise to flexibility unaccompanied by flow, then there must be a three dimensional gel network present. They discovered that a gel structure existed even in solution of 4% PVC in 96% plasticizer. They further noted that the gel structure apparently became tighter when kept

at room temperature since the shear modulus steadily increased.

Taylor and Tobolsky⁽⁸⁸⁾ made stress relaxation measurements at various temperatures on PVC containing a range of plasticizer types and levels. They concluded that PVC is semi-crystalline in nature, the crystallites can be considered to act as cross-links. The action of the plasticizer is similar to their effect on completely amorphous polymers, but the crystallites remain stable under their action. This work has been continued by Hata and Tobolsky⁽⁸⁹⁾ who noted some anomalous behaviour, depending on the heat history of the sample used. The behaviour of plasticized PVC can be usefully compared to the behaviour of unplasticized PVC at high temperatures. Crugnola et al⁽⁹⁰⁾ have studied the stress relaxation of PVC in the temperature range 100 - 180°C. They also attributed the elastic nature of the PVC response to crystallite cross-links. Sabia and Eirich^(91,92) studied the viscoelastic behaviour of PVC at large deformations using stress relaxation and creep experiments. They proposed two mechanisms for viscoelastic behaviour of PVC in creep. Firstly, elongation of amorphous regions, followed by deformation of the crystallites, so resulting in flow and set.

CHAPTER 3

EXPERIMENTAL TECHNIQUES3.1 Plan of Procedure

This work is a part of the large programme being undertaken in the Institute of Polymer Technology.

The aim of the above mentioned programme is the study of inter-relationships between PVC powder morphology, processing conditions, structure and properties of mouldings.

In this work investigations have been made on rigid PVC simply because plasticizers change the entire properties of PVC. A very careful formulation (3 pph of Tl35 stabiliser and 0.5 pph of calcium stearate as lubricant) was used in order to have the minimum effects of additives on the properties as well as excellent clarity and finished surface of the moulded sheets.

Two commercial grade PVC resins have been used for this work. The first material was Breon M-80/50, mass PVC supplied by B P Chemicals Ltd. The second was Corvic D55/09, suspension PVC, manufactured by ICI. They will be referred to as M-PVC and S-PVC respectively throughout this work. Technical data for these two resins is given in Tables 4 and 5. From published

literature the crysallinity in both materials is expected to be in the range of 10-15%.

This research project was aimed to find the relationship between structure and mechanical properties of Poly (vinyl chloride). In order to investigate structural changes and corresponding property changes in the absence of high shear forces present in injection moulding, it was planned to prepare compression moulded sheets from dry blends at various mould temperatures. Since mouldings produced below 160°C exhibit incomplete fusion of powder particles, mould temperatures above 160°C were used.

Other research workers⁽⁹⁶⁾ working on the compounding area of this programme, had established the optimum conditions for dry-blending. So it was also decided to use the same optimum conditions for dry-blending in this project.

Structural changes were examined by X-ray diffraction and differential thermal analysis techniques. The mechanical tests for tensile, Young's modulus were carried out on an Instron testing machine, while Charpy was used for impact tests.

New structures were introduced by thermal treatment and any changes in structure and properties were examined using the same techniques. It was hoped that the correlation between structure and properties of heat

treated samples would confirm the investigations in structure and properties relationship of untreated samples.

TABLE 4

Technical Data of M80/50⁽⁹⁷⁾

Specific viscosity (0.5% solution in cyclohexane)	0.39 - 0.41
K - value	56 - 58
Viscosity No. (Iso method R174: 1961)	78 - 82
Bulk density (BS 2782, Part 5, method 501A)	640 - 680 kg/m ³
Particle size 99.9% min. 90% min 6% min	< 250 μ m < 100 μ m < 63 μ m

Measurements of molecular weight on G.P.C. apparatus by
RAPRA (Rubber & Plastics Research Association)

Molecular Weight	M-PVC	S-PVC
Weight average molecular weight (\bar{M}_w)	66,700	76,470
Number average molecular weight (\bar{M}_n)	29,400	34,030

TABLE 5

Technical data sheet⁽⁹⁸⁾ for Corvic D55/09, 1

Property	Unit	Value	Test Method
K value	-	62	No. 1
Viscosity Number	-	95	150 - R174
Packing Density	g/ml	0.64	No. 2
Apparent Density	g/ml	0.59	150 - R60
Relative Density		1.40	Archimedes Method
Weight passing 60 mesh (250 μ m)	%	99.9	No. 3
Weight passing 200 mesh (75 μ m)	%	5	No. 3
Volatile content	%	0.2	No. 4

No. 1: Calculated from relative viscosity data obtained by method ISO-R174.

No. 2: From volume of 20 grams of polymer in cylinder dropped 30 times from a height of 51 mm.

No. 3: By sieving dry polymer for 30 minutes in humid air (BS 410: 1969).

No. 4: Weight loss after one hour at 135°C.

3.2 Preparation of Blends

In the present work the following formulation was used for both M-PVC and S-PVC.

Formulation

PVC resin	100 pph by weight
T-135, Thiotin (stabilizer)	3 pph by weight
Calcium Stearate (lubricant)	0.5 pph by weight

This simple formulation was used to achieve the following properties:

- a) The minimum effect of additives on the properties of PVC.
- b) Excellent clarity and finish surface of the moulded sheets.
- c) Good dispersibility of ingredients.

Thiotin stabilizer is the most suitable stabilizer which gives excellent clarity and surface finish in rigid PVC. Primarily it is a heat stabilizer but it also gives good light stability, non-staining and non-toxic properties. Calcium stearate acts as internal lubricant and has good dispersibility. These additives were supplied by Akzo Chemic U.K. Ltd. They have

been added at levels to impart minimum effects on mechanical properties of PVC.

Dry-blends of formulation described above from both M-PVC and S-PVC were prepared in an 8 litre T.K. Fielder mixer using the optimum conditions determined previously⁽⁹⁶⁾. The working capacity of the mixer chamber is about 3 Kg with impeller speeds ranging from 500 - 4000 revolutions per minute. The mixer is fitted with stock temperature measurement facilities, jacket temperature control and a separate cooling mixer. The cooling mixer has an arrangement to circulate cold water in the inner jacket and equipped with rotor that operates at relatively low speeds. An iron/constantan thermocouple protrudes through the baffle to measure the blend temperature.

The jacket was heated to 75°C by steam in order to minimise the mixing cycle and to attain a high blend temperature of 120°C. About 2 kilograms mass was placed in the mixing chamber and the rotor speed was set to 3500 revolutions per minute. After the temperature of the mass reached 50°C, the stabilizer was added through the window in the lid of the mixing chamber. Due to the high speed of the impeller, the components were thoroughly mixed and intensive frictional heat was developed. The temperature of the mass increased gradually and in 15-20 minutes it reached

120°C. The blend was discharged, at this temperature, into the cooling mixer through a pneumatic valve. The mass was cooled for about 3 minutes at the speed of 1000 revolutions per minute.

Mixing cycles for S-PVC took longer than M-PVC, due to the morphological differences between the two resins. In S-PVC mixing cycles, less frictional heat is generated and hence less rapid rise in temperature occurs compared to the M-PVC. This happens because S-PVC resin particles have a skin or membrane around them, and therefore the particle's surface is smoother. Moreover S-PVC particles have less regularity in shape and wider particle size distribution.

The blending conditions are given in Table 6. Table 7 shows the typical properties of Thiotin-Tl35, stabilizer.

TABLE 6

Optimum Blending Conditions

Rotor speed	3500 r.p.m.
Jacket temperature	75°C
Temperature of stabilizer addition	50°C
Blend discharge temperature	120°C
Cooling mixer rotor speed	1000 r.p.m.
Cooling time	2-3 minutes

TABLE 7

Typical Properties of Stabilizer

Type	Thiotin T-135
Colour (garden)	1
Density	1.1 gm/ml at 20°C
Reflective index	1.508 at 20°C
Viscosity ρ	< 0.5 Poise at 20°C

3.3 Preparation of Mouldings

Compression moulded sheets were prepared from both M-PVC and S-PVC powder blends at various temperatures ranging from 160°C to 220°C in steps of 10°C.

20 x 20 cm² sheets of thickness 1 mm and 3 mm were prepared in an electric press. 200 gm of powder blend for 3 mm thick sheet and 80 gm of 1 mm thick sheet, was placed in the preheated mould. The mould was heated for 15 minutes in the press at a fixed temperature and a constant pressure of 25 tons on 8 inch diameter. The mould was then cooled down to 50°C by circulating cold water through the press platen. The cooling cycle took 7-8 minutes.

In order to investigate the effect of cooling rate on structure and properties of PVC, a few sheets were cooled by ice cold water to reduce the cooling cycle to 5 minutes. Figure 8 shows the two different rates of cooling.

Moulded sheets were stored at -21°C in a deep-freezer to inhibit any free volume changes during storage.

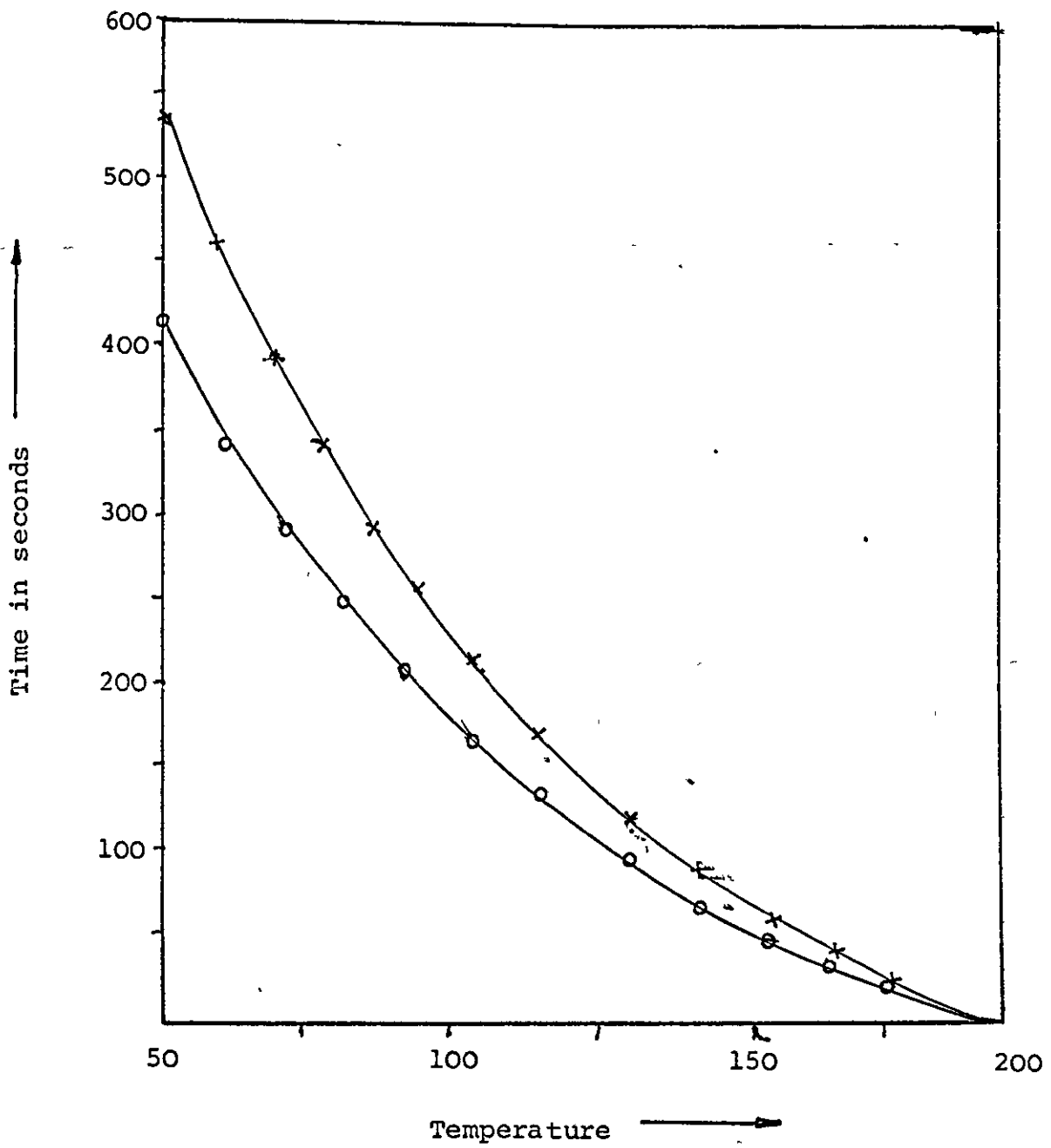


FIGURE 8 Rate of cooling
o Fast cooling
x Slow cooling

3.4 Physical Characterisation

3.4.1 Particle Size Distribution

The size and size distribution of resin particles are reflected in the properties such as surface area, bulk and apparent densities and powder flow. These parameters also have a profound effect on the processing behaviour. During processing, large resin particles would require more processing to break them down and the time to achieve this would depend on bulk density of the resin. It is, therefore, desirable for the resin to have narrow particle size distribution with minimum of fines or oversize.

Particle size and size distribution are usually determined by sieve analysis using a stack of standard ~~sieves~~ sieves in the range of 12-300 BS mesh sizes. Other methods such as microscopy, electrical conductivity and relative motion between particles and fluid are also used for particle size analysis. The choice of the method depends on particle size range and form of the specimen.

In the present work an optical method was used to analyse the particle size of both M-PVC and S-PVC dry blended resins. The optical method involves the use of a Zeiss TGZ3 particle size analyser. In this method the diameter of each particle is measured and

hence it becomes essential to observe sufficient numbers of particles. At least 1000 particles were analysed for each sample at a magnification of X100. Each particle on the micrograph was analysed by adjusting the area of the iris to coincide with the area of the particle. On pressing the footswitch, the particle size is recorded automatically on the counter.

3.4.2 Density of PVC Powder Blends

One of the important physical characteristics of polymer resins, in establishing processing conditions, is bulk/apparent density. In the present work bulk and apparent densities were measured by usual methods.

Bulk density: Bulk, tap or packing density are three different terminologies for the same thing. About 100 grams of dry-blended powder were vibrated in a tall cylinder until the volume was constant. The bulk density was then calculated simply by dividing the weight of the PVC powder by its volume. The average of three determinations is reported.

Apparent density: Apparent density was measured by BS 2782, part 5-1970, 501A method.

The standard funnel was supported vertically with its lower orifice 20 mm above the measuring cup. The measuring cup was coaxial with the funnel. The bottom of the funnel was closed with a cardboard sheet and about 100 grams of PVC blended powder was placed in the funnel, then the cardboard sheet was slid away so that powder filled the cup and overflowed. The powder in the measuring cup was levelled off and

the cup was tapped gently to settle the powder. The cup and powder was weighed and the weight of the powder was obtained by difference. Volume of the cup was taken as 80 cm^3 . The apparent density was then calculated by dividing the weight of the powder by the volume of the cup - 80 cm^3 .

Flow rate

In order to measure the flow rate, 25 grams of powder was allowed to flow through the funnel and time in seconds was recorded. The flow rate was measured using the same apparatus and procedure as described for the apparent density.

3.5 Thermal Techniques

3.5.1 Thermal Treatment

From the literature review, in Section 2.5, it is clear that thermal treatment (annealing) is a useful method of modifying the polymer structure, and thermal properties are a potentially useful method of studying polymer structures.

Therefore, in the present work, samples were heat treated in order to introduce various structures and then to study the corresponding properties.

In order to provide a uniform thermal history, samples from one specific moulding temperature were chosen for heat treatment. Two sets of samples 'a and b' from both M-PVC and S-PVC moulded sheets at 200°C were prepared for heat treatment.

- a) Samples from both M-PVC and S-PVC moulded sheet at 200°C were annealed at temperatures between 80°C to 170°C for times varying from 0.5 hours to 5 hours. No pre-treatment was given to this set of samples. In order to see the effect of rate of cooling on structure and properties, a few samples were quenched in ice/water mixture after being annealed, whereas the rest of the samples were cooled to ambient temperatures in air.

- b) This set of samples was subjected to a pre-treatment prior to being annealed. The pre-treatment was carried out in an attempt to remove the existing order. Samples from both M-PVC and S-PVC moulded sheet at 200°C were wrapped in aluminium foil and placed in an air circulating oven for 5 minutes at 210°C. Samples were then quenched immediately in ice/water mixtures. The quenched samples were then annealed at temperatures between 80°C to 150°C for times varying from 0.5 to 5 hours.

Samples from both sets "a and b" were wrapped in aluminium foil to prevent them sticking to the surface of the oven and to retain their surfaces smooth. They were annealed in an air circulating oven and were brought to ambient temperature just by cooling in air. A few samples from set "a" were quenched in ice/water mixture after being annealed. The heat treated samples were stored at -21°C in the deep freezer to inhibit any morphological changes which may otherwise take place.

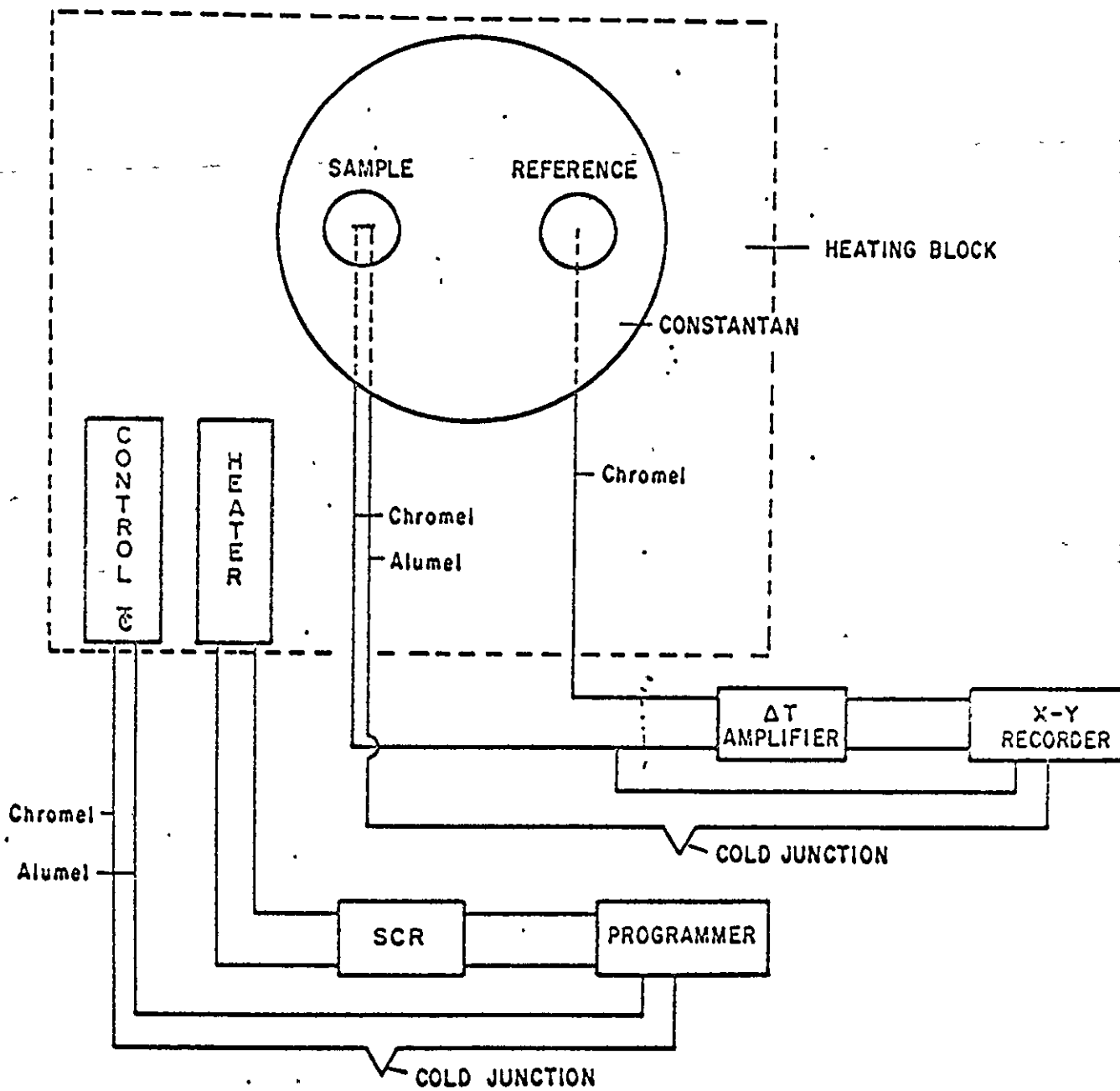
3.5.2 Differential Thermal Analysis (DTA)

Differential thermal analysis is a technique for studying the thermal behaviour of materials as they undergo physical and chemical changes during heating or cooling. The sample to be examined is heated at a linear rate alongside an inert reference. The temperature difference is monitored by thermocouples situated underneath the sample and reference.

A Du Pont 900 thermal analyser, fitted with a "DSC" cell was used. The heart of the analyser is the solid state electronic temperature programmer controller, which permits a wide range of temperature scanning conditions. Heating, cooling, isothermal, hold and cyclic operations are selected by a "programme mode" switch. The heating or cooling rates and the starting temperature of the programme can be varied to suit individual needs. The 900 X-Y recorder plots chemical, physical and mechanical properties on the Y-axis as a function of sample temperature or time on X-axis. A plot of ΔT as a function of either temperature or time is known as a thermogram.

A schematic diagram of "DSC" cell is shown in figure 9. Samples and reference pans made of aluminium are placed on the raised platforms or thermoelectric disc, which is made of constantan. Chromel

FIGURE 9: SCHEMATIC FOR DSC CELL



wire is welded at the centre of the base of each platform. Thermocouple junctions thus formed are used for measuring the temperature difference between sample and reference. The signal between these two junctions is fed to the 900 amplifier, and observed on the Y axis of the recorder. An alumel wire is also welded to the centre of the front raised platforms, forming a chromel-alumel thermocouple, which is used to measure the temperature of that platform.

The corresponding cold junction of the thermocouple is placed in crushed ice at 0°C and the output observed on the X-axis of the recorder. The constantan disc also serves to transfer heat radially inward from the heating block to the sample and reference which are otherwise thermally isolated. A chromel-alumel thermocouple situated close to the heater winding is used to operate the temperature programmer-controller via a feedback mechanism. The sample chamber is protected from external temperatures by a series of shields and lids and the entire cell is kept covered with a glass bell jar.

Thermograms were run on samples from both annealed and unannealed PVC moulded sheets. Samples of weight 10 ± 1 mg were cut from the same position of moulded sheets and three runs were recorded for each

specimen. The cell was cooled to -40°C by pouring liquid nitrogen into a surrounding steel jacket. When the temperature was brought to -40°C , the cooling jacket was quickly replaced by a steel cover and the entire cell was covered with the glass bell jar. The heating rate was used $20^{\circ}\text{C}/\text{minute}$ with the sensitivity of $0.2^{\circ}\text{C}/\text{inch}$ in an atmosphere of dry nitrogen. All thermograms were recorded from -40°C to 200°C and a few were recorded to 220°C .

3.5.3 Thermal Mechanical Analysis (TMA)

The instrument used was a Du Pont 900 thermal analyser equipped with a thermo-mechanical analyser attachment. The Du Pont 941 thermo-mechanical analyser measures vertical displacement as a function of temperature or time. The analyser comprises a moveable core differential transformer to which is coupled a quartz probe to sense displacement changes as small as 10^{-7} mm. Movement of the cone in the transformer results in a change in output of the transformer which is fed to the Y-axis of the recorder. A thermocouple attached to the sample holder tube contacts the sample and provides an output proportional to the sample temperature. The voltage, compensated with a suitable reference junction, is applied to the X-axis of the recorder. The sample and probe head are surrounded by a cylindrical heater containing a control thermocouple. In penetration measurements, the probe which can be weighted or loaded, sinks into the sample when the sample changes from solid to glassy state.

The penetration thermograms were obtained using the penetration probe. The probe was loaded with 10 gram weight and the trace was recorded from -40°C with a heating rate of $5^{\circ}\text{C}/\text{min}$.

3.6 X-Ray Diffraction

A particularly effective way of examining partially crystalline polymers, is by X-ray diffraction. Polymer specimens, whether fibres, sheets or moulding with no preferred molecular orientation, give diffraction patterns having not only fairly sharp crystal diffraction, but also broad peaked diffuse scattering like that given by liquids or glasses.

The crystalline and amorphous scattering in the diffraction pattern can be separated from each other, the crystalline fraction is equal to the ratio of integrated crystalline scattering to the total scattering, both crystalline and amorphous and expressed as percentage crystallinity of the polymer specimens.

For both experimental and theoretical reasons, it is useful to separate X-ray diffraction effects into small-, and wide-angle regions according to the size of the angle of deviation from direct beam, designated by 2θ . Small-angle diffraction (SAXD) refers to effects observed at angles smaller than about 2° or 3° . Wide angle diffraction (WAXD) encompasses effects that are observed above at all larger angles. In the present

work the PVC diffraction pattern is observed from 12° up to $46^\circ 2\theta$.

X-rays are generated when high energy electrons impinge on a metal target, such as copper. By doing so a spectrum of wavelengths is produced as shown below in figure 10.

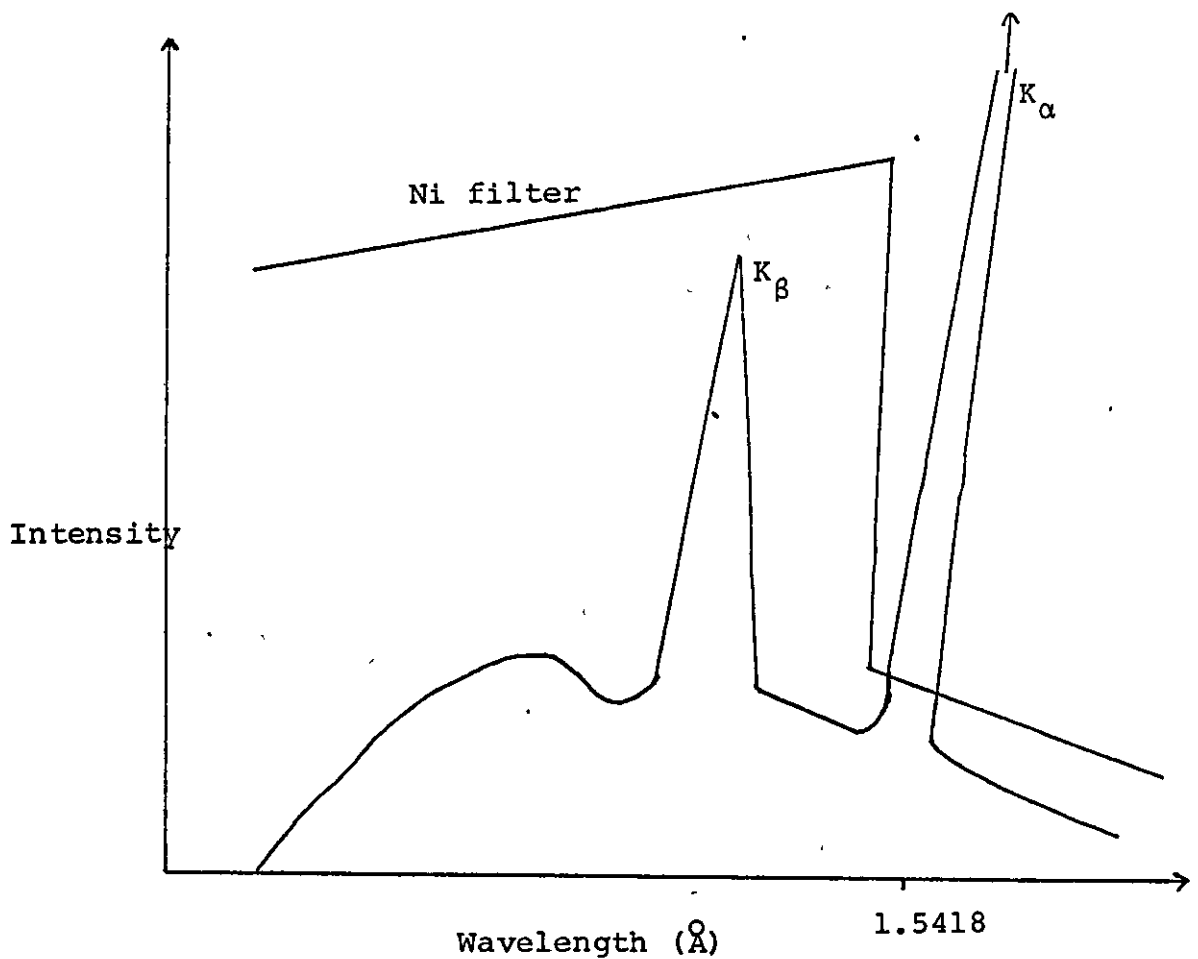


FIGURE 10 Intensity curve for X-rays from copper target

The spectrum can be seen to consist of two parts - a broad band of continuous or white radiation, and a set of two sharp peaks K_{α} and K_{β} , K_{α} being the most intensive. By selecting an appropriate filter, the unwanted wavelengths can be avoided and the radiation of a desired wavelength can be obtained. A Ni filter is used to allow $\text{Cu } K_{\alpha}$ radiation to pass through.

When a polymer specimen is subjected to X-rays, the crystallites present in the sample diffract X-ray beams from parallel planes for incident angles θ , which are determined by the Bragg equation:

$$n\lambda = 2d \sin\theta.$$

where:

- λ = the wavelength of the radiation
- d = the distance between the parallel planes in the crystallites.
- θ = the angle of incidence.
- n = an integer.

Poly (vinyl chloride) has an X-ray diffraction pattern which is of low intensity and, therefore, requires special conditions to be observed. The X-ray

diffraction spectra were recorded using a "Jeol DX-GE-2S" X-ray generator, with DX-GO-S, vertical goniometer, electronic counting device SX-CR-2, and a chart recorder CR-RD-1. The operating conditions used for all samples are given in table 8.

TABLE 8

X-ray tube	40 kV 30 mA
Range	2×10^3 CPS
Time constant	2
Scan speed	$1^\circ/\text{minute}$
Receiving slit	0.2°
Scattering slit	2°
Divergence slit	2°
Angular range	$12 - 46^\circ 2\theta$

The schematic diagram of the diffractometric apparatus used for measuring crystallinity in PVC, is shown in figure 11.

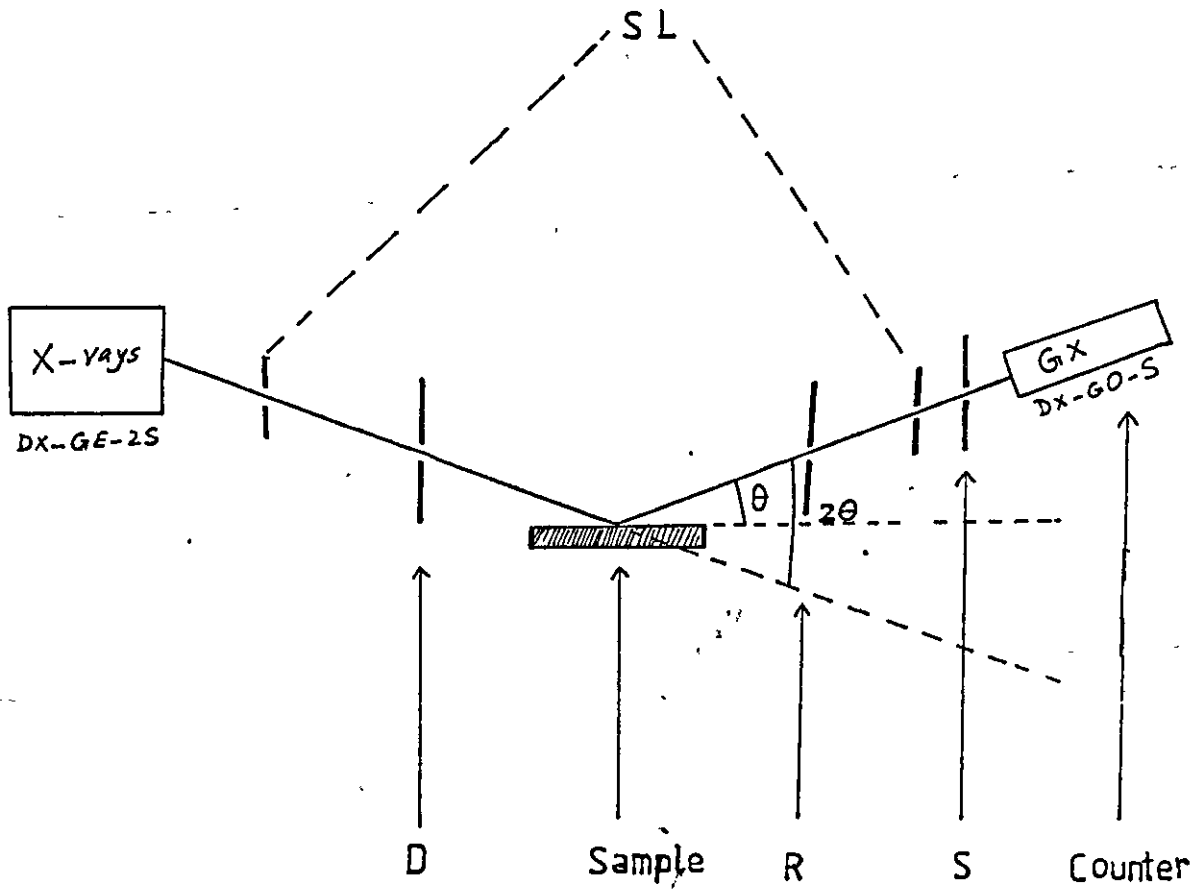


FIGURE 11

Schematic diagram of diffractometer

D = divergence : 2°
 R = receiving slit : 0.2°
 S = scattering slit: 2°
 SL = soller slits :

Ni filtered Cu K_{α} radiation falls on the surface of the specimen and crystallites present in the sample diffract X-rays. The diffracted rays pass through slits 'R' and 'S' and are received by the counter GX. The slit S minimises the air scattered X-rays that can be received by the counter GX. The pulses from counter GX are fed into an electronic device, SX-CR-2, which averages the measured intensities over 2 second intervals, which are finally registered by the recorder. A plot of average intensity as a function of Bragg angle 2θ is obtained.

3.7 Mechanical Properties

3.7.1 Tensile Properties

A tensile test, having been decided upon, it is necessary to choose the shape of the specimen. Different standards organisations have chosen different profiles. The profile used in the present work is according to the ASTM, D-638, shown in figure 12⁽⁹⁹⁾.

The tensile behaviour of all samples has been investigated using an Instron Universal Testing machine. The machine incorporates a highly sensitive electronic weighing system to detect and record the load on the

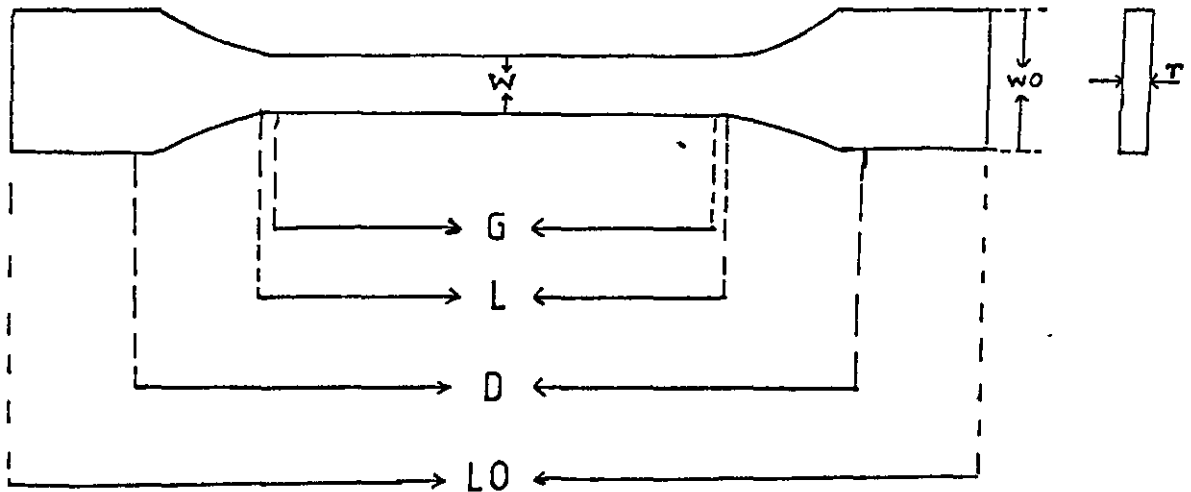


FIGURE 12⁽⁹⁹⁾

Width of the narrow section	$W = 3.0 \text{ mm}$
Gauge length G	$= 7.62 \text{ mm}$
Length of the narrow section L	$= 9.53 \text{ mm}$
Grips distance D	$= 25.4 \text{ mm}$
Overall length LO	$= 64.0 \text{ mm}$
Width of the specimen WO	$= 9.53 \text{ mm}$
Thickness of strip T	$= 3.0 \text{ mm}$

specimen. The moving cross-head is operated by two vertical drive screws from a servo-controlled drive system which provides for selection of a wide range of testing speeds. The recorder is equipped with a strip chart which is driven synchronously with respect to the cross-head over a wide range of testing speeds. Because of synchronism, the chart need not necessarily be operated at the same speed as the cross-head. The chart may be stopped whenever the pulling jaw is stationary and thus extension axis of the chart may be magnified or demagnified.

Preparation of the Samples

10 sets of tensile bars were prepared:

1. Bars from moulded sheets (M-PVC and S-PVC) at various temperatures from 160°C - 220°C.
2. Bars from 200°C moulded sheet cooled by ice/water mixture in the press (M-PVC).
3. Bars from quenched samples. Samples from 200°C moulded sheets were quenched from 210°C in ice/water mixture (M-PVC and S-PVC).
4. Bars from annealed samples. Samples from 200°C moulded sheet were annealed at various temperatures and cooled in the air (M-PVC and S-PVC).

5. Bars from annealed samples. Samples from 200°C moulded sheet were annealed at various temperatures and quenched in ice/water mixture. (M-PVC).
6. Bars from annealed samples. Samples from 200°C moulded sheets were quenched from 210°C in ice/water mixture and then annealed at various temperatures and cooled in the air.

Samples were cut from moulded and heat treated sheets into strips of dimension 64 mm x 9.53 mm. These strips were then shaped by machining (Dumbell shape as shown in figure 12⁽⁹⁹⁾). Marks left by coarse machining operation were carefully removed with a file and filed surfaces were then smoothed with fine abrasive papers. The cross-sectional area for each sample was measured by a micrometer. At least three readings for each specimen were taken and an average recorded.

Tensile tests were performed on all 10 sets of specimens at ambient temperature and on sets 1, 2 and 3 tests at elevated temperatures of 40°C, 55°C and 70°C were also performed.

For tests at elevated temperatures, an air circulating oven was used which fits on the machine.

The oven was regulated for one hour at the test temperature. Each test specimen was held in between

the jaws for five minutes in the oven to allow the specimen to acquire the test temperature. It was pre-checked by inserting a thermocouple probe inside a specimen and left in the oven, set at test temperature. In just about 5 minutes time the specimen had acquired the temperature of the oven.

Six determinations on each sample were carried out, and mean values calculated. The values of elongation were calculated using the initial gauge value and final cross-head separation.

The operating conditions of the Instron are given in Table 8:

TABLE 8

CTM load cell full deflection	50 Kg
Effective gauge length	9.8 mm
Cross head speed	10 mm/min
Chart speed	100 mm/min

3.7.2 Impact Strength

In the present work a Charpy Impact Tester was used. Both notched and unnotched specimens were tested at ambient temperatures. The Charpy Impact Tester in the laboratory uses small bars of rectangular shape. The size and geometry of the specimens used is according to the size of the Charpy test supporter. Figure 15 shows the Charpy test piece and the support and in figure 16 the dimensions of the specimen are shown.

Samples for impact tests were cut from M-PVC and S-PVC moulded sheets into rectangular bars of dimension 6 x 44 mm. The bars were notched 2.5 mm deep in the direction parallel to the moulded surfaces. The sides of the bars were smoothed by a fine abrasive paper.

The test specimen was mounted on the span support, notch facing the support (see figure 15). The pendulum striker was allowed to hit the sample centrally behind the notch (see figure 15) and the excess energy was then measured by the angle of the swing. Six determinations for each sample were carried out, the average value of the parameter was recorded.

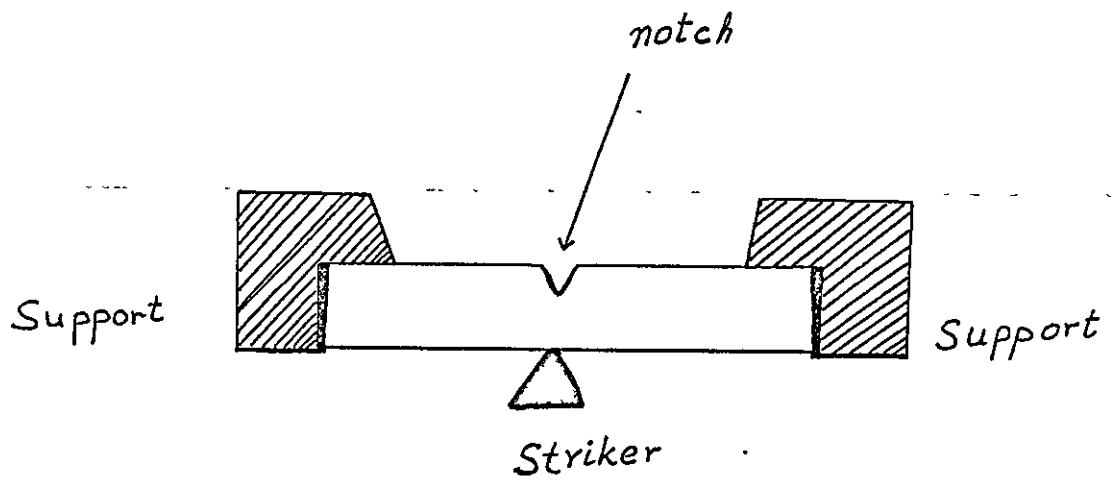


FIGURE 15

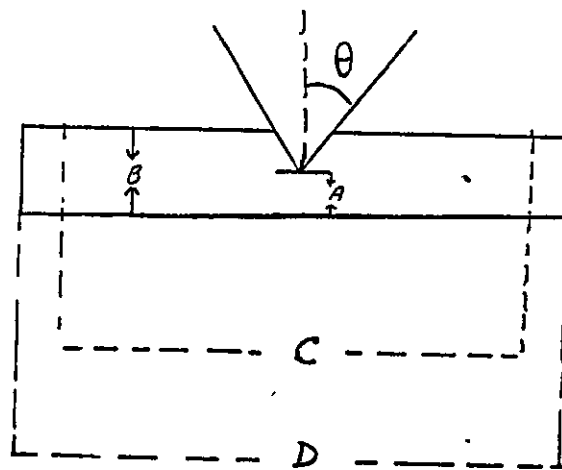


FIGURE 16

$$A = 3.5 \text{ mm}$$

$$B = 6.0 \text{ mm}$$

$$C = 34.0 \text{ mm}$$

$$D = 44.0 \text{ mm}$$

$$T = 3.0 \text{ mm}$$

$$\theta = 22.0 \text{ mm}$$

CHAPTER 4

EXPERIMENTAL RESULTS4.1 Physical Properties

In this section results of physical properties studied on powder blends from both M-PVC and S-PVC are reported. These physical parameters would help in understanding the behaviour of the materials.

4.1.1 Particle Size Distribution

Particle size distribution for both M-PVC and S-PVC powder blends was carried out using "ZEISS TG23" particle analyser as described in sec. 3.4.1. Particles are plotted against % occurrence of particles; results are shown in Fig. 17.

M-PVC has a narrower distribution of particle size which results in higher bulk and apparent densities, better absorption of additives.

4.1.2 Density of Powder Blends

Bulk and apparent densities of both M-PVC and S-PVC powder blends as prepared in sec. 3.2 were measured by usual methods explained in sec. 3.4.2. The values of these parameters are listed in the table 9.

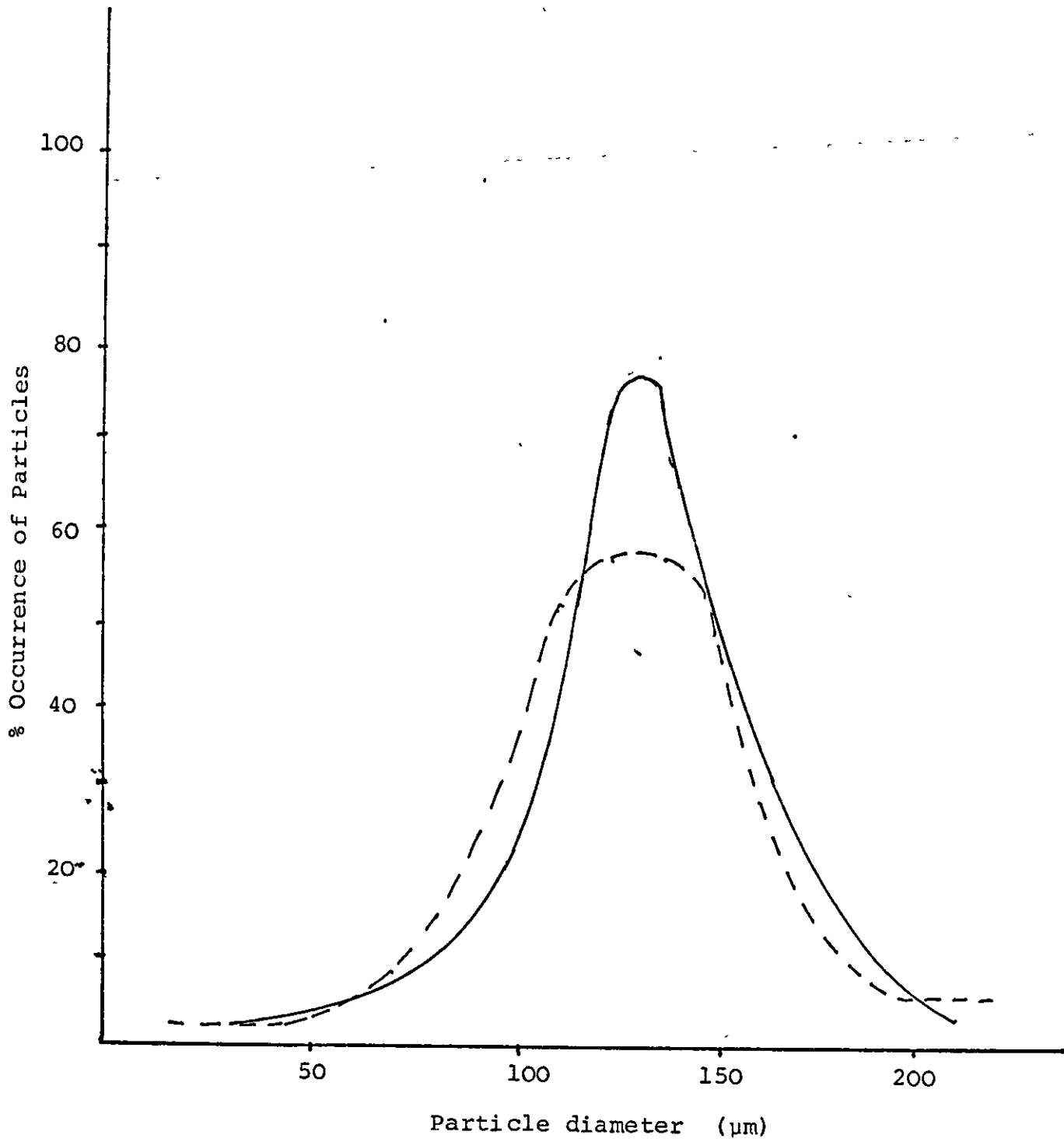


FIGURE 17 Particle size distribution (—) = M-PVC
(---) = S-PVC

TABLE 9

Bulk and apparent densities for M-PVC and S-PVC

Type of Blend	Bulk Density Kg/m ³	Apparent Density Kg/m ³	Flow Rate kg/sec
M-PVC powder blend	760	690	82
S-PVC powder blend	685	620	105

Bulk and apparent densities of M-PVC are higher than that of S-PVC. This can be attributed to the known morphological difference between two resins. M-PVC resin particles have no skin or membrane around them, therefore, the additives are absorbed more uniformly as compared to the S-PVC particles which are covered with a skin. Moreover narrow particle size distribution and regularity in shape also help M-PVC resin to absorb additives more uniformly.

4.2 Thermal Properties

4.2.1 Differential Thermal Analysis (DTA)

Thermograms of moulded sheets annealed and quenched samples were recorded using the Du Pont 900 thermal analyser fitted with a 'DSC' cell. The general construction and principle of the analyser and the cell have already been described in Section 3.5.2. The thermograms were recorded from -40°C to 200°C and in some cases up to 220°C , using a heating rate of $20^{\circ}\text{C}/\text{minute}$ and a sample weight of $10 \pm 1 \text{ mg}$. An empty aluminium sample pan was used as the inert reference.

The areas of peaks observed in the thermograms were traced and weighed on a four figure balance. Weights in milligrams were converted into areas in cm^2 by comparing the weight of a piece from the same paper of the known area. To obtain values of these areas in energy units, the cell was calibrated using Indium, melting point 157°C , heat of fusion 28.4 kJ/kg .

Calculation for Heat of Fusion, ΔH_f

$$A = KW \Delta H_f$$

$$A = \text{Area of the peak}$$

$$W = \text{Weight of the sample}$$

$$K = \text{A constant}$$

$$\Delta H_f = \text{Heat of fusion}$$

Area of the peak and weight of the sample are known from the thermogram, ΔH_f , heat of fusion is to be found and the only unknown left is the constant "K".

Calculation for the constant "K"

ΔH_f , heat of fusion for indium is known, therefore value of "K" the constant is found from the above equation.

The "K" value is used in determining heat of fusion, ΔH_f , for all other samples:

$$\Delta H_f = \frac{A}{W} \times \frac{1}{K}$$

Five determinations were carried out to obtain the value of "K" and the standard deviation was found to be 5% of the mean.

The thermograms obtained for PVC powder-blend and moulded sheets at temperatures from 160°C to 220°C are shown in figure 19 for M-PVC. In the case of the powder-blend sample, the thermogram consists of three transitions. The first transition at approximately 56°C is due to non-uniform distribution of liquid tin stabiliser. The uptake of tin stabiliser depends on the particle size and size distribution of resin particles. During blending operations, some particles absorb tin stabilisers more quickly than the others, which results into a glass transition at a

lower temperature in the thermogram of the powder-blend. This transition is absent in the moulded sheets from the same blends. Thus it is reasonable to assume that all the resin particles have a uniform absorption of tin stabiliser during moulding at 160°C and higher temperatures.

The second base-line shift at 78°C is assigned to the glass transition temperature, T_g . The last transition is in the form of a deep and broad endotherm starting at 155°C extending to 200°C . This transition is designated by a letter "A" (see figure 19).

aging → Thermograms for moulded sheets have also three transitions, except 160° moulded sheet which has only two. The transition observed in powder-blend samples at 56°C is absent, whereas the remaining two transitions (T_g and A) are common in the thermograms of all other samples. However " T_g " has been shifted to 74°C : transition "A" decreases in magnitude and occurs at a higher temperature as the moulding temperature increases. In thermograms of samples moulded at 170°C and above, a new transition is observed which starts at 104 to 112°C and extends to 200 to 212°C . This transition is designated by a letter "B" and the magnitude of the transition increases with the increase in moulding temperature (see figure 19). The values in energy units for both these transitions, A and B, are listed in Table 10.

The enthalpy changes in the transitions A and B, are plotted against moulding temperature in figures 20 and 21, respectively.

Figure 22 shows the thermograms P and Q of 160°C moulded M-PVC. Thermogram P is the initial run, whereas Q is the rerun. The thermogram Q was obtained when the sample was taken to 200°C in D.T.A. and then cooled slowly to -40°C.

The thermogram Q shows an endothermic effect which starts at 110°C and extends to 206°C. This thermogram is very similar to the one obtained for 210°C moulded sample.

The thermograms obtained for S-PVC moulded samples and blended powder are similar to that of M-PVC, however, the glass transition, T_g , was higher and transition "B" was absent up to 170°C moulding. The thermograms are shown in figure 23. The values in energy units for these transitions are listed in table 11.

Figure 24 shows the thermogram for a quenched sample. The thermogram consists of a base line shift at 72°C which is assigned to glass transition, T_g . Soon after the glass transition an exothermic peak is obtained at 88°C which is followed by a broad endothermic peak starting at 98°C and extending to 200°C. All the transitions merge into one another. The glass transition is lower than that in the

unquenched samples. Values obtained for exo- and endothermic changes are given in Table 12.

With the heat treated samples, sharper endothermic changes are observed and appear at approximately 20°C above the annealing temperature. The transition is designated by a letter "C" (see figure 25). The starting temperatures of this transition for M-PVC and S-PVC are given in Table 13 and the influence of annealing time on melting temperature is shown in Figure 26.

In all thermograms of heat treated samples, a portion of the broad endotherm "B" observed in its original thermogram is still present. This portion of the thermogram will be called the transition "B'", (see figure 25). The values in energy units for the transitions C and B' are listed in Table 15.

The change in enthalpy with annealing temperature for transitions C and B' is plotted in figure 27. The heat of fusion for transition C passes through a maxima while for transition "B'" passes through a minima at 110°C annealing temperature. Figure 28 shows the plot of the ratio of two transitions against the annealing temperature.

The effect of annealing time on the magnitude of annealing effect for transitions C and B' is shown in figures 29 and 30 respectively, and the values in energy units are listed in Table 16.

From the above table it is noted that magnitude of annealing effect increases in transition "C" whereas decreases in transition "B'" as the annealing is prolonged. It is also noted that the magnitude of annealing effect on both transitions C and B' is maximum at 110°C annealing temperature.

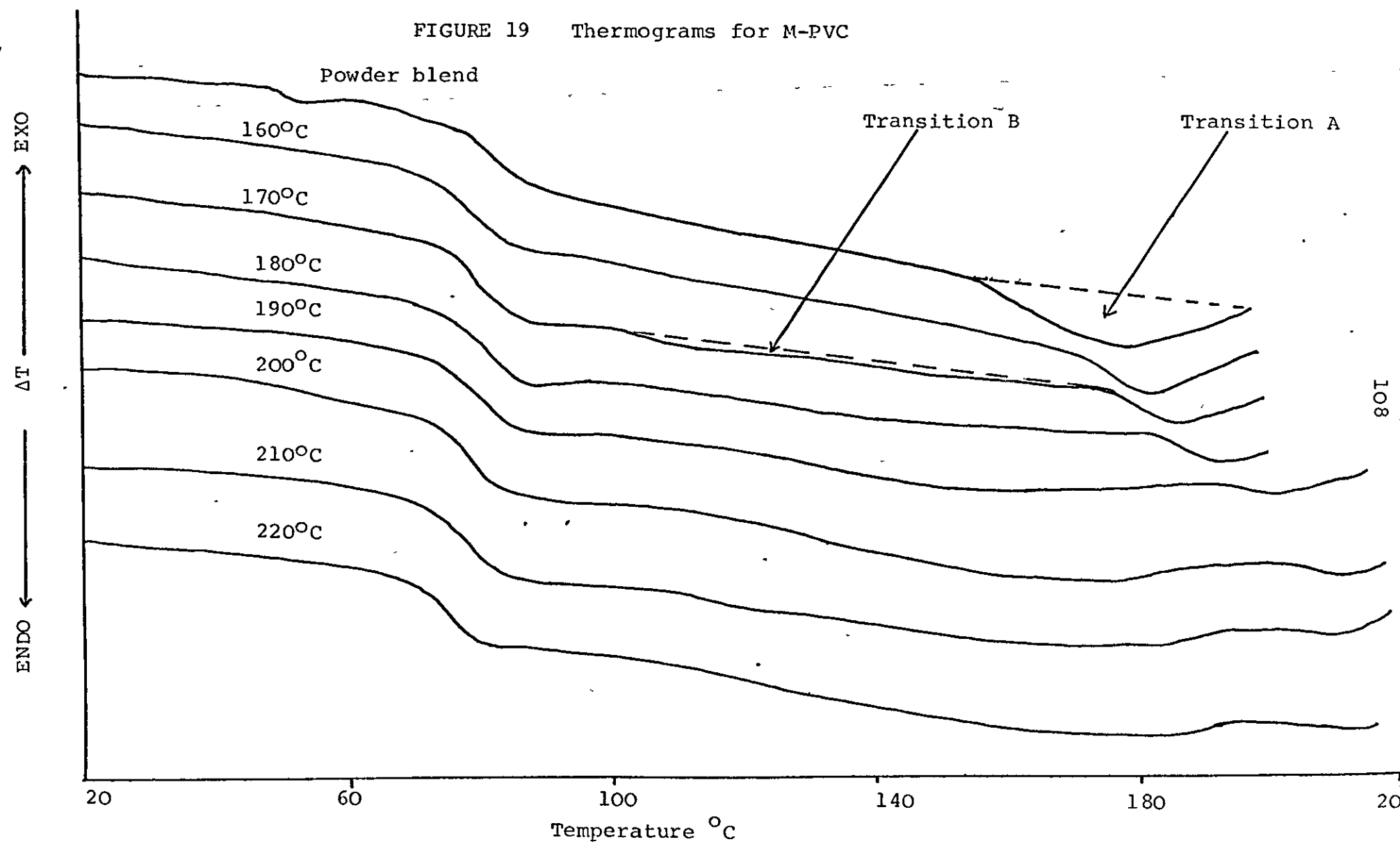
In order to see the effect of cooling rate on the structure of PVC, thermograms from samples cooled at different rates were also obtained. Figure 31 shows the thermograms R and S obtained from S-PVC annealed at 110°C, but cooled at different rates. Thermogram 'R' obtained from the sample cooled in air to ambient temperature and thermogram 'S' from the sample quenched in ice/water mixture after being annealed. D.T.A. could not detect any difference between the two samples.

Figure 32 shows the thermograms T and U obtained from 200°C moulded M-PVC sheet cooled at different rates as described in Section 3.5.1. Again there was no significant difference in their thermograms.

4.2.2 Thermomechanical Analysis

The glass transition temperatures of the moulded samples were measured using Du Pont thermal analyser equipped with a thermomechanical analyser attachment. The glass transition temperature does not change with moulding temperature for both polymers. T_g recorded for M-PVC is 74°C and that of S-PVC 75°C.

FIGURE 19 Thermograms for M-PVC



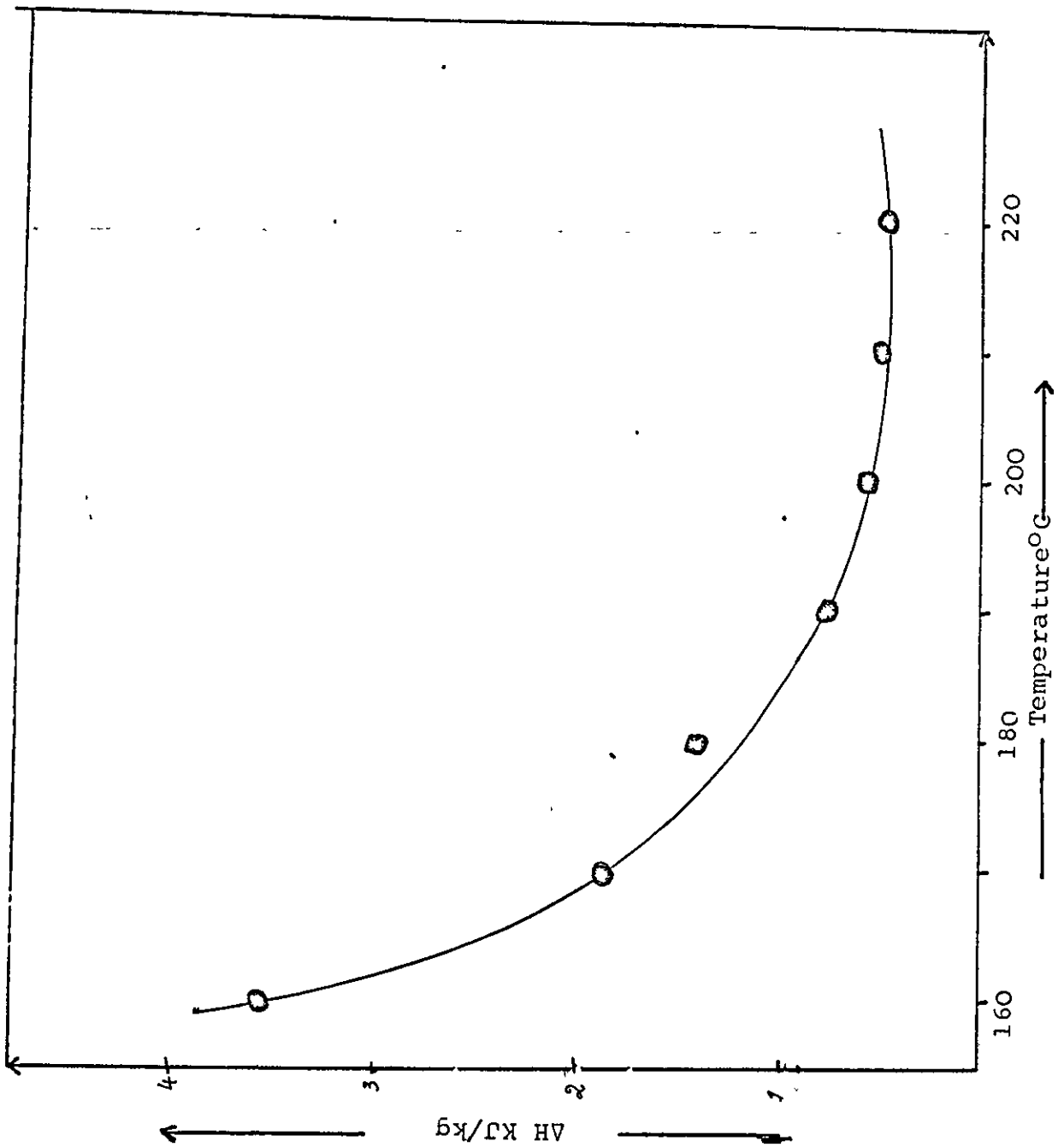


FIGURE 20 Enthalpy change in transition "A" vs
moulding temperature for M-PVC

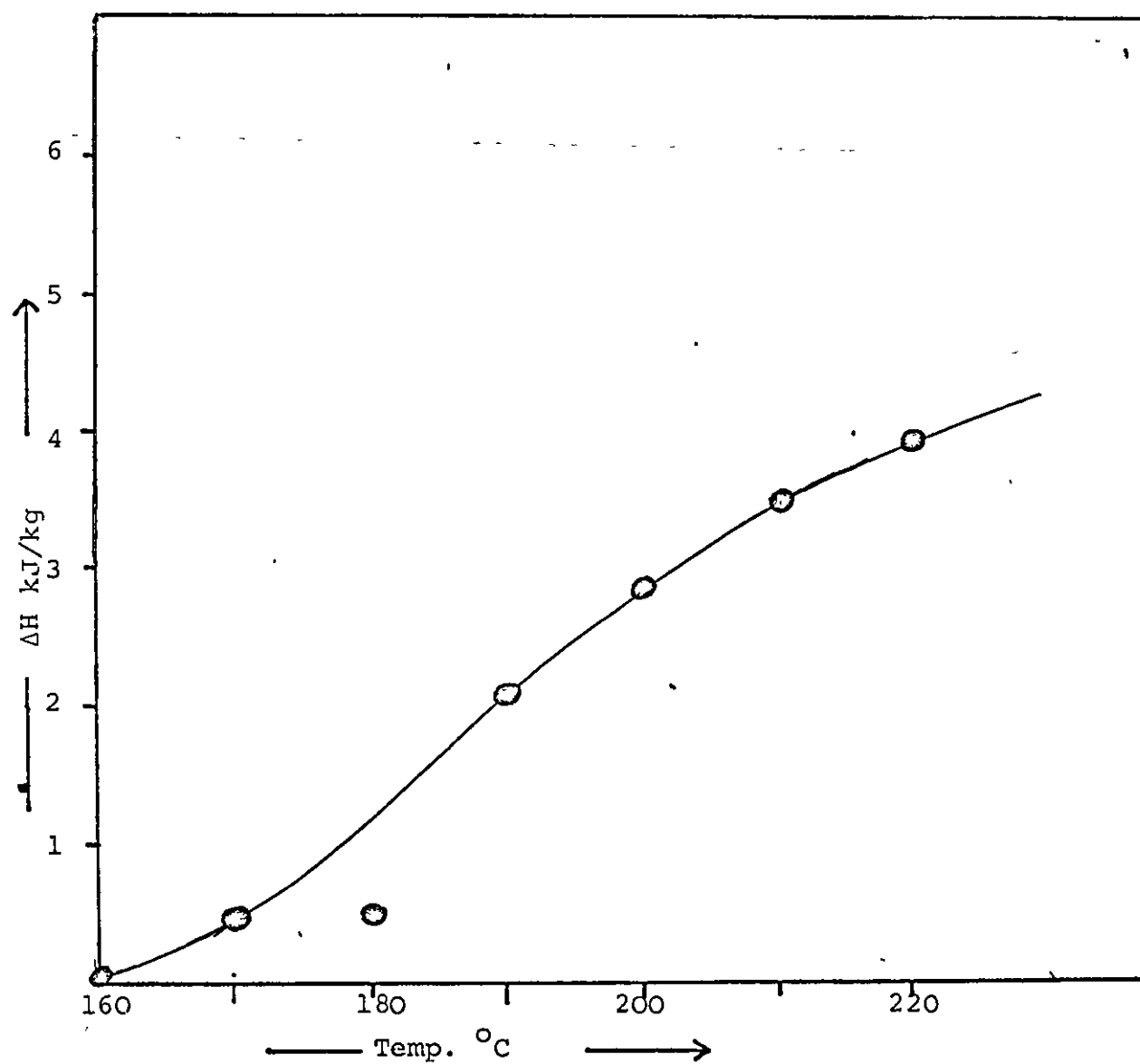


FIGURE 21 Enthalpy change in transition "B" vs
moulding temperature for M-PVC

FIGURE 22 Thermograms for M-PVC (-) 1st run (---) 2nd run

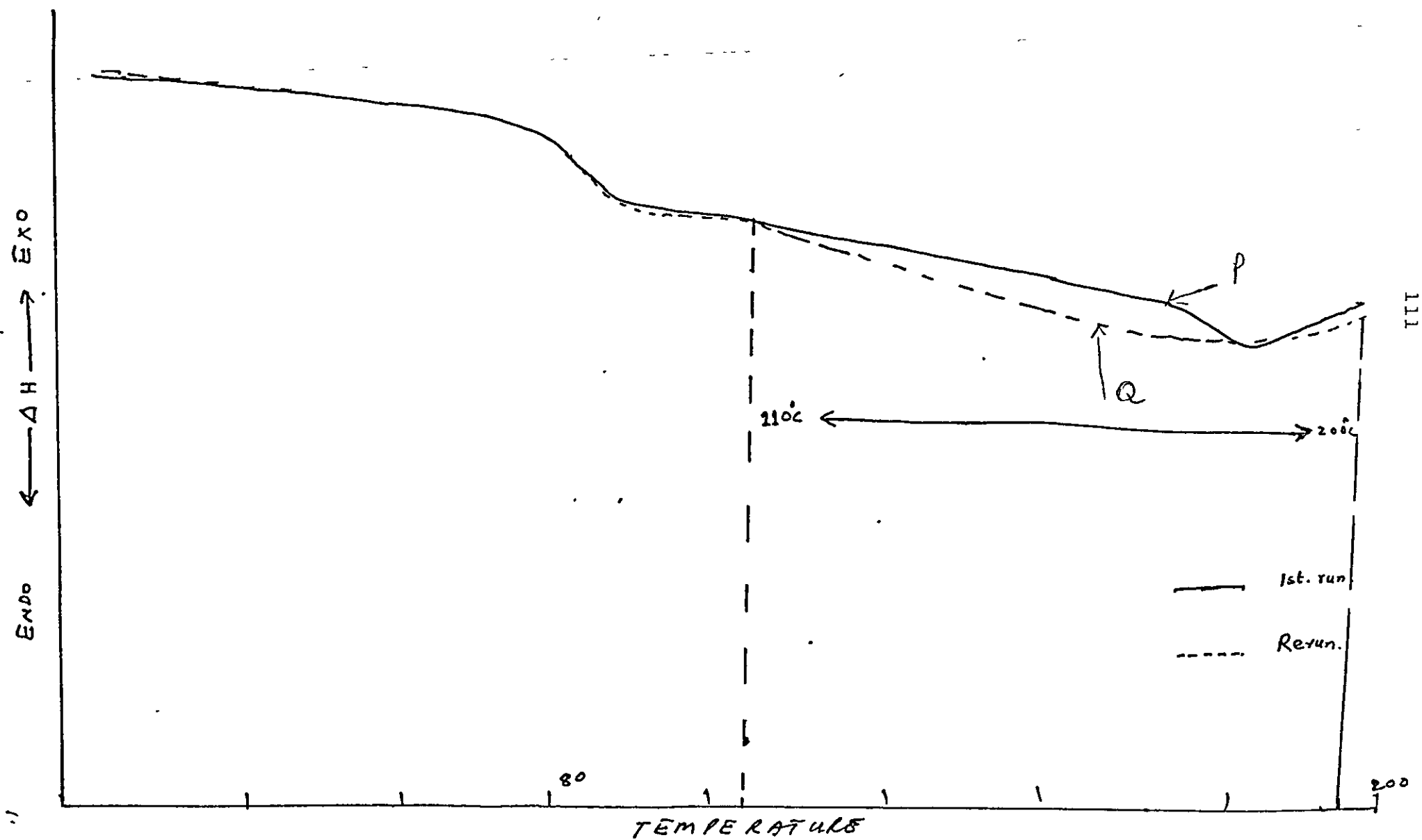


FIGURE 23 Thermograms for S-PVC

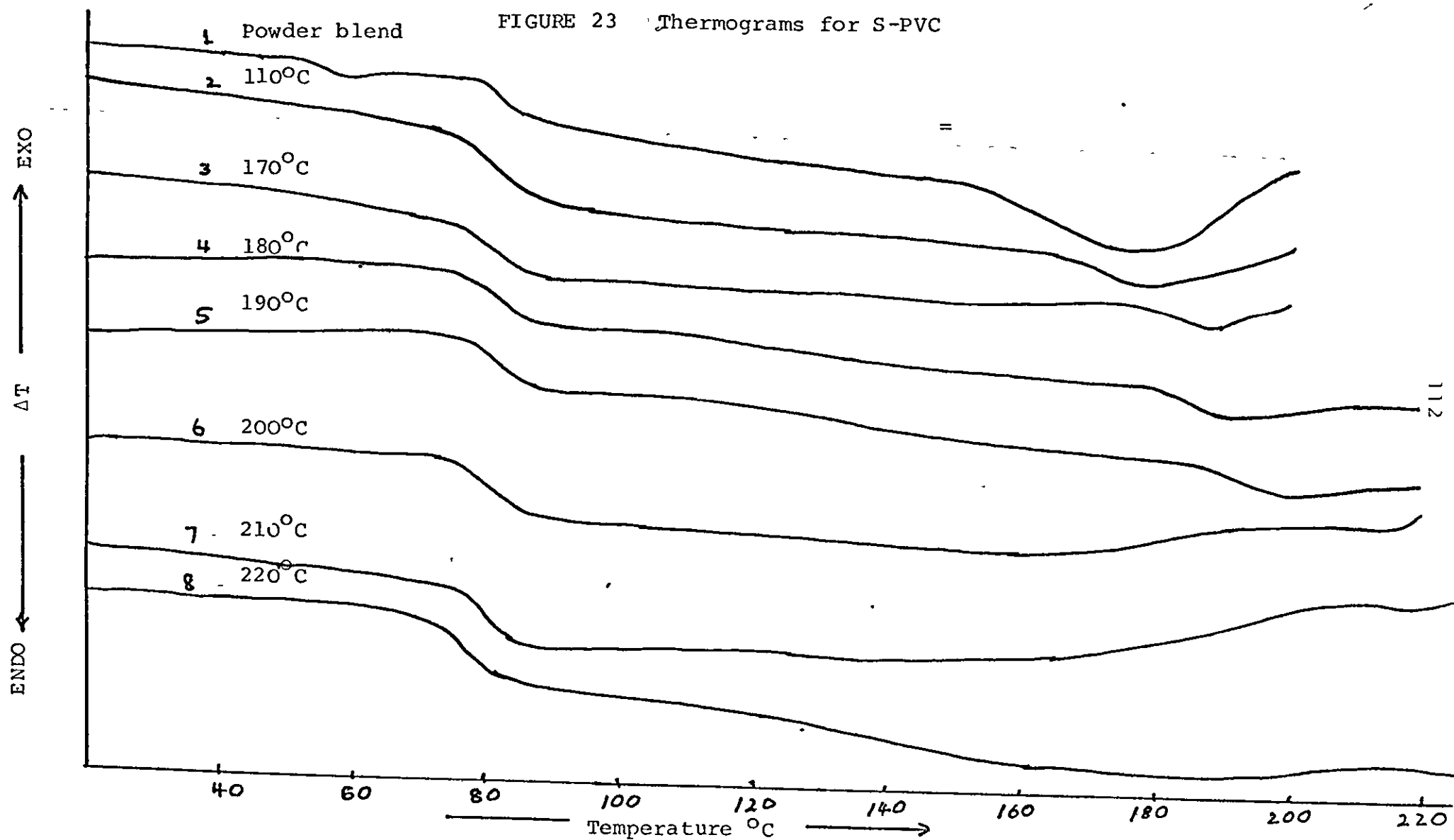
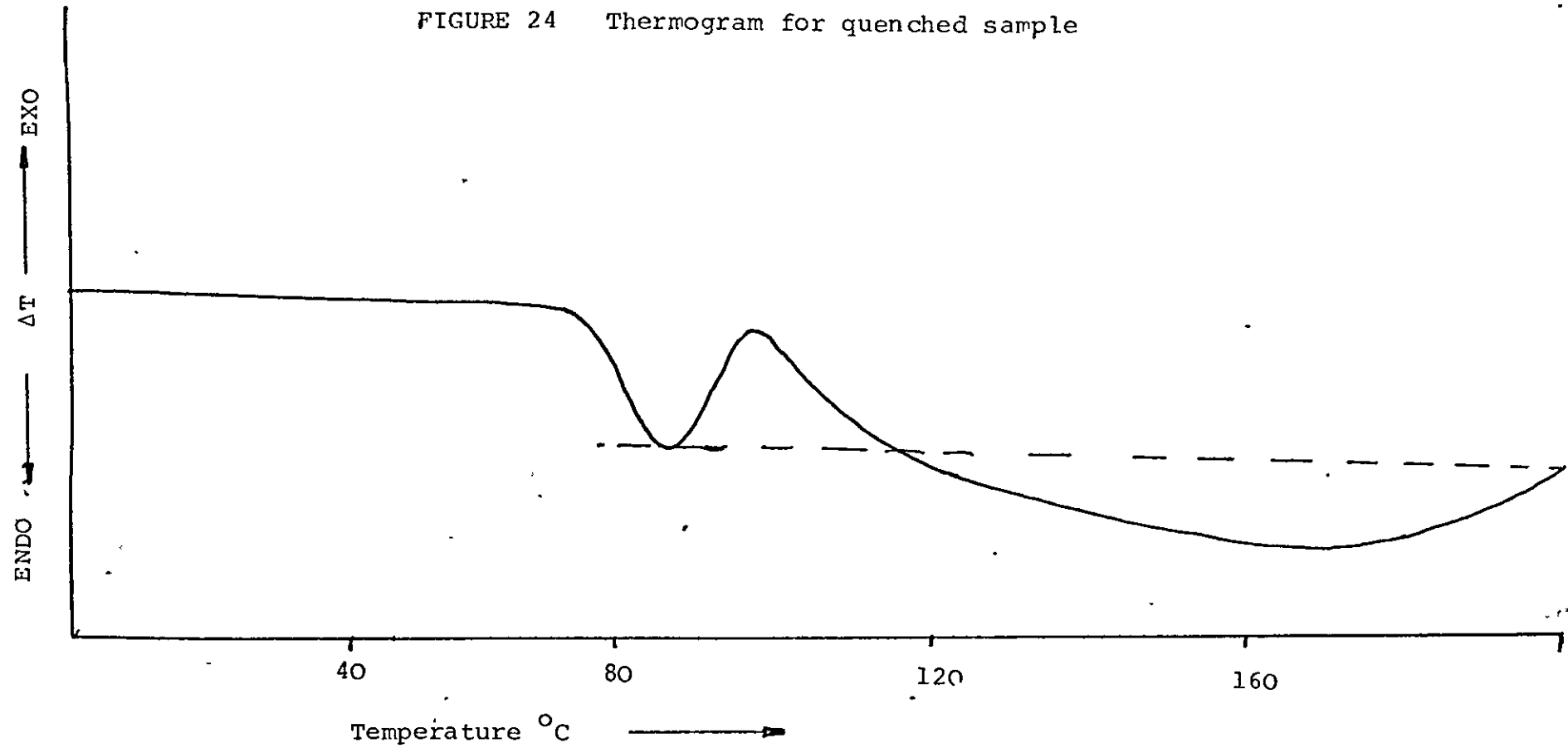


FIGURE 24 Thermogram for quenched sample



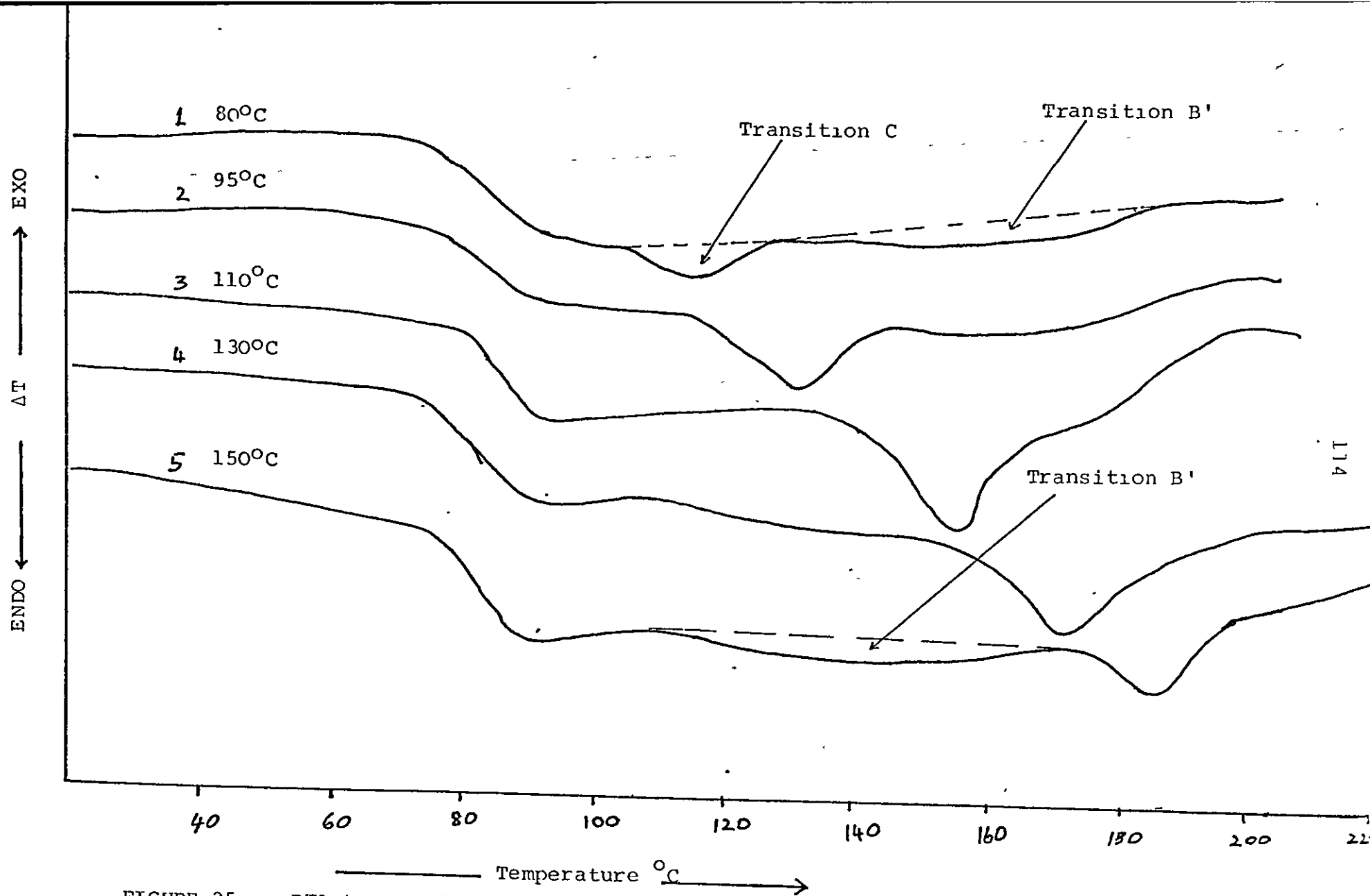


FIGURE 25 DTA traces for M-PVC annealed for 5 hours

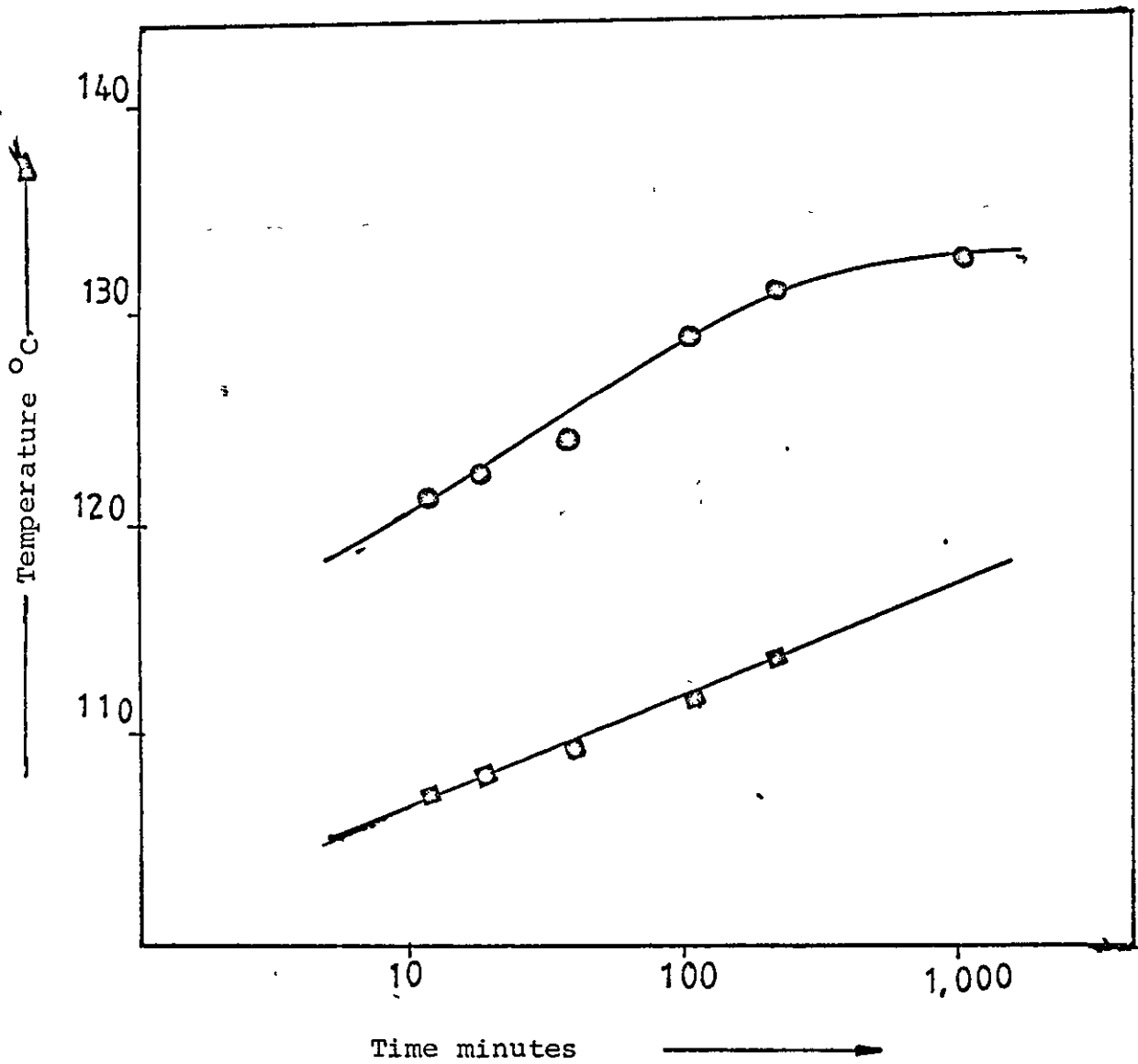


FIGURE 26 Annealing time vs melting temperature

- = M-PVC moulded at 110 °C.
- = M-PVC " " 95 °C.

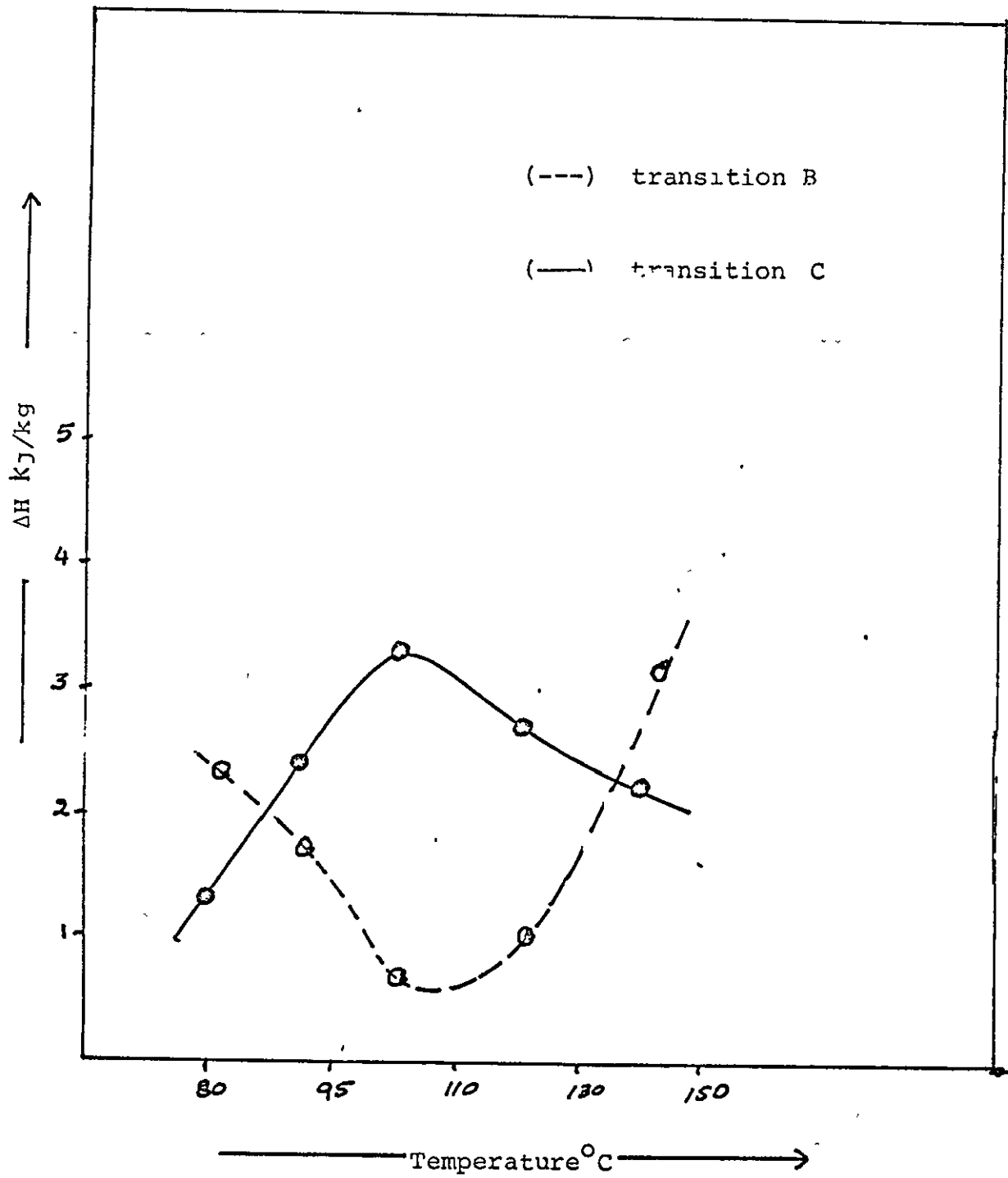


FIGURE 27 Enthalpy change in transitions B and C for M-PVC as a function of annealing temperature

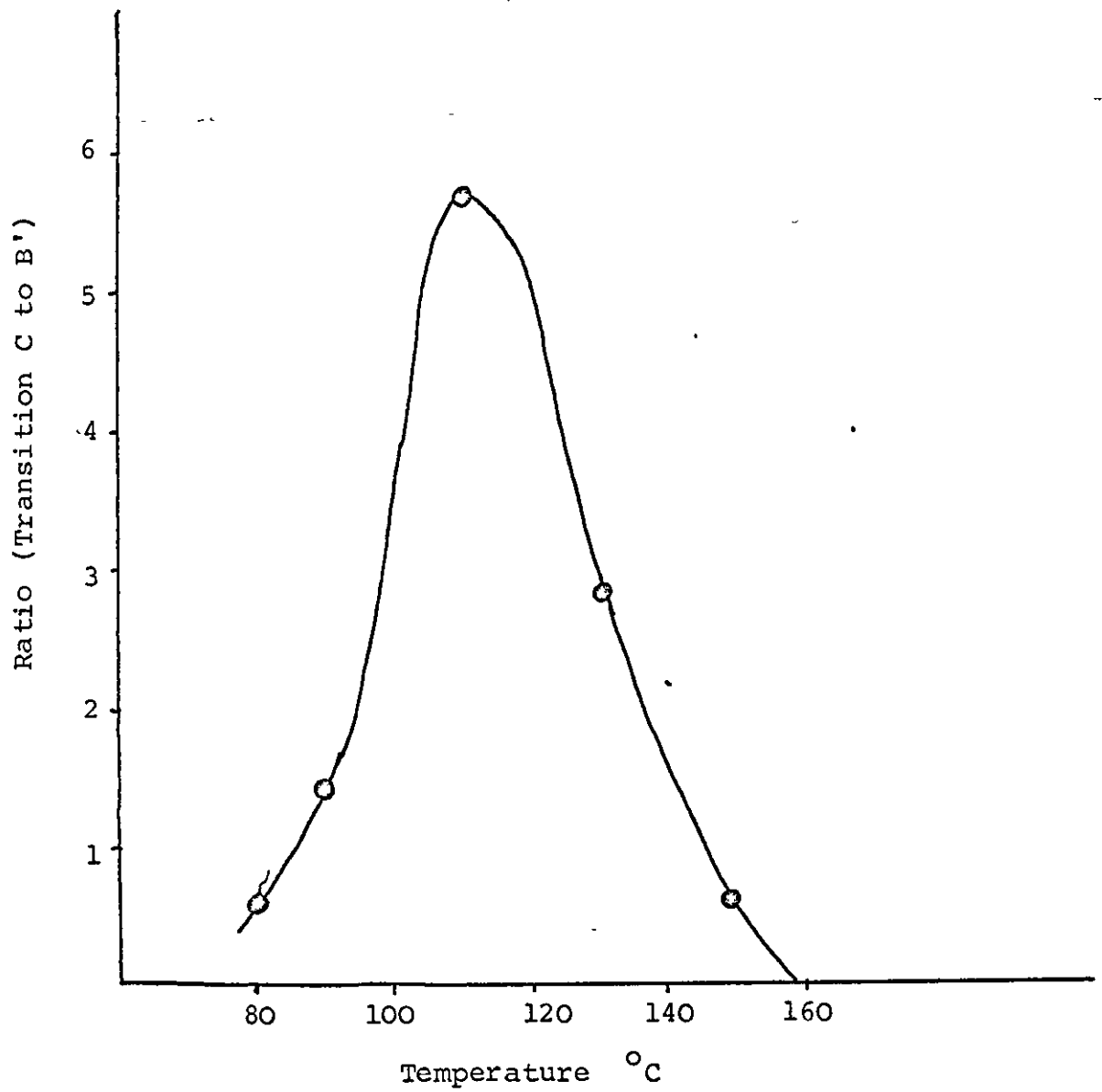


FIGURE 28 Annealing temperature vs ratio of transition C to B

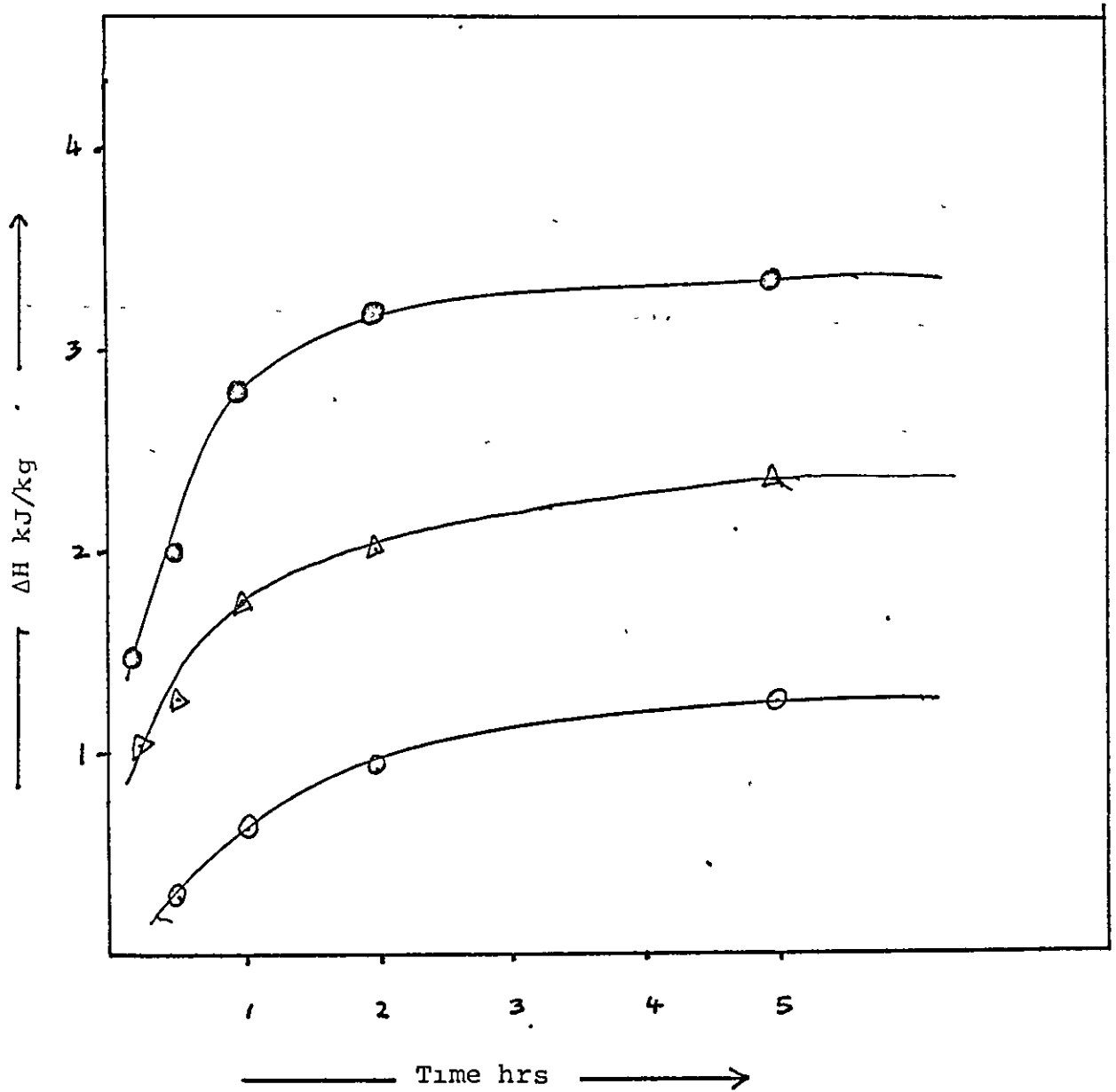


FIGURE 29 Enthalpy change in transition C as a function of annealing time.

● - 110°C

Δ - 95°C

○ - 80°C

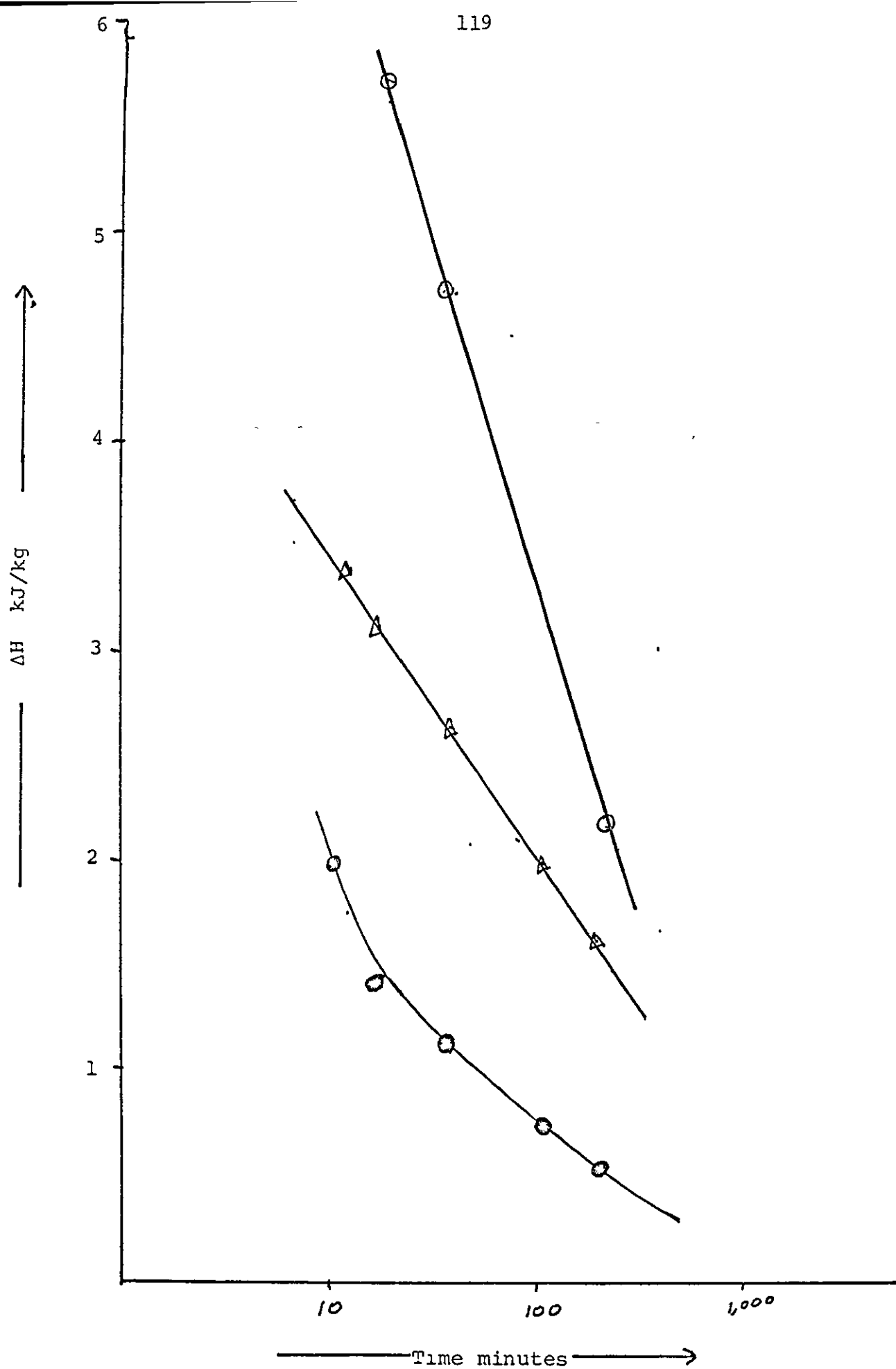


FIGURE 30 Enthalpy change in transition B as a function of annealing time: O = 80°C
 Δ = 95°C
 ● = 110°C

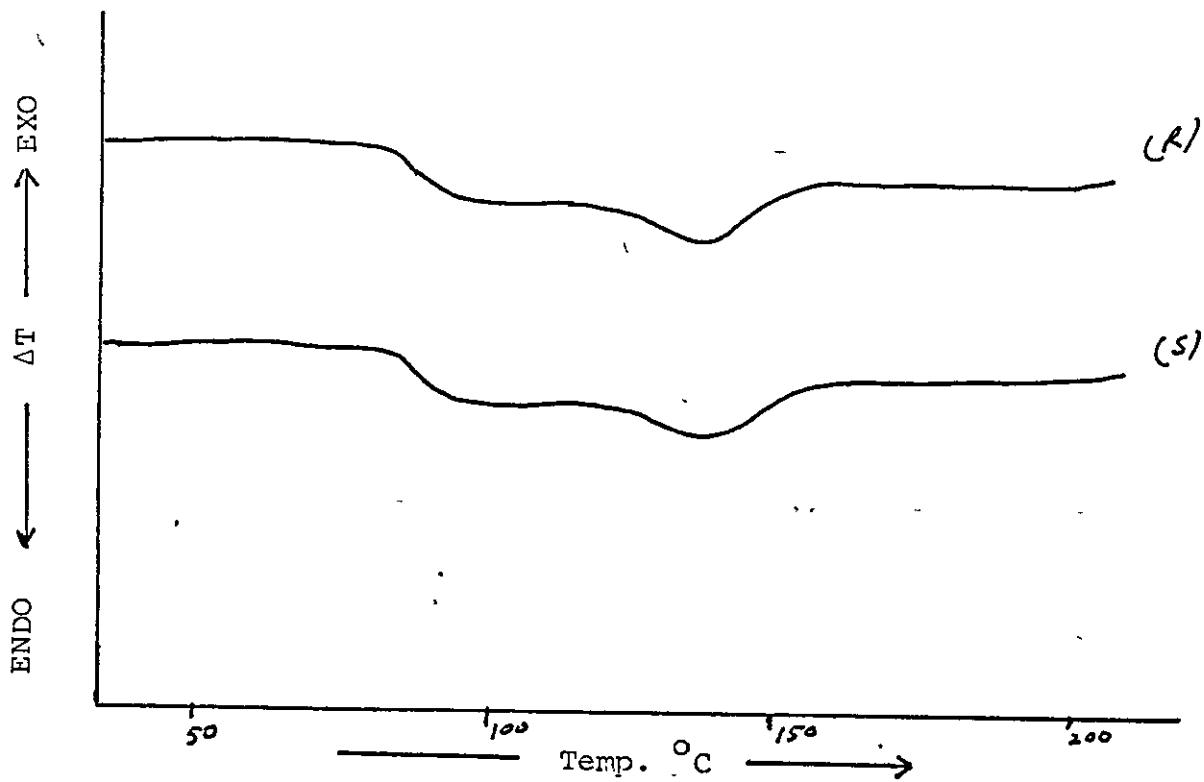


FIGURE 31 M-PVC annealed at 110°C
(R) cooled in air (S) fast cooled

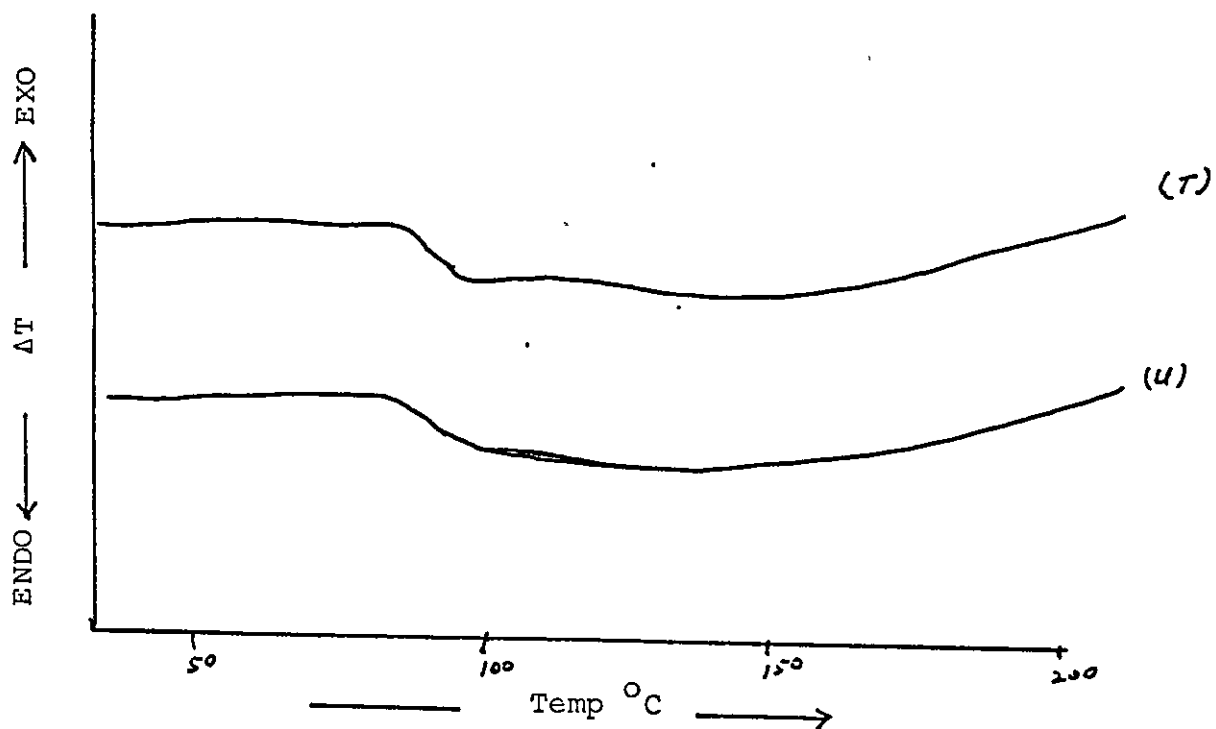


FIGURE 32 M-PVC samples cooled at different rates in the mould.
(T) Ordinary water (U) Ice water

TABLE 10

M-PVC

Type of Sample	T _g °C	Melting temperature °C	Melting area ΔH_f kJ/kg "A"	Melting area ΔH_f kJ/kg "B"
Powder-blend	56,78	155°C	4.02	-
160°C	74	170.5	3.73	-
170°C	74	175	1.98	3.58
180°C	74	182	1.48	3.86
190°C	74	192	0.78	7.11
200°C	74	206	0.62	8.68
210°C	74	206	0.50	9.93
220°C	74	206	0.50	10.76

A+B

4.02

3.73

5.56

5.54

7.89

9.30

10.43

11.26

TABLE 11

S-PVC

Type of Sample	Tg °C	Melting temperature °C	Melting area ΔH_f kJ/kg "A"	Melting area ΔH_f kJ/kg "B"
Powder blend	56,79	153	4.00	-
160°C	75	166	3.50	-
170°C	75	177	1.94	-
180°C	75	182	1.82	2.59
190°C	75	186	1.77	2.59
200°C	75	206	0.53	9.52
210°C	75	212	0.46	13.99
220°C	75	212	0.47	13.40

A+B

4.00

3.5

1.94

4.41

4.36

10.05

14.45

13.97

Table 12Enthalpy Change Values for Quenched Samples

Type of Sample	Tg. °C	Exothermic Peak kJ/kg	Endothermic Peak kJ/kg
M-PVC	72	5.26	8.26
S-PVC	72	5.80	8.58

Table 13Effect of Annealing Time on the Starting Temperature of Transition "C" in M-PVC

Annealing Time	Annealing Temperature °C	80	95	110	130	150
15'	Starting Temperature	-	107°C	121°C	-	-
30'	of transition	98°C	108°C	122°C	-	-
60'	"C"	96°C	109°C	124°C	-	-
120'	"C"	96°C	111°C	128°C	-	-
300'	"C"	96°C	113°C	132°C	149°C	170°C
1000'	"C"	-	-	132°C	-	-

Table 14

Effect of Annealing Time on the Starting Temperature of Transition "C" in S-PVC

Annealing in time minutes	Annealing Temperature °C	80°C	95°C	110°C	130°C	150°C
15	Starting Temperature	-	108°C	122°C		
30	"	96°C	108°C	122°C		
60	"	96°C	109°C	124°C		
120	"	96°C	111°C	129°C		
300	"	97°C	114°C	134°C	149°C	171°C

Table 15

Effect of Annealing Temperature on the Magnitude of Annealing Effect for M-PVC Annealed for 5 Hours

Annealing Temperature °C	ΔH_f kJ/kg Transition "C"	ΔH_f kJ/kg Transition "B"	Ratio C:B'
80	1.26	2.18	0.578
95	2.36	1.66	1.421
110	3.32	0.58	5.724
130	2.62	0.92	2.840
150	2.22	3.24	0.685

TABLE 16

Effect of Annealing Time on the Magnitude of Annealing Effect for M-PVC on Transitions C and B'

<div>Annealing time in minutes</div> <div>Annealing Temperature</div>	80°C		95°C		110°C	
	ΔH_f	kJ/kg	ΔH_f	kJ/kg	ΔH_f	kJ/kg
	C	D	C	D	C	D
15	-	-	1.04	3.41	1.45	2.20
30	0.29	5.63	1.20	3.11	2.00	1.40
60	0.63	4.74	1.81	2.65	2.80	1.10
120	0.86	4.91	1.91	2.02	3.15	0.70
300	1.26	2.18	2.36	1.66	3.32	0.58

4.3 X-Ray Diffraction

X-ray diffraction patterns for both M-PVC and S-PVC, moulded and annealed samples were obtained on Jeol DX-GE-25 diffractometer. The operating conditions have been described in Section 3.6

Percentage crystallinity was calculated for all the samples by using the following formula over a limited 2θ range 12° - 36° .

$$\% \text{ Crystallinity} = \frac{X_c}{X_c + X_a} \times 100$$

where:

X_c = area of the crystalline portion

X_a = area of the biomodeal amorphous background.

To obtain the diffraction trace for amorphous PVC, several attempts were made to convert the polymer into amorphous state by quenching from high temperatures to different cooling systems. The temperature, time and cooling system used for quenching are given in Table 17.

TABLE 17

Polymer	Temperature °C	Time in Minutes
M-PVC	190	10'
	200	5'
	205	5'
	210	5'
	220	3'

The following three cooling systems were used:

- i) Liquid nitrogen.
- ii) Solid CO₂/methanol.
- iii) Ice/water.

These conditions were chosen following studies of thermal stability of the materials and the literature review of the melting of PVC. The intention was to use the highest temperature possible in an attempt to remove existing order whilst keeping degradation to a minimum. A successful amorphous trace was obtained from M-PVC quenched from 210°C into an ice/water mixture. The amorphous trace obtained (see figure 34) is similar to that used by other workers (39,41,47).

Templates were made from the amorphous trace by reducing the intensity axis. The points were selected on the original trace at each $\frac{1}{2}^{\circ} 2\theta$. The values of these points in arbitrary units of intensity on Y-axis were reduced to nine-tenths, eight-tenths, ... one-tenth of their original values and plotted against 2θ . In this way ten templates (see figure 34) were obtained as in reference 100.

In order to calculate percentage crystallinity, the appropriate amorphous trace was fitted to the experimental curve such that its trough touched the experimental curve at points A, B and C as shown in figure 35. In this way crystalline portions were separated from amorphous regions. The straight line AC indicates the background level. Areas for both amorphous and crystalline portions above base line AC were measured by planimeter and % crystallinity was calculated using the above equation. Five determinations were made for each diffraction trace and the mean value has been reported.

The values of calculated crystallinity for M-PVC and S-PVC moulded samples are listed in Tables 18 and 19 respectively. From the Tables it is noted that the value of crystallinity decreases as the moulding temperature is raised. The sample moulded at the highest temperature has the lowest value of crystallinity. This has

been shown by plotting a graph in between percentage crystallinity and the moulding temperature (see figure 36).

Figures 37 and 38 show the typical X-ray diffraction traces for M-PVC and S-PVC moulded samples at temperatures of 160°C and 220°C. Crystalline peaks were observed at 16° 2θ from lattice planes (010) and (200), 18° 2θ from (110), 24-26° 2θ from (210), (210) and (111), 41° 2θ from (220) and (410) and a less pronounced peak at 31° 2θ from lattice planes (310). The assignment of the lattice spacings, is according to the literature⁽⁴¹⁾.

The reflection from (110) at 18° 2θ was quite sharp in the X-ray diffraction traces for samples moulded at low temperature and it continued to decrease with other reflections as the moulding temperature was increased. In the X-ray trace for 220°C, moulded sample, all reflections are reduced in size as compared to the reflections in that of 160°C moulded sample.

X-ray diffraction traces for heat treated samples were also obtained using the same technique. Samples from both M-PVC and S-PVC annealed for 5 hours at various temperatures, have been analysed. The percentage

crystallinity has been calculated in the similar way as that for moulded samples. The values are listed in Tables 20 and 21 for M-PVC and S-PVC respectively.

From the table it is noted that the annealing causes increase in the amount of crystallinity and is maximum at 110°C annealing temperature.

Typical X-ray traces for heat treated samples are shown in Figures 39 and 40 for M-PVC and S-PVC respectively. A close examination of the traces reveals that the reflection from all planes are sharper for heat treated samples and the peak height is maximum at an annealing temperature of 110°C .

In Figures 41 and 42 percentage crystallinity values for heat treated samples are plotted against the annealing temperature. The value of crystallinity passes through a maxima at 110°C .

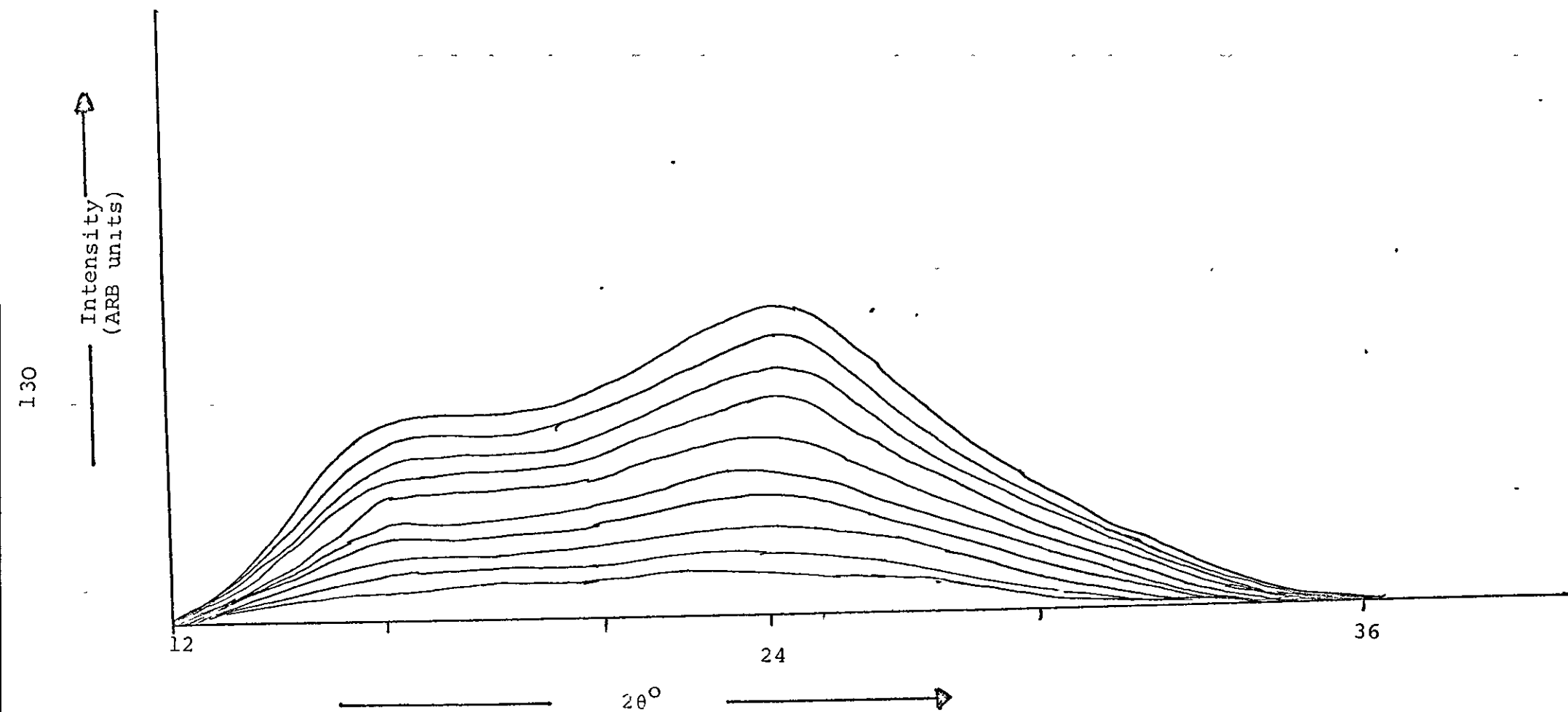


FIGURE 34 Templates made from amorphous trace

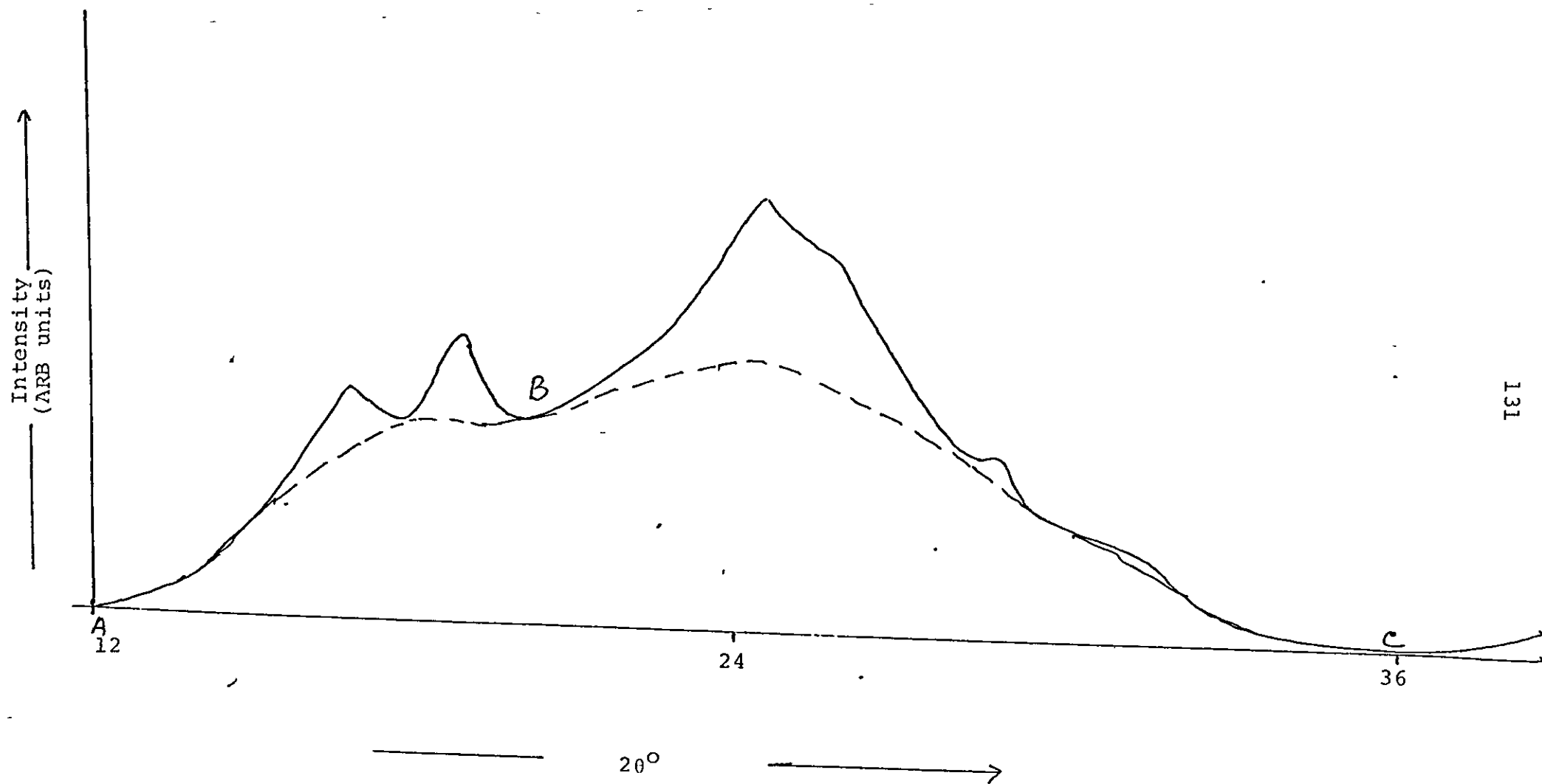


FIGURE 35

Amorphous trace fitting

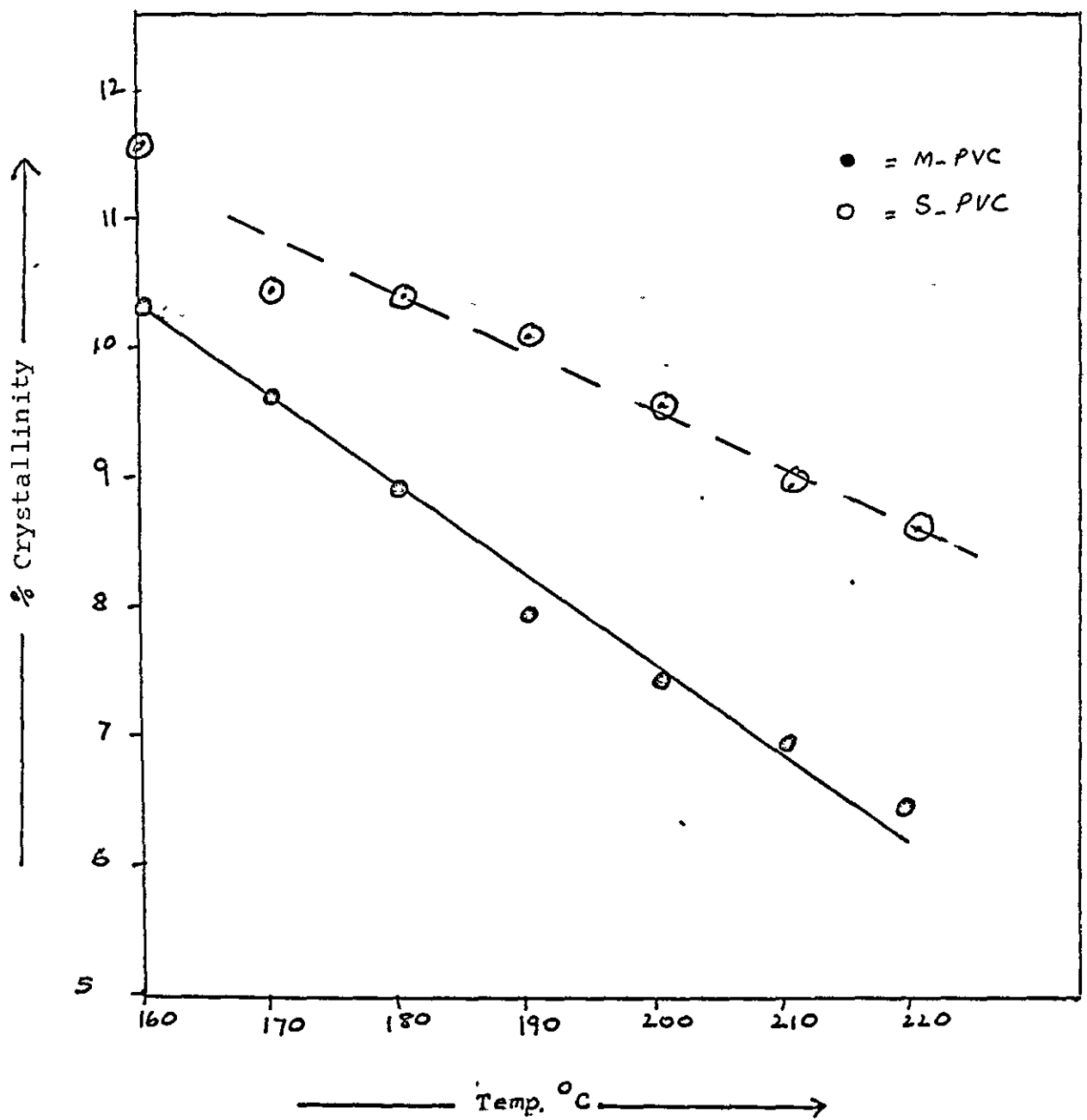


FIGURE 36 Percentage crystallinity as a function of moulding temperature

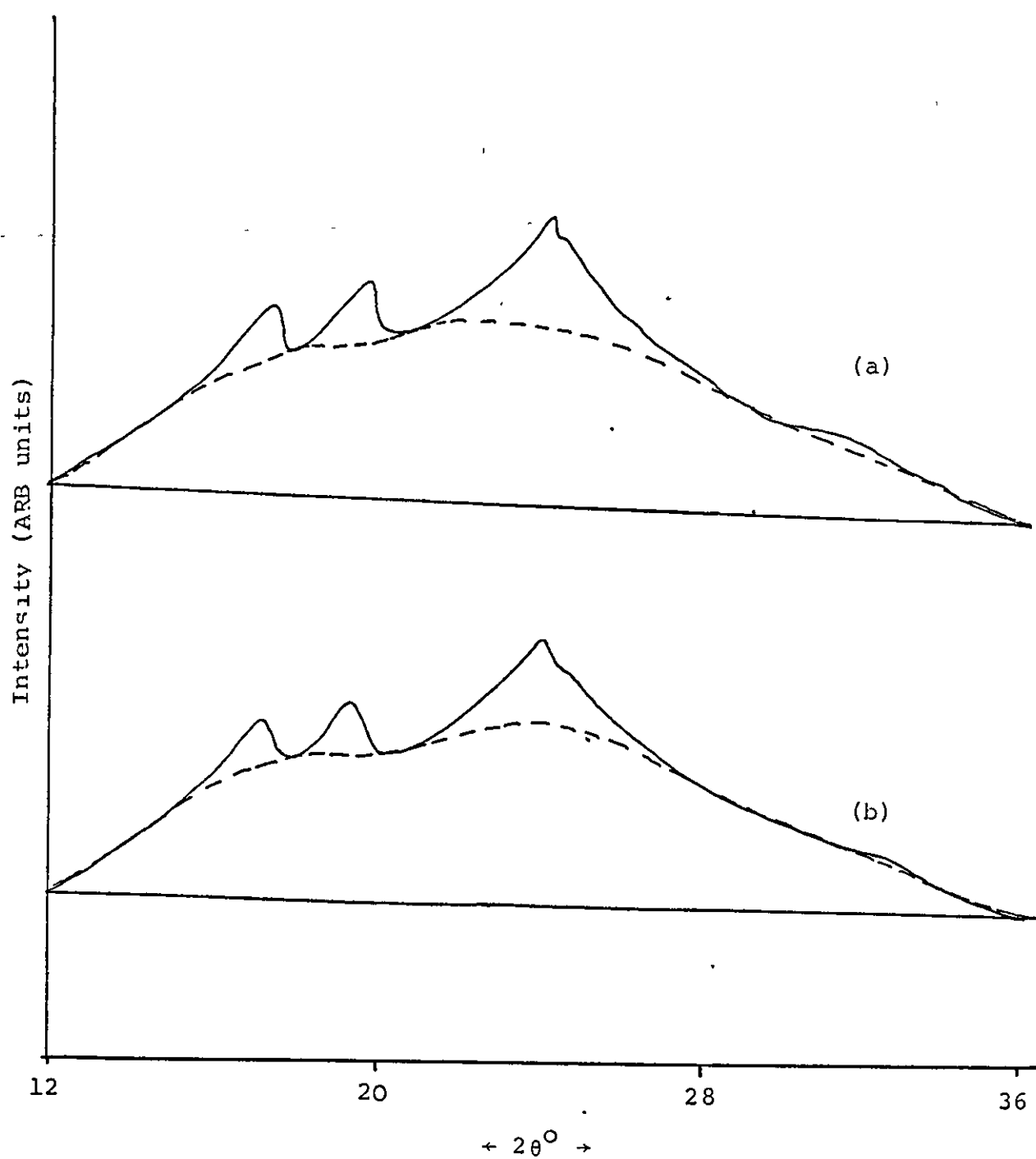


FIGURE 37 X-ray diffraction pattern for M-PVC moulded at
a) 160°C and b) 220°C

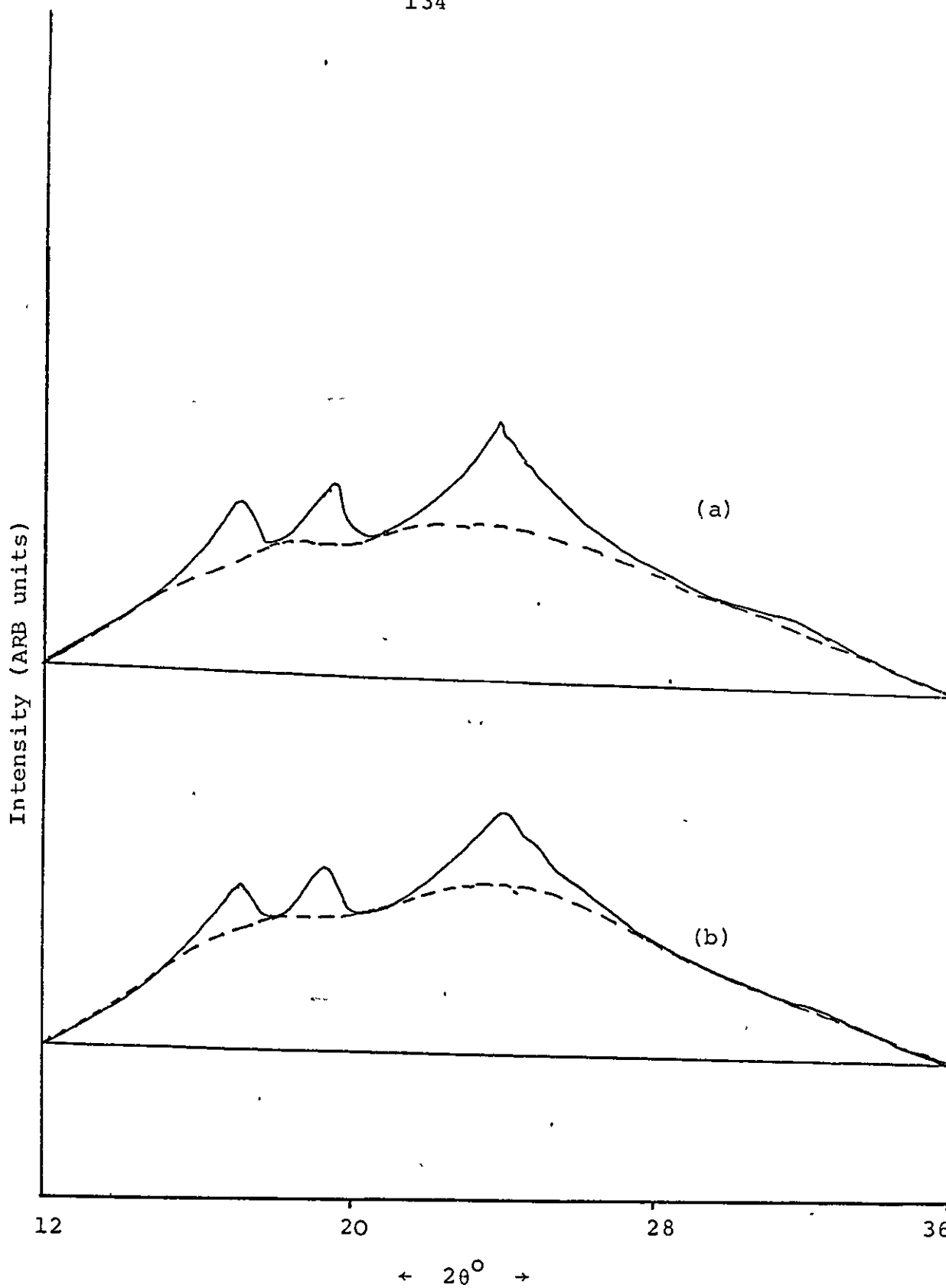


FIGURE 38 X-ray diffraction patterns for S-PVC annealed at (a) 160°C (b) 220°C

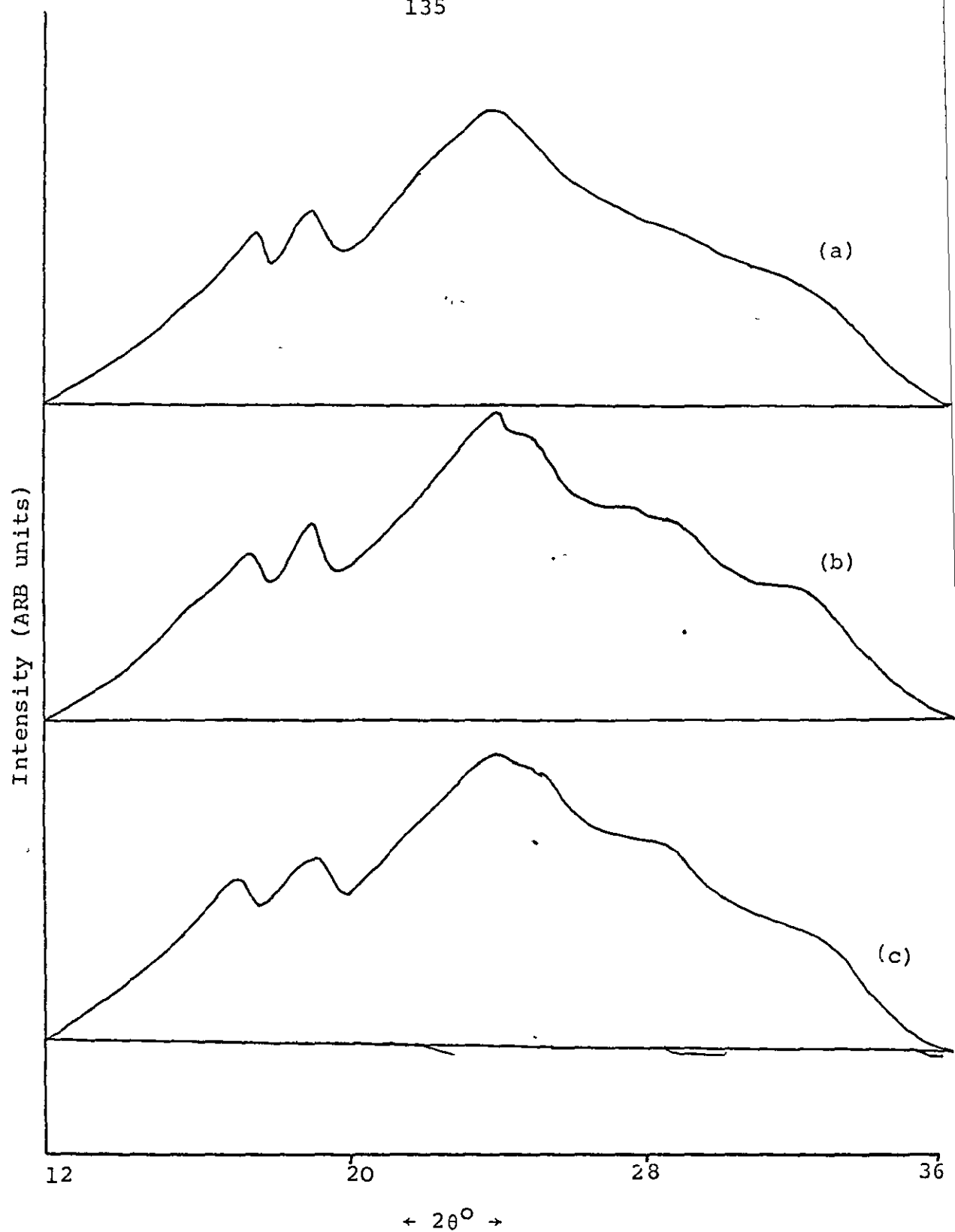


FIGURE 39 M-PVC annealed for 5 hours at (a) 80°C (b) 110°C and (c) 150°C

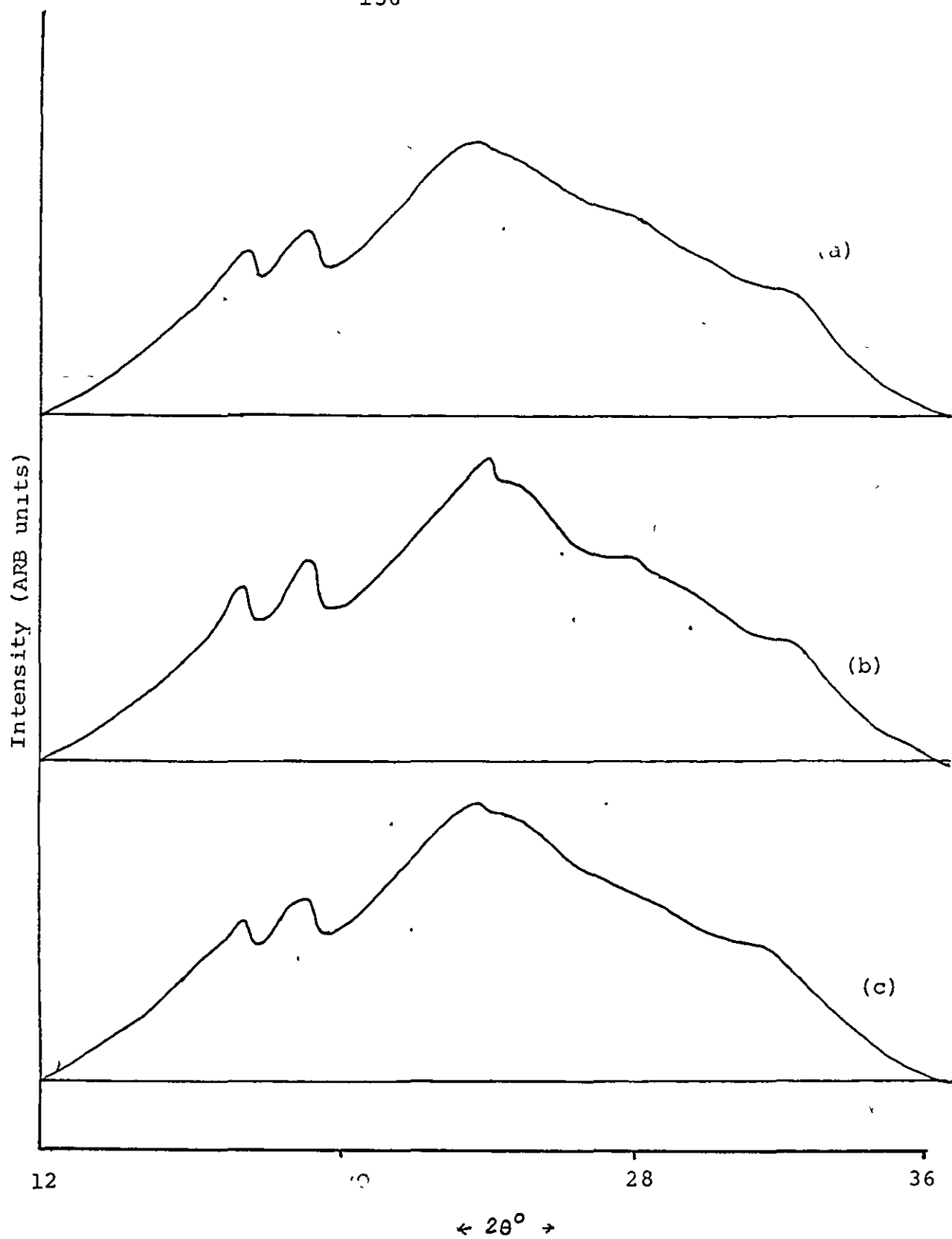


FIGURE 40 S-PVC annealed for 5 hours at; (a) 80°C .
(b) 110°C (c) 150°C .

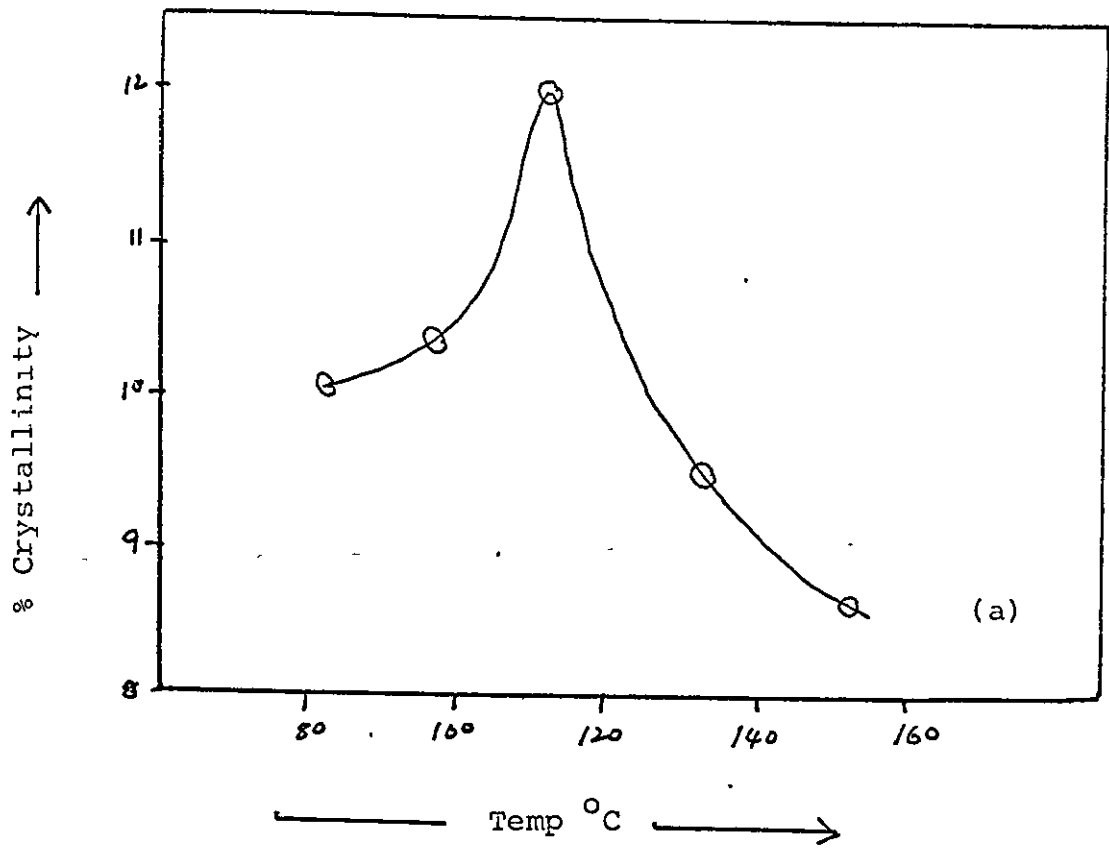


FIGURE 41 % Crystallinity as a function of annealing temperature a) S-PVC, b) M-PVC

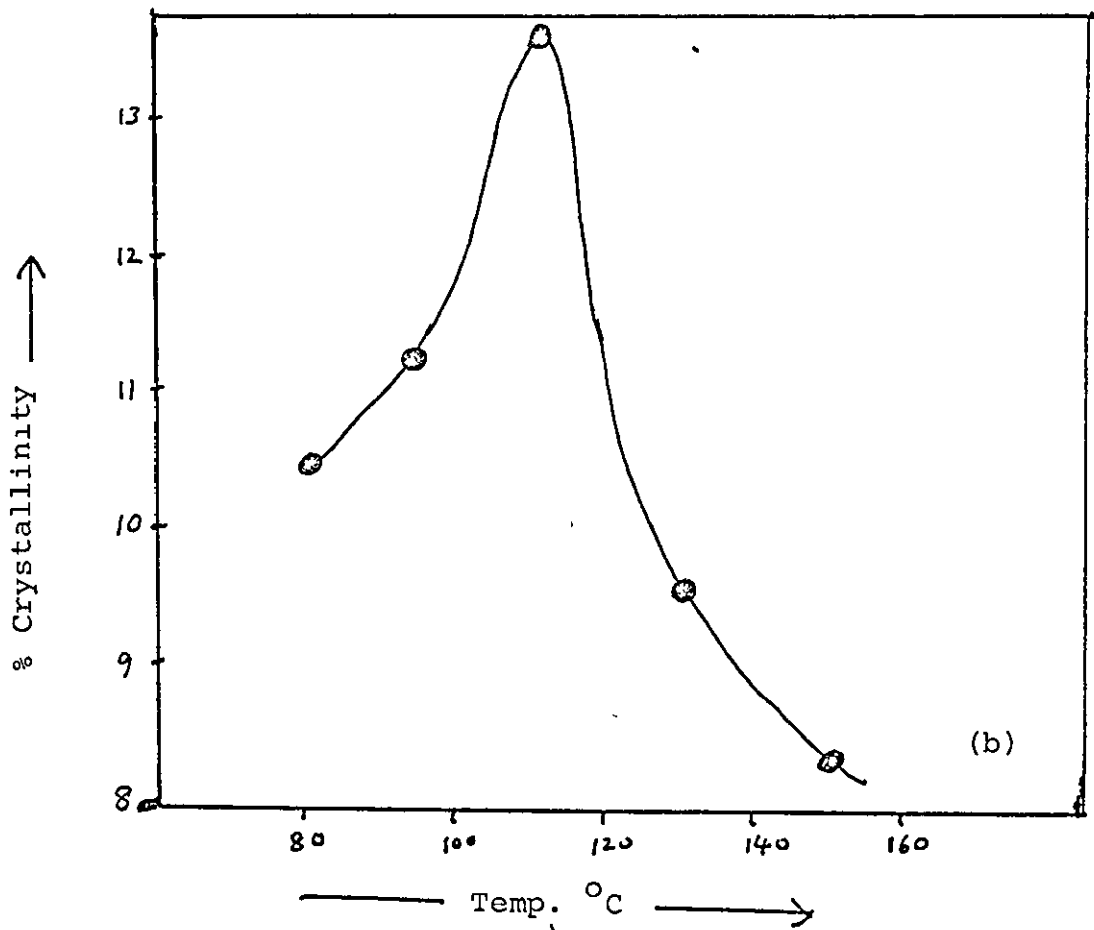


TABLE 18

Percentage Crystallinity for M-PVC at Various Moulding Temperatures

Moulding Temperature	% Crystallinity
160°C	10.3
170°C	9.6
180°C	8.9
190°C	7.9
200°C	7.4
210°C	7.0
222°C	6.3

TABLE 19

Percentage Crystallinity for S-PVC at Various Moulding Temperatures

Moulding Temperature	% Crystallinity
160°C	11.52
170°C	10.42
180°C	10.33
190°C	10.16
200°C	9.55
210°C	8.79
222°C	8.54

TABLE 20M-PVC Annealed at Various Temperatures for 5 hours

Annealing Temperature	% Crystallinity
80°C	10.29
95°C	10.93
110°C	13.28
130°C	9.43
150°C	8.33

TABLE 21S-PVC Annealed for 5 hours at Various Temperatures

Annealing Temperature	% Crystallinity
80°C	10.06
95°C	10.29
110°C	11.96
130°C	9.43
150°C	8.06

4.4 Mechanical Properties.

4.4.1 Tensile Properties :

Samples from M-PVC and S-PVC, moulded at different temperatures, and heat treated material were tested on an Instron universal testing machine. Details of the operation conditions have been given in section 3.7.1.

Typical stress strain curves for MPVC and SPVC moulding made at different temperatures are shown in figures 42-45. The mode of deformation was found to be dependent on moulding temperature and the type of resin. For instance in M-PVC mouldings, ductile failure was observed whereas mouldings made from similar blends with S-PVC failed in a brittle manner, without yielding at moulding temperatures below 190°C . Cold-drawing was observed in M-PVC at a moulding temperature of 190°C and above, while in S-PVC it was not observed until a moulding temperature of 210°C . This was followed by the specimen breaking at the necked region. It is clear from figures 42-45 that as the moulding temperature is raised the type of failure changes progressively from brittle fracture to necking rupture to cold drawing.

The results of the yield stress or breaking stress in case of brittle failure, and elastic modulus for M-PVC and S-PVC are given in tables 22 and 23. The stress and modulus values are shown as a function

of moulding temperature in figures 46 and 47 respectively. Initially the M-PVC has higher value of yield stress than S-PVC but after reaching to 200°C moulding temperature the values are approximately same. In the case of M-PVC an increase of 7% was observed in yield stress whereas in S-PVC yield was increased by 88%. Elastic modulus also increased with the rise in moulding temperature but again there was a sharp increase of 36% in the case of S-PVC while in M-PVC only 21% increase in the value of modulus was observed. The elongation at break for M-PVC was much higher than S-PVC and the elongation at break for S-PVC 200°C moulded sample was approximately equal to the M-PVC 180°C moulded sample. Figures 48-51 show the typical stress-strain curves for M-PVC and S-PVC 180° and 200°C mouldings, tested at elevated temperatures. The mode of deformation changed considerably in the case of S-PVC. Samples from S-PVC moulded at 180°C show brittle failure at ambient temperature while ductile failure with necking was observed at elevated temperatures. The mode of deformation at elevated temperature for M-PVC was similar to that at ambient temperature, however the magnitude of elongation was larger at elevated temperatures.

The values of yield stress and modulus decreased at elevated temperatures from both M-PVC and S-PVC and tend to the same value as the test

temperature is increased. This has been shown in figures 53 - 55.

Tensile tests were also carried out for M-PVC quenched samples at ambient and elevated temperatures. Typical curves for quenched material are shown in figure 52. The values of yield stress and modulus are plotted against test temperatures, in figures 54 and 55 respectively. The quenched samples break just after yielding at ambient temperature, but cold-drawing is observed in the same sample at elevated temperatures. Yield stress and modulus decrease as the test temperature is increased. Figure 56 shows the typical stress-strain curves for annealed samples from M-PVC quenched material. The mode of deformation for all the samples is similar in that the samples break just after yielding. The values of yield stress are given in table 29. The samples annealed at 110°C shows the highest value of yield stress.

Figures 58 and 59 show the typical stress strain curves for 200°C moulded sheets from M-PVC and S-PVC annealed at various temperatures. The values of yield stress are listed in table 28, and these values of yield stress are plotted as a function of annealing temperature (see figure 57).

The mode of deformation in the case of M-PVC annealed samples changes from cold drawing to less ductile and after reaching an annealing temperature

of 110°C the order is reversed. Whereas in the case of S-PVC the mode of deformation is little changed. From table 28 it is noted that tensile yield stress increases on annealing. The maximum value of yield stress was obtained for samples annealed at 110°C, these samples also had minimum value of elongation at break.

In order to see the effect of cooling rate on mechanical properties, tests were performed on M-PVC, 200°C moulded samples cooled at different rates. Figure 60 is the plot of yield stress against the test temperature of two M-PVC samples cooled at different rates. There is no significant difference in the values of yield stress of the two specimens at variety of test temperature.

Calculation of Tensile Properties:

1) Yield Stress, σ_y .

Yield stress was calculated by using the following formula:

$$\sigma_y = F/A$$

where σ_y = yield stress

F = load at the yield point

A = Cross-sectional area of the original specimen.

2) Young's Modulus, E.

Young's modulus was calculated from the load-extension curve by drawing a tangent from a point on

the uniformly extended portion of the curve. A normal was drawn from a point of the tangent to the strain axis, and by using the following formula the value of 'E' was obtained;

$$E = \frac{\text{stress}}{\text{strain}} = \frac{F/A}{\Delta L/L_0}$$

where F = Force at any point on the tangent

A = Area of cross-section of the original specimen

ΔL = Change in length at the point where force is considered.

L_0 = The effective gauge length of the original specimen.

N.B. Due to the use of small size sample an extensometer could not be used to record the actual extension, therefore, percentage strain was calculated from load-extension curve. Hence the values for moduli reported here may not be absolute values but can be used for a comparative study.

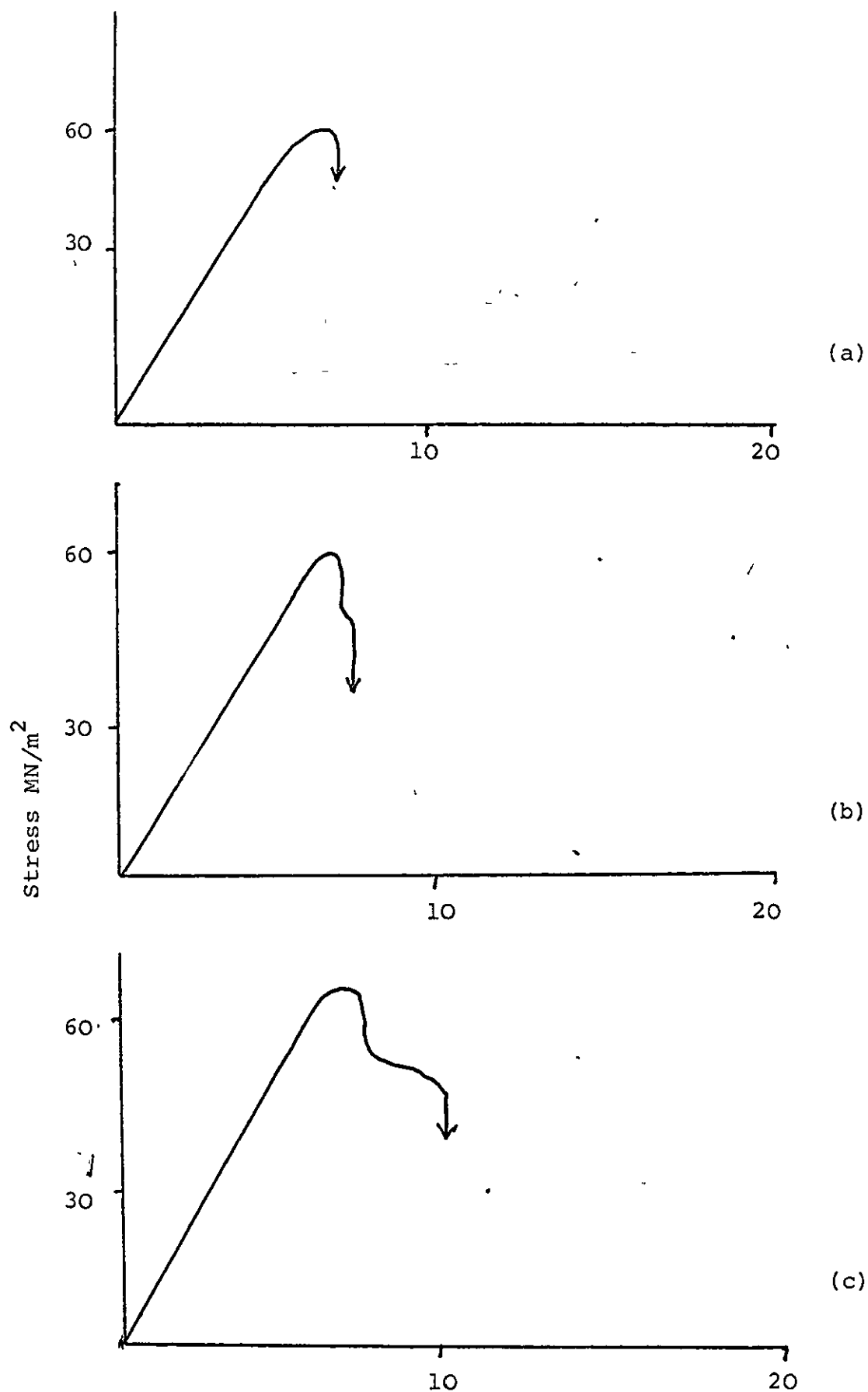


FIGURE 42 Stress-strain curves for M-PVC moulded at (a) 160°C, (b) 170°C and (c) 180°C

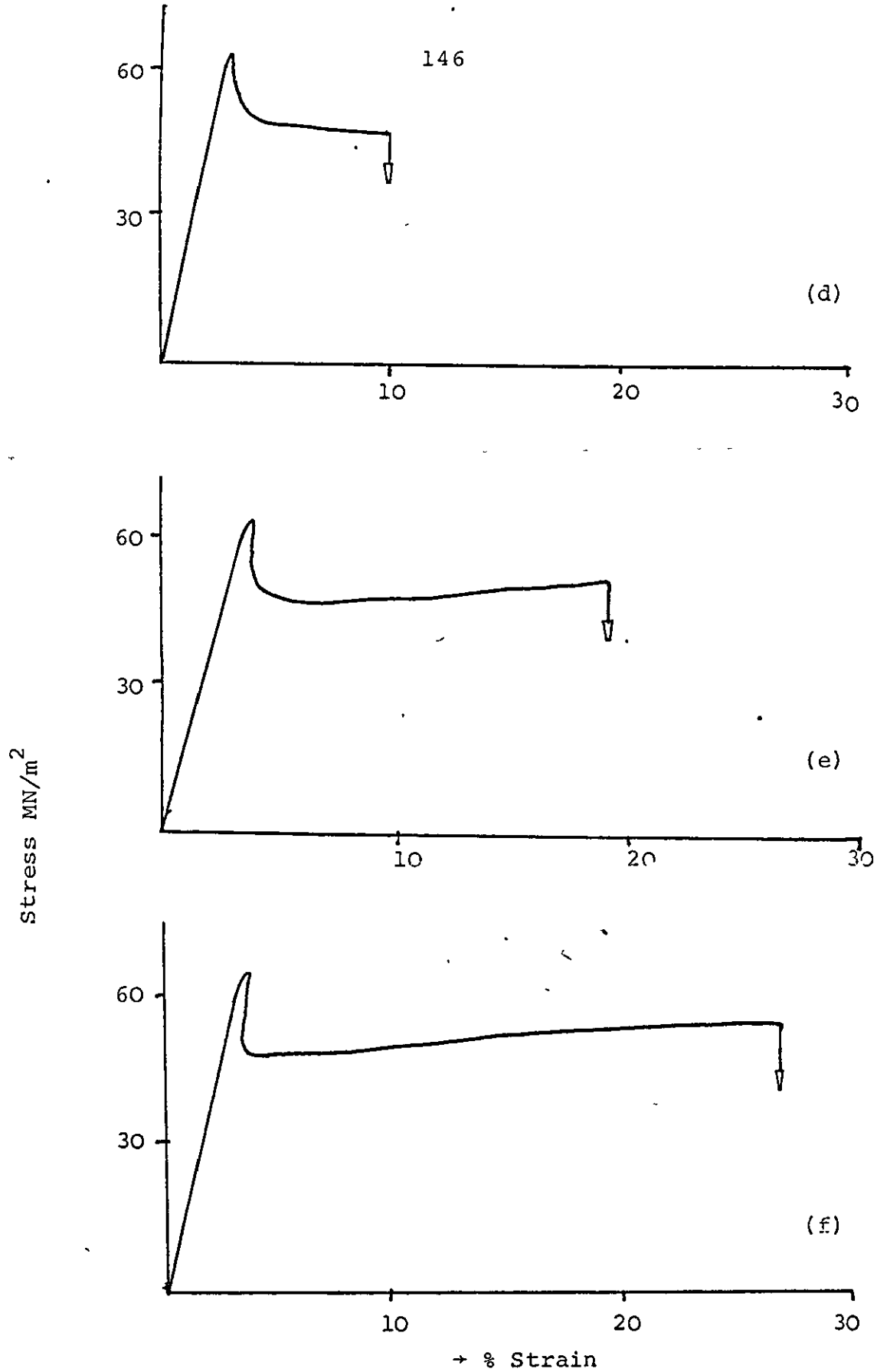


FIGURE 43 Stress-strain curve for M-PVC moulded at:
(a) 190°C (b) 200°C and (c) 210°C)

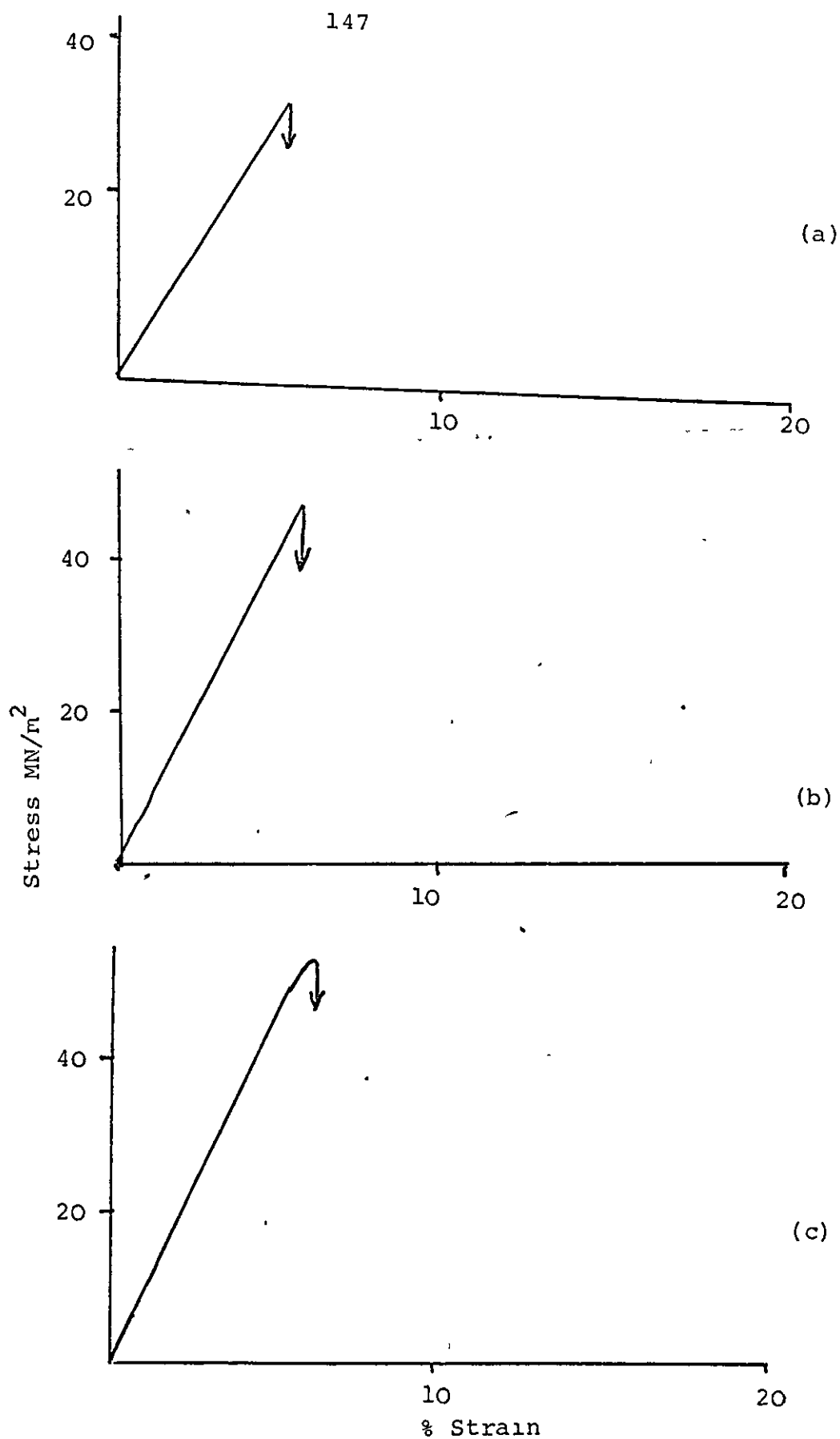


FIGURE 44 Stress-strain curves for S-PVC moulded at (a) 160°C (b) 170°C and (c) 180°C

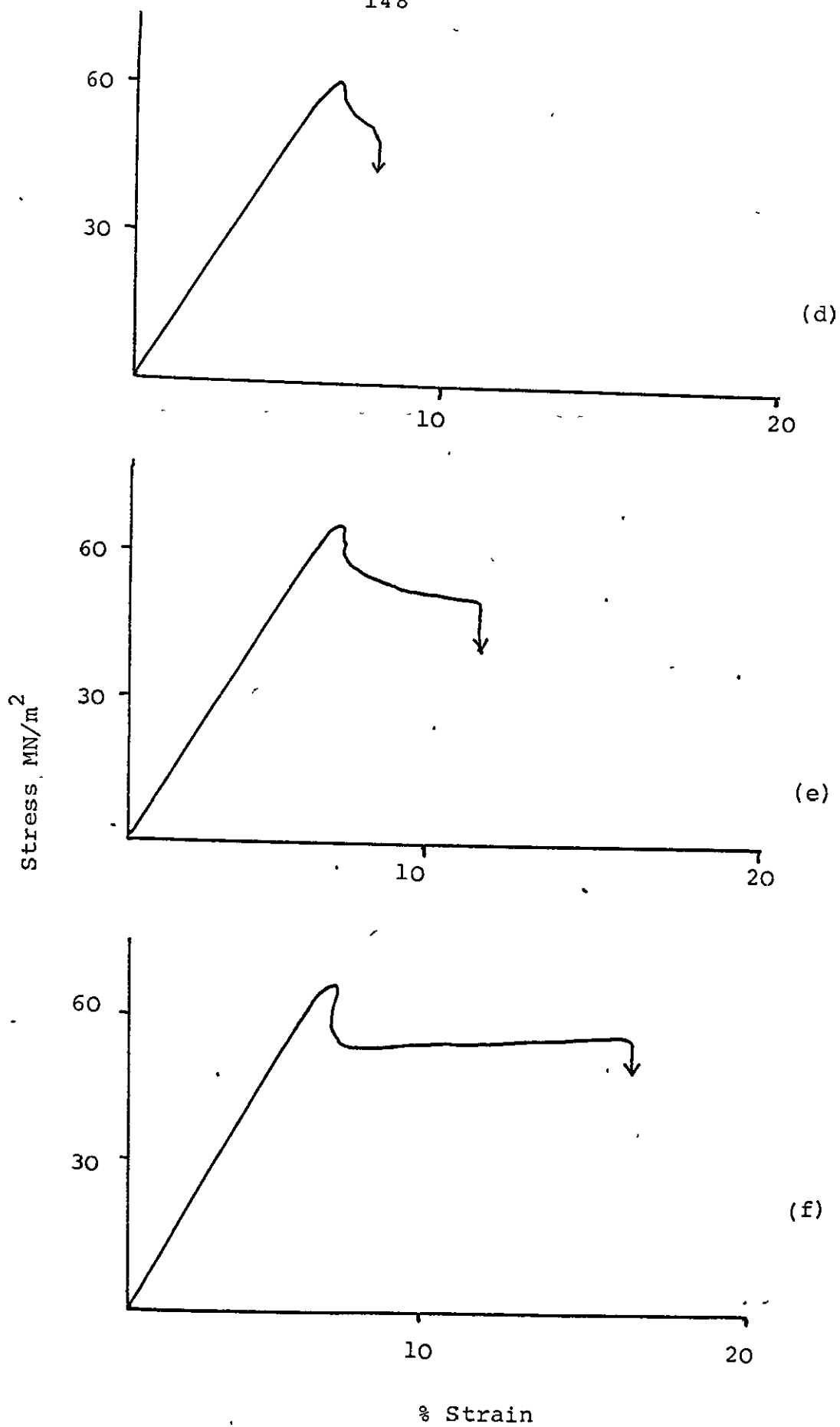


FIGURE 45 Stress-strain curves for S-PVC moulded at (a) 190°C (b) 200°C and (c) 210°C

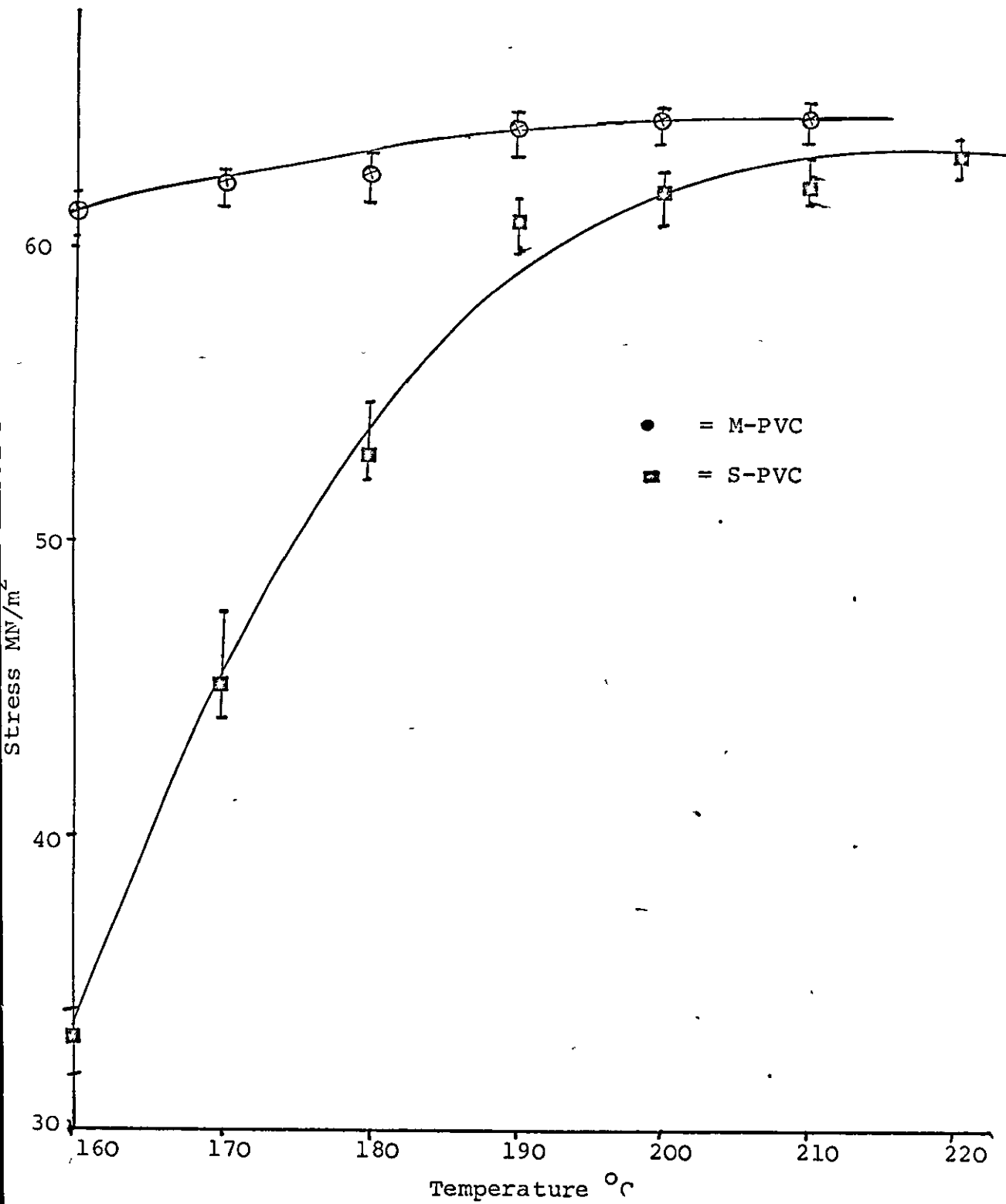


FIGURE 46 Yield stress as a function of mould-temperature

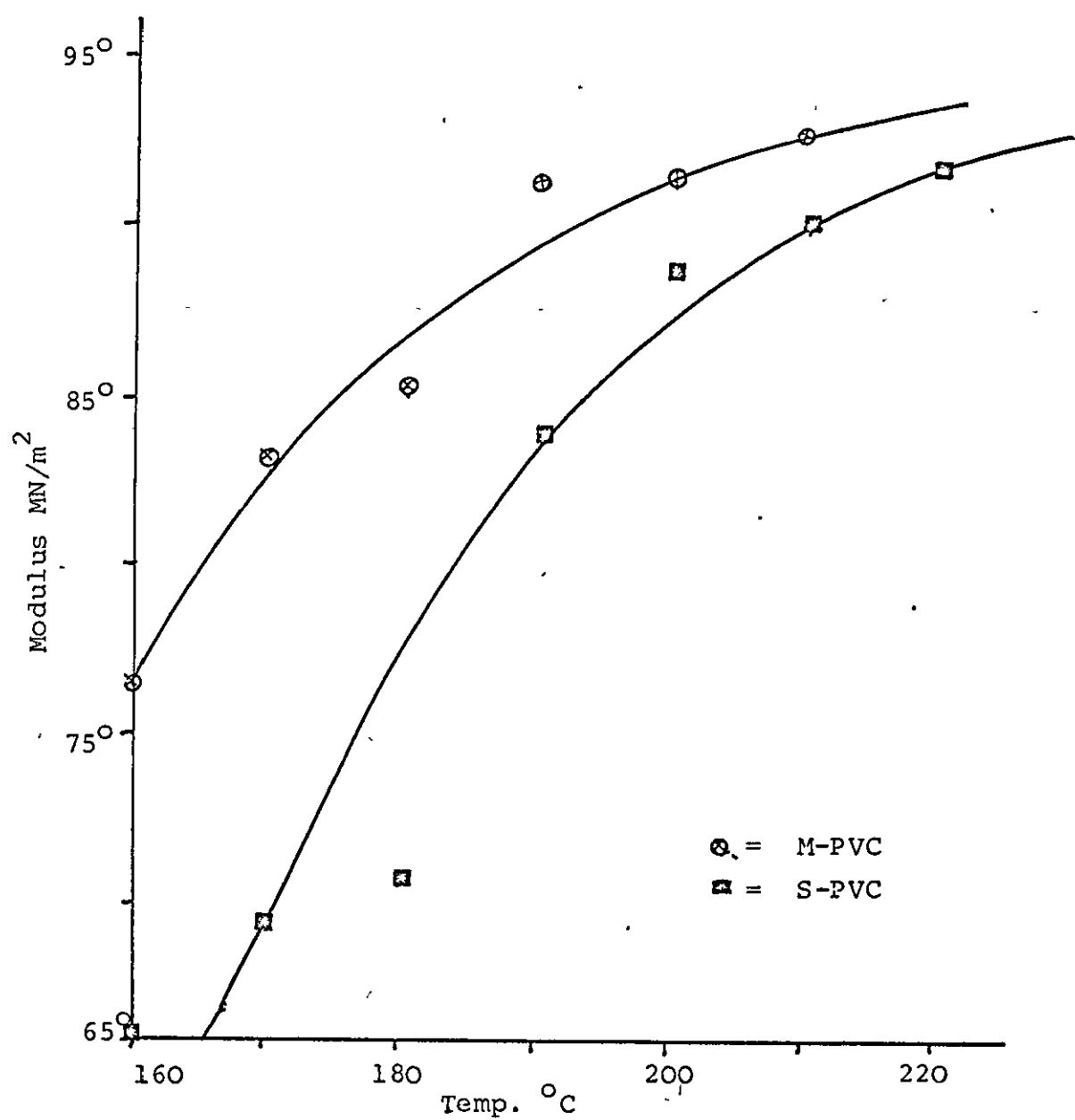


FIGURE 47 Elastic modulus as a function of moulding temperature

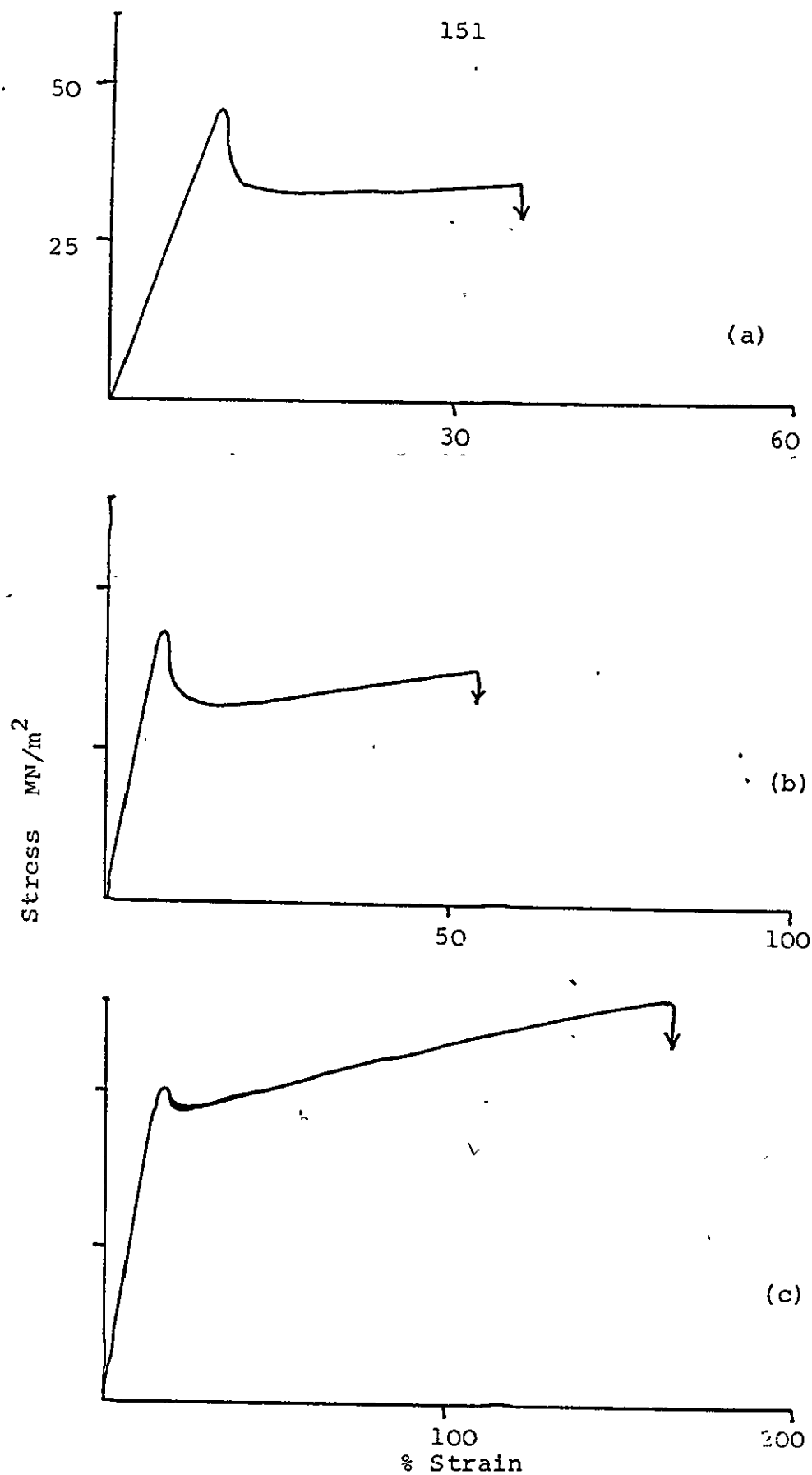


FIGURE 48 Stress-strain curves for 180°C M-PVC moulding at elevated temperatures:
(a) 40°C, (b) 55°C (c) 70°C

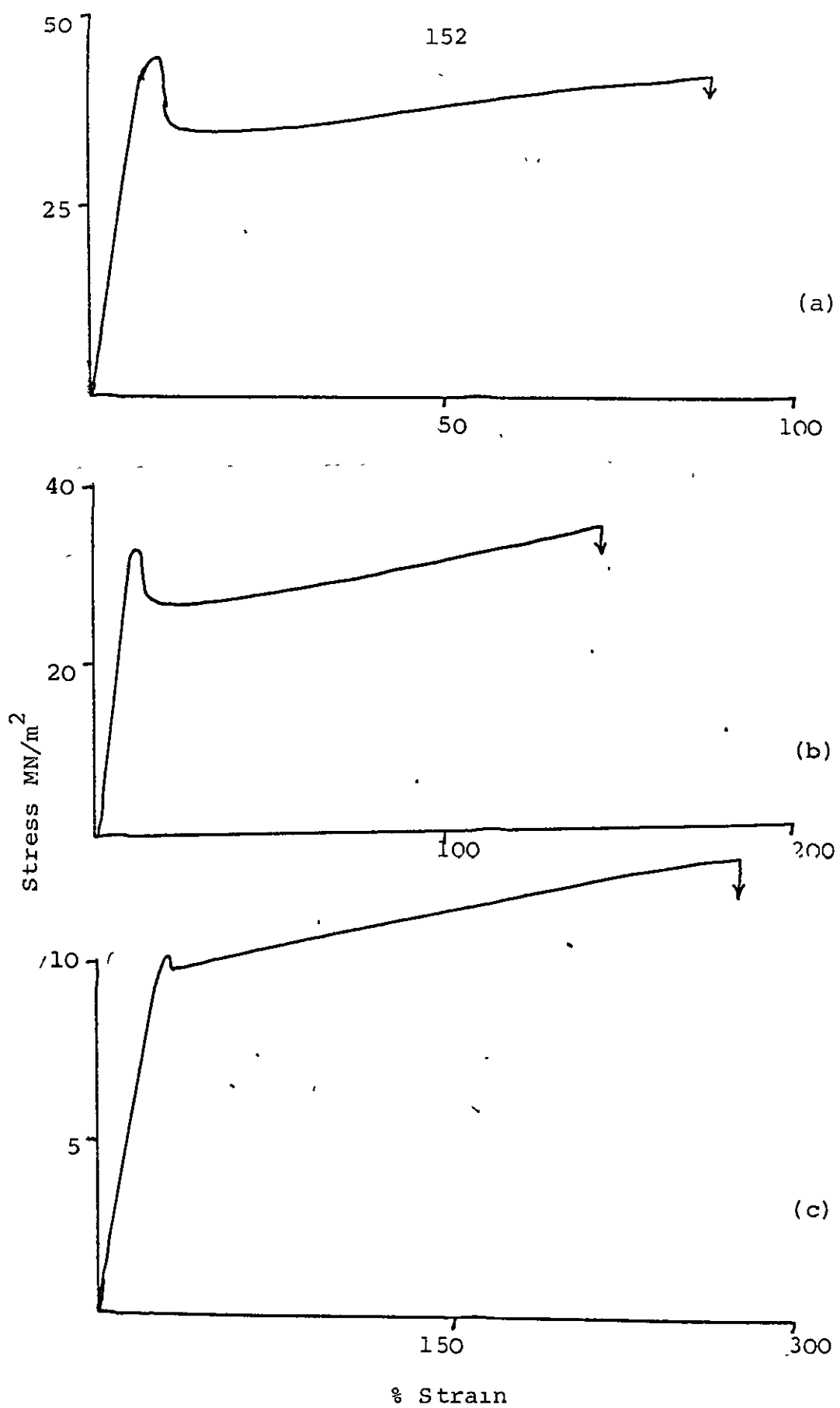


FIGURE 49 Stress-strain curves for 200°C M-PVC moulding at elevated temperatures:
(a) 40°C, (b) 55°C and (c) 70°C

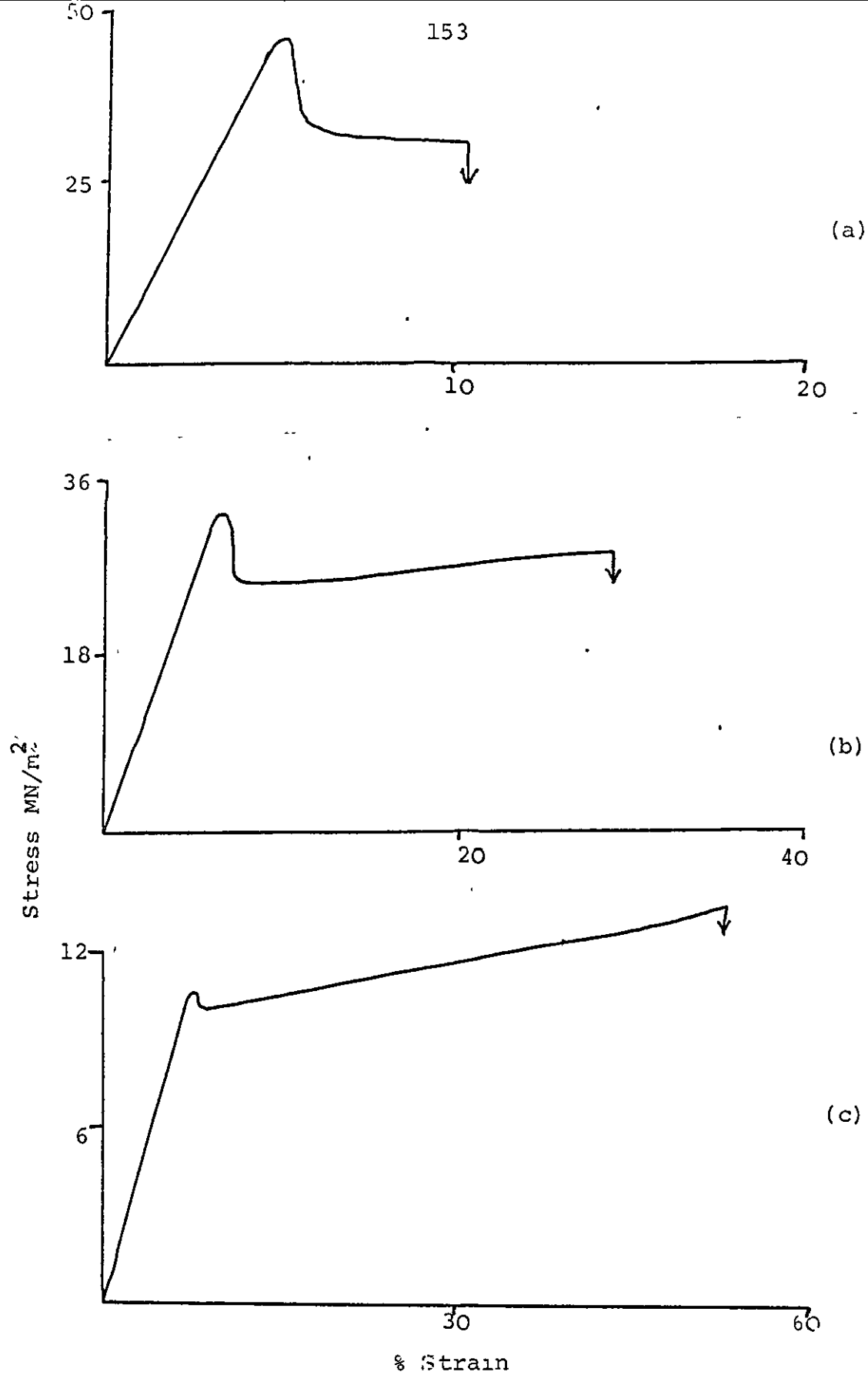


FIGURE 50 Stress-strain curves for 180°C S-PVC moulding elevated temperatures:
(a) 40°C, (b) 55°C and (c) 70°C

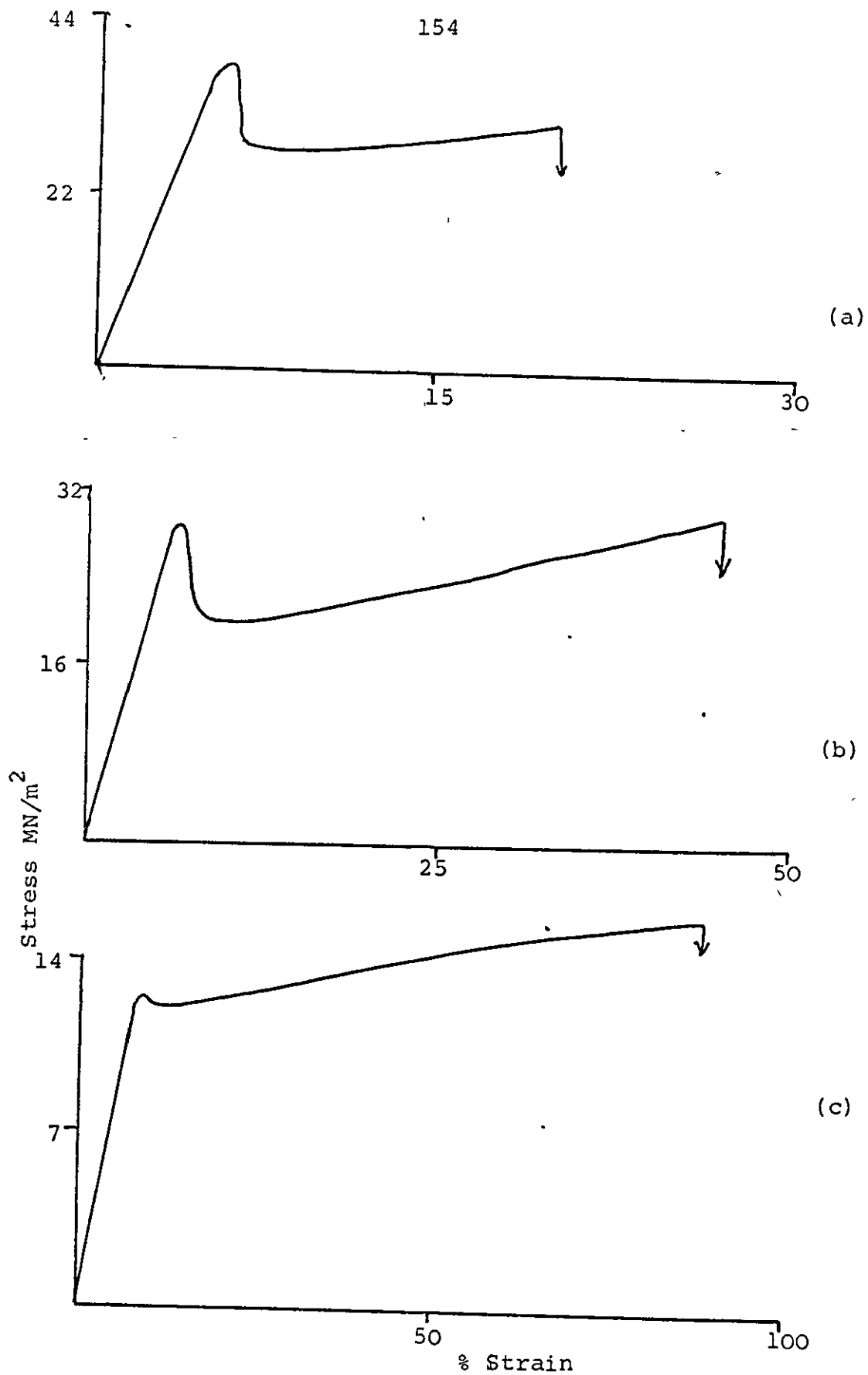


FIGURE 51 Stress-strain curves for 200°C S-PVC moulding at elevated temperatures:
(a) 40°C, (b) 55°C and (c) 70°C

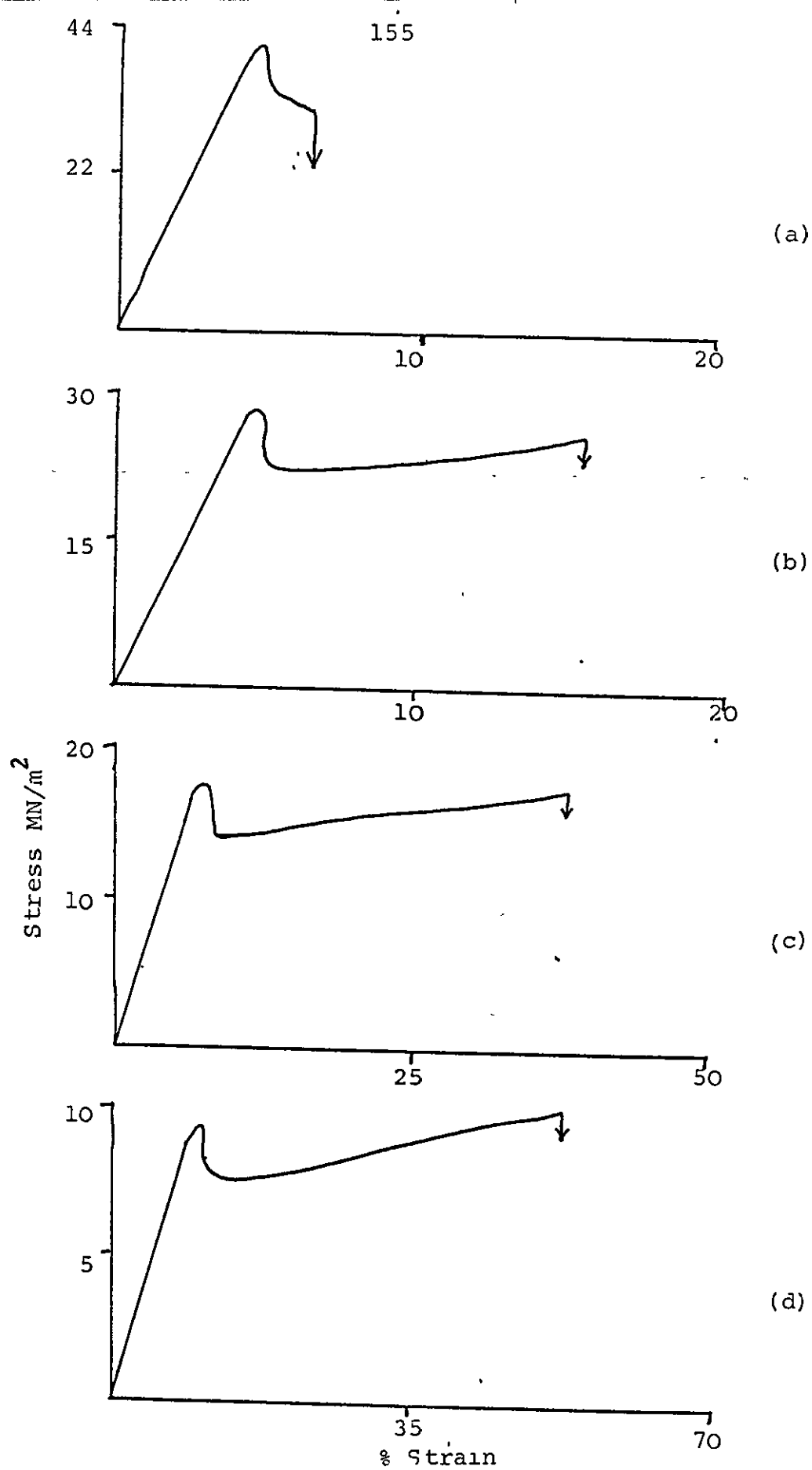


FIGURE 52 Stress-strain curves for quenched M-PVC at various temperatures: (a) 25°C, (b) 40°C (c) 55°C (d) 70°C

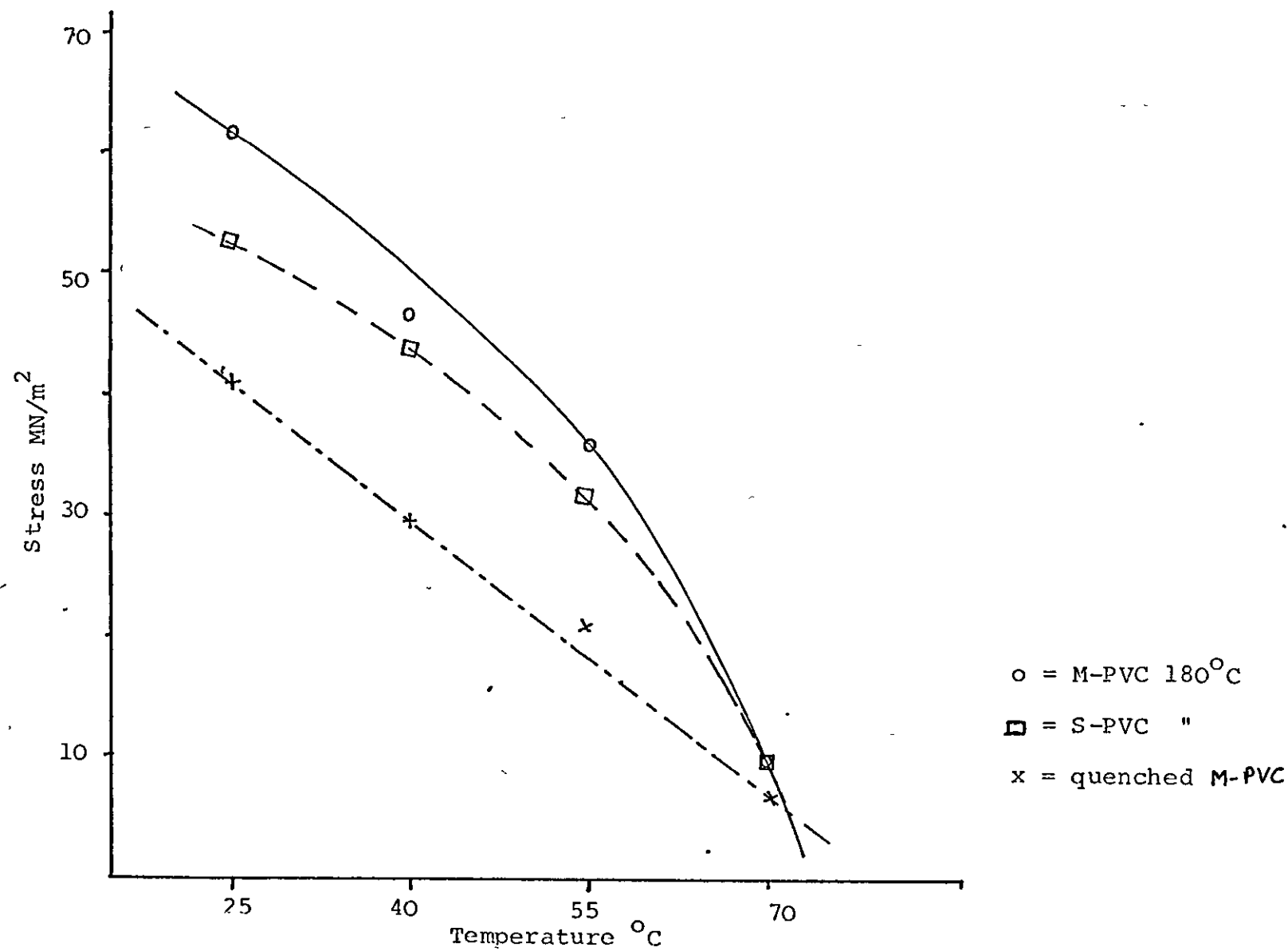


FIGURE 53 Yield stress as a function of test temperature

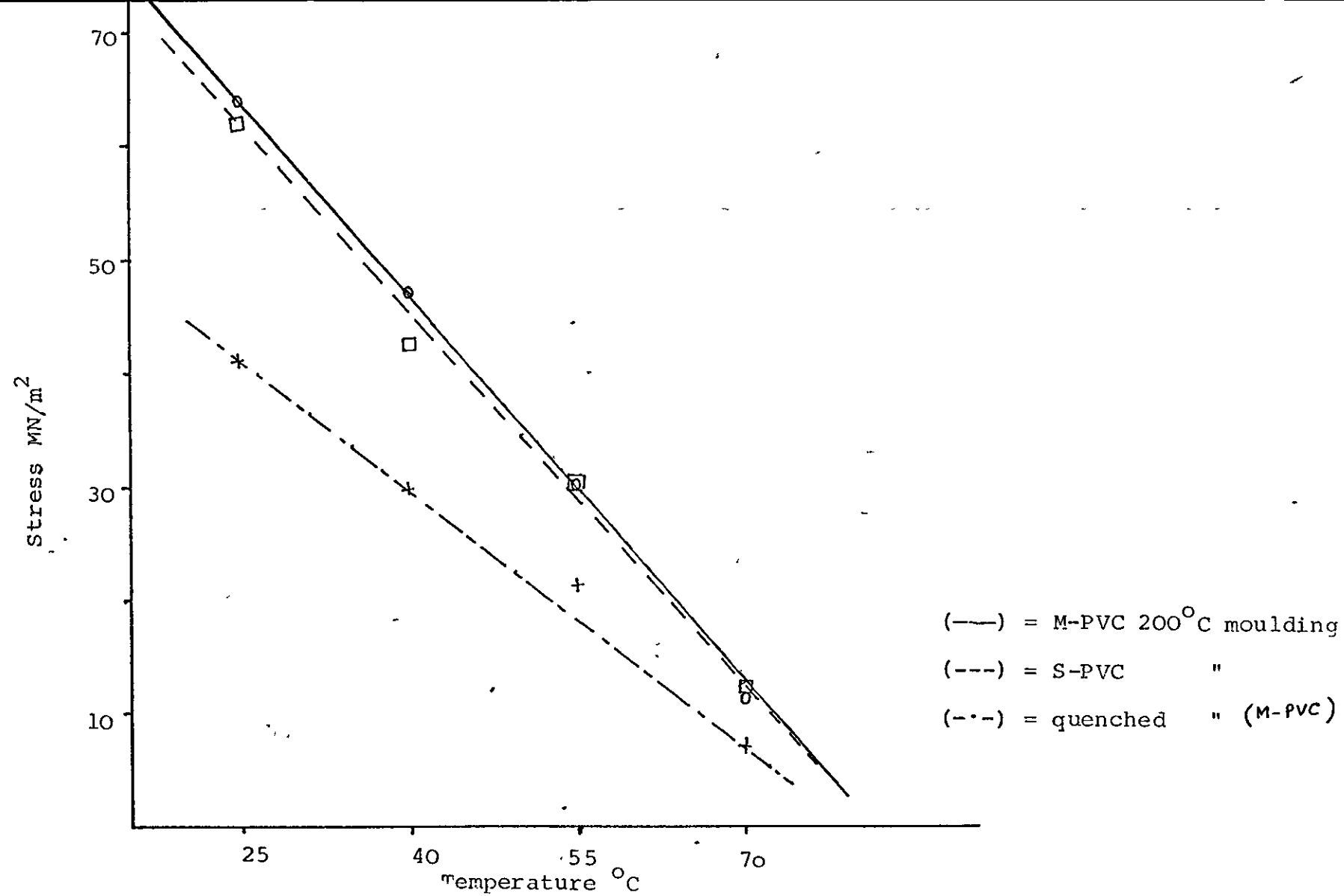


FIGURE 54 Yield stress as a function of test temperature

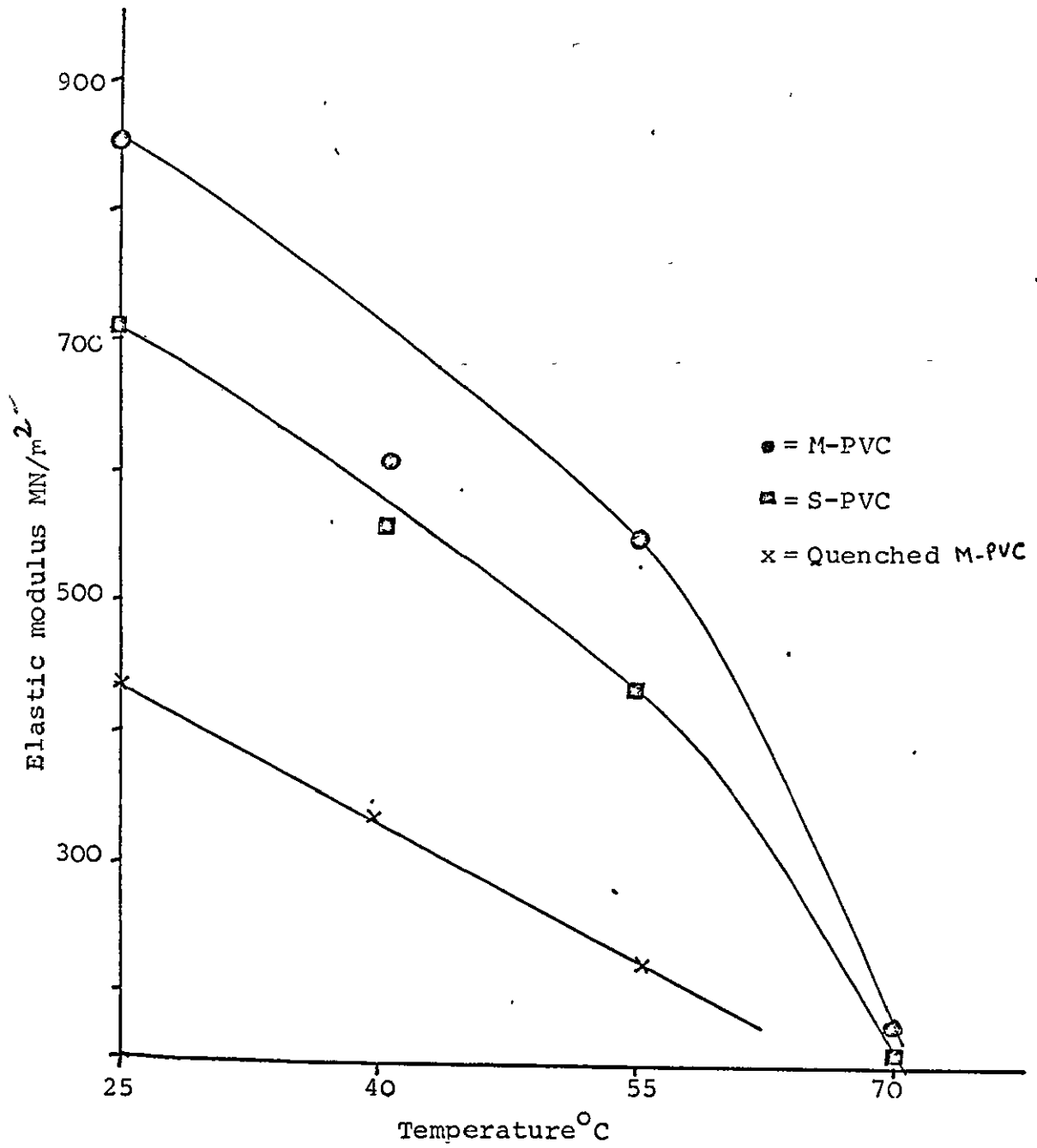


FIGURE 55 Elastic modulus as a function of temperature

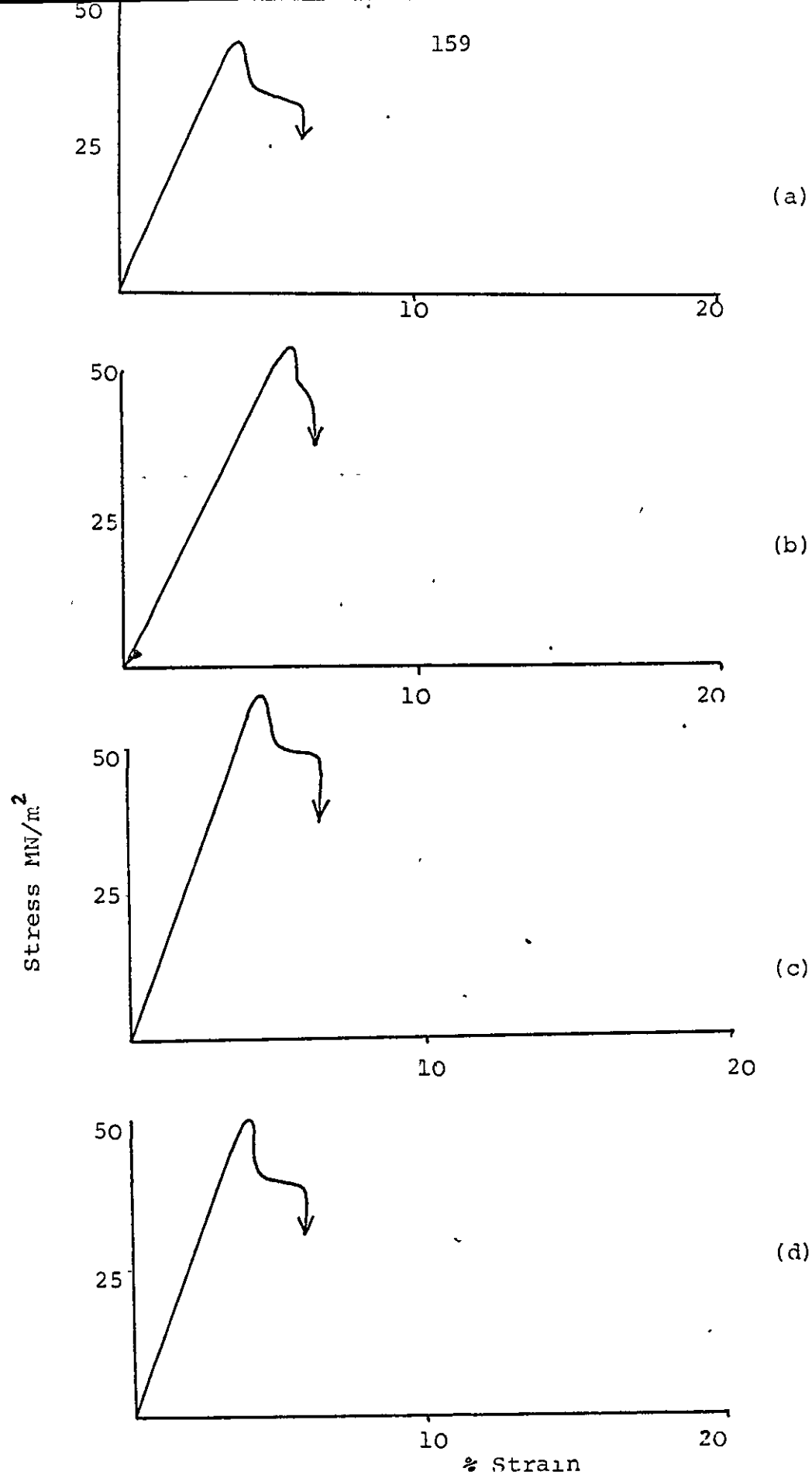


FIGURE 56 Stress-strain curves for quenched M-PVC annealed for 5 hours at various temperatures.
(a) quenched (b) 80°C (c) 110°C (d) 150°C

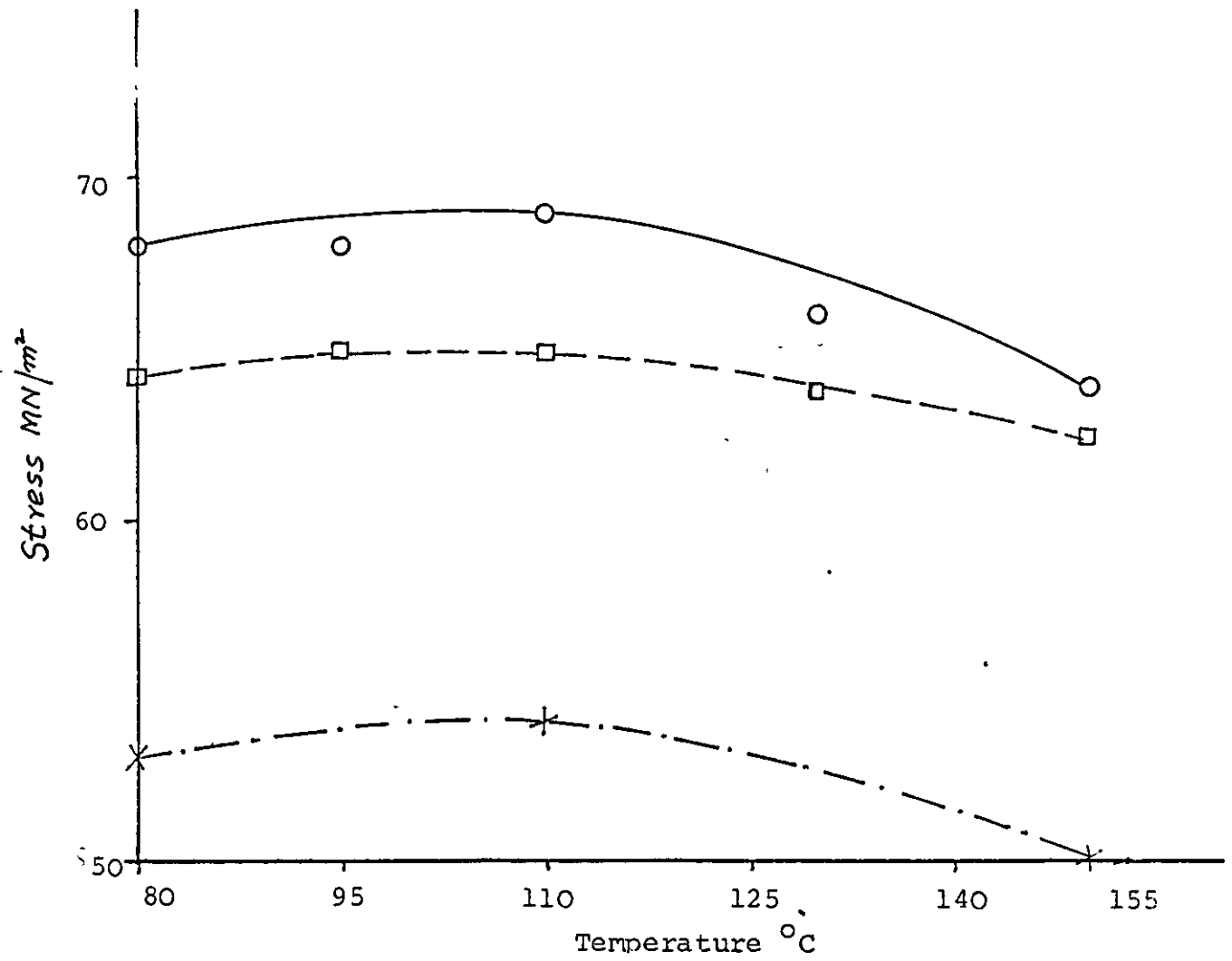


FIGURE 57: Nominal yield stress as a function of annealing temperature.

○ = M-PVC

□ = S-PVC

X = Quenched M-PVC

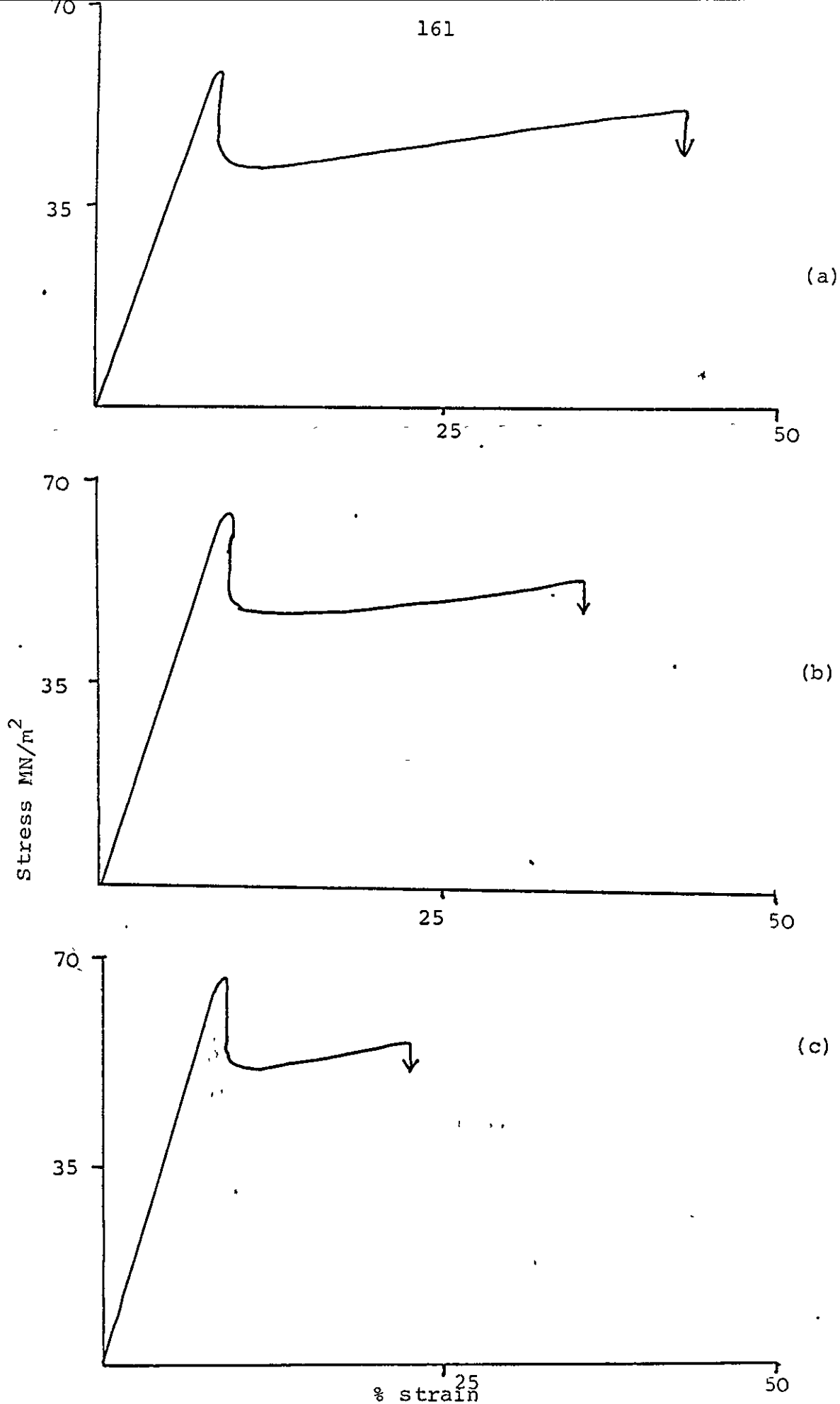


FIGURE 58 Stress-strain curves for M-PVC annealed for 5 hours at (a) unannealed, (b) 80°C and (c) 95°C

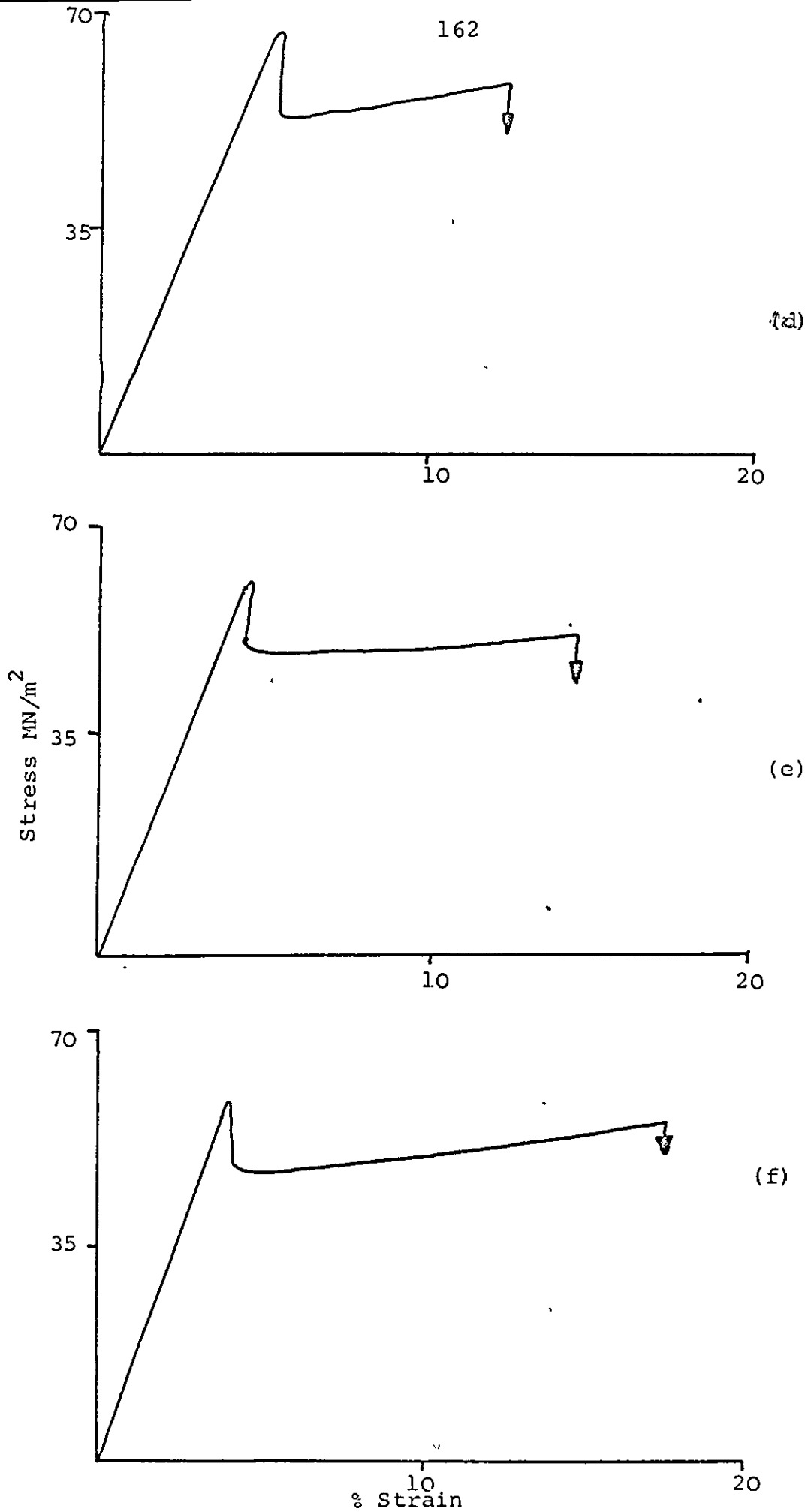


FIGURE 59 Stress-strain curves for M-PVC annealed for 5 hours at (d) 110°C (e) 130°C (f) 150°C

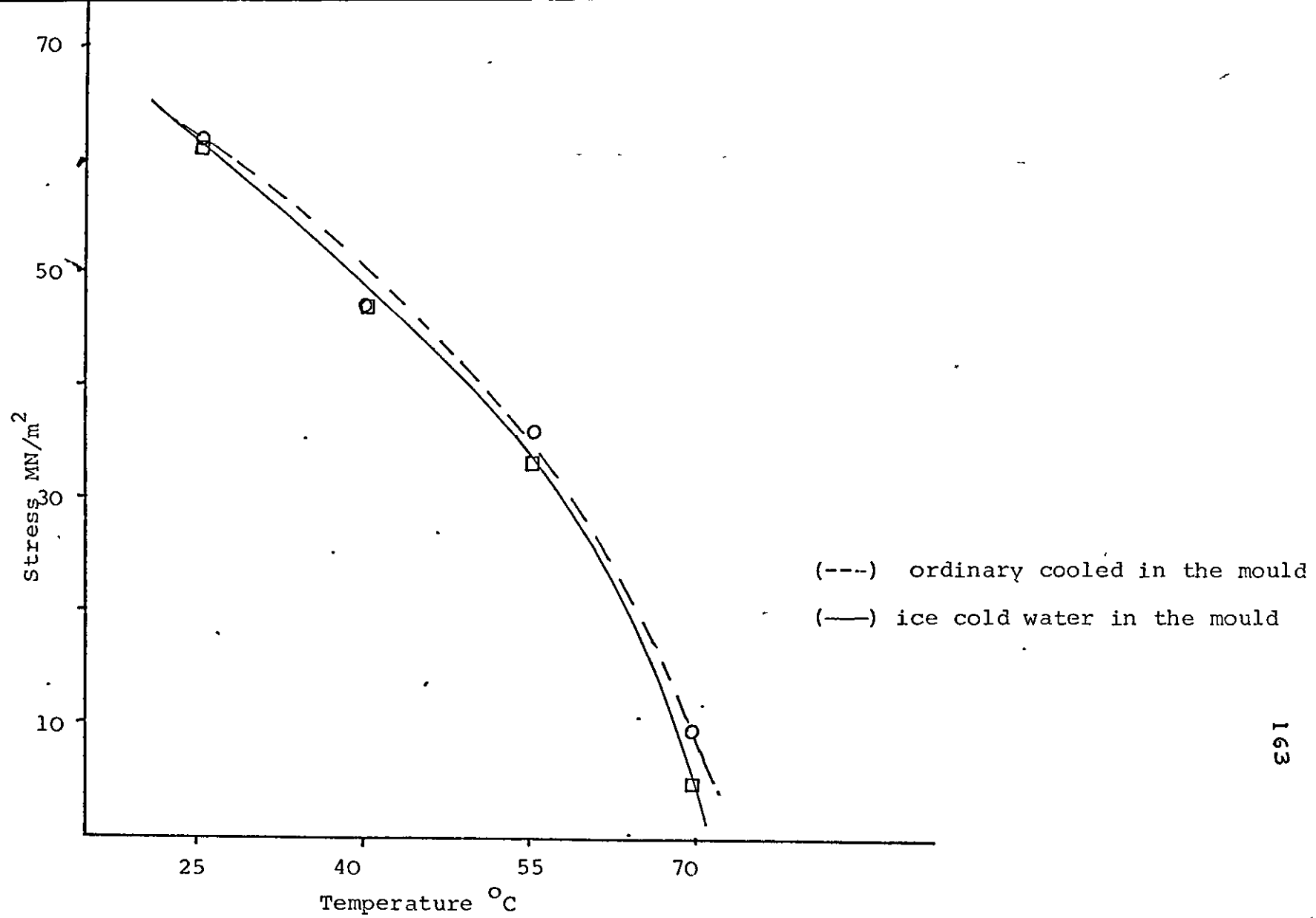


FIGURE 60 Effect of cooling rate on yield stress

TABLE 22 Effect of moulding temperature
on nominal yield stress and Young's
Modulus in M-PVC.

Moulding Temp. °C	Nominal Yield Stress MN/m ²	Young's Modulus MN/m ²
160	61	762
170	62	826
180	62	849
190	64	914
200	64	914
210	64	927

Moulding Temperature °C	Nominal Yield Stress MN/m ²	Young's Modulus MN/m ²
160	33	660
170	45	692
180	53	706
190	61	835
200	62	885
210	62	898
220	63	913

TABLE 23: Effect of moulding temperature on nominal yield stress and Young's modulus in S-PVC.

Test Temperature	M-PVC		S-PVC	
	Nominal Yield Stress MN/m ²	Young's Modulus MN/m ²	Nominal Yield Stress MN/m ²	Young's Modulus MN/m ²
25°C	62	849	53	706
40°C	46	604	44	556
55°C	35	566	32	442
70°C	10	183	10	160

TABLE 24: Nominal yield stress and Young's modulus for M-PVC and S-PVC 180°C mouldings at ambient and elevated temperatures.

Test Temperature	M-PVC		S-PVC	
	Nominal Yield Stress MN/m ²	Young's Modulus MN/m ²	Nominal Yield Stress NM/m ²	Young's Modulus NM/m ²
25°C	64	917	62	885
40°C	47	626	42	575
55°C	30	-	30	450
70°C	12	-	12.5	-

TABLE 25: Nominal yield stress and Young's modulus for M-PVC and S-PVC 200°C mouldings at elevated temperatures.

Test Temperature	Nominal Yield Stress MN/m ²	Young's Modulus MN/m ²
25	41	415
40	29	338
55	21	250
70	8	-

TABLE 26: Yield stress and modulus values for M-PVC quenched material at elevated temperatures.

Annealing Temperature	Yield Stress MN/m ²
unannealed (quench)	41
80°C	53
110°C	54
150°C	50

TABLE 27: Effect of annealing temperature on yield stress in quenched M-PVC

Annealing Temperature	Unannealed Sample	80°C	95°C	110°C	130°C	150°C
M-PVC	64	68	68	69	65	64
S-PVC	62	64	65	65	64	63
Quenched M-PVC	41	53	-	54	-	50

TABLE 28: Effect of annealing on the nominal yield stress
(samples annealed for 5 hrs)

4.4.2 Impact Strength

Impact strength tests were carried out on both notched and unnotched samples from M-PVC and S-PVC using a Charpy impact tester. The value of the energy to break the specimen was divided by the area beneath the notch and by the cross sectional area in case of unnotched samples. The energy to break per unit area in MN/m of the specimens has been reported.

Table 29 shows the results for unnotched samples. In the case of S-PVC the value of impact strength increases with the increase in moulding temperature. The mode of deformation was brittle for 160°C and 180°C moulded samples, but the sample moulded at 200°C failed in a ductile manner i.e. it had good impact strength.

However the M-PVC samples were highly ductile and except for the sample moulded at 160°C could not be broken by the highest weight tup available. Therefore notched specimens were prepared for both M-PVC and S-PVC mouldings to carry out impact tests.

The values of impact strength for notched samples are listed in table 30. Again impact strength increases with the increase in moulding temperature for both polymers. M-PVC samples have a higher value of impact strength than samples of S-PVC. The mode of deformation, in the case of M-PVC, was ductile whereas in S-PVC brittle failure was observed.

Figures 61 and 62 show the impact strength as a function of moulding temperature.

TABLE 29

Effect of moulding temperature on impact strength of unnotched samples

$\times 10^2$ MN/m

Moulding Temperature °C	M-PVC	S-PVC
160	1.7	0.64
180	did not break	0.88
200	did not break	4.40

TABLE 30

Effect of moulding temperature on impact strength of notched samples

$\times 10^2$ MN/m

Moulding Temperature °C	M-PVC	S-PVC
160	0.37	0.114
180	1.11	0.170
200	1.56	0.431

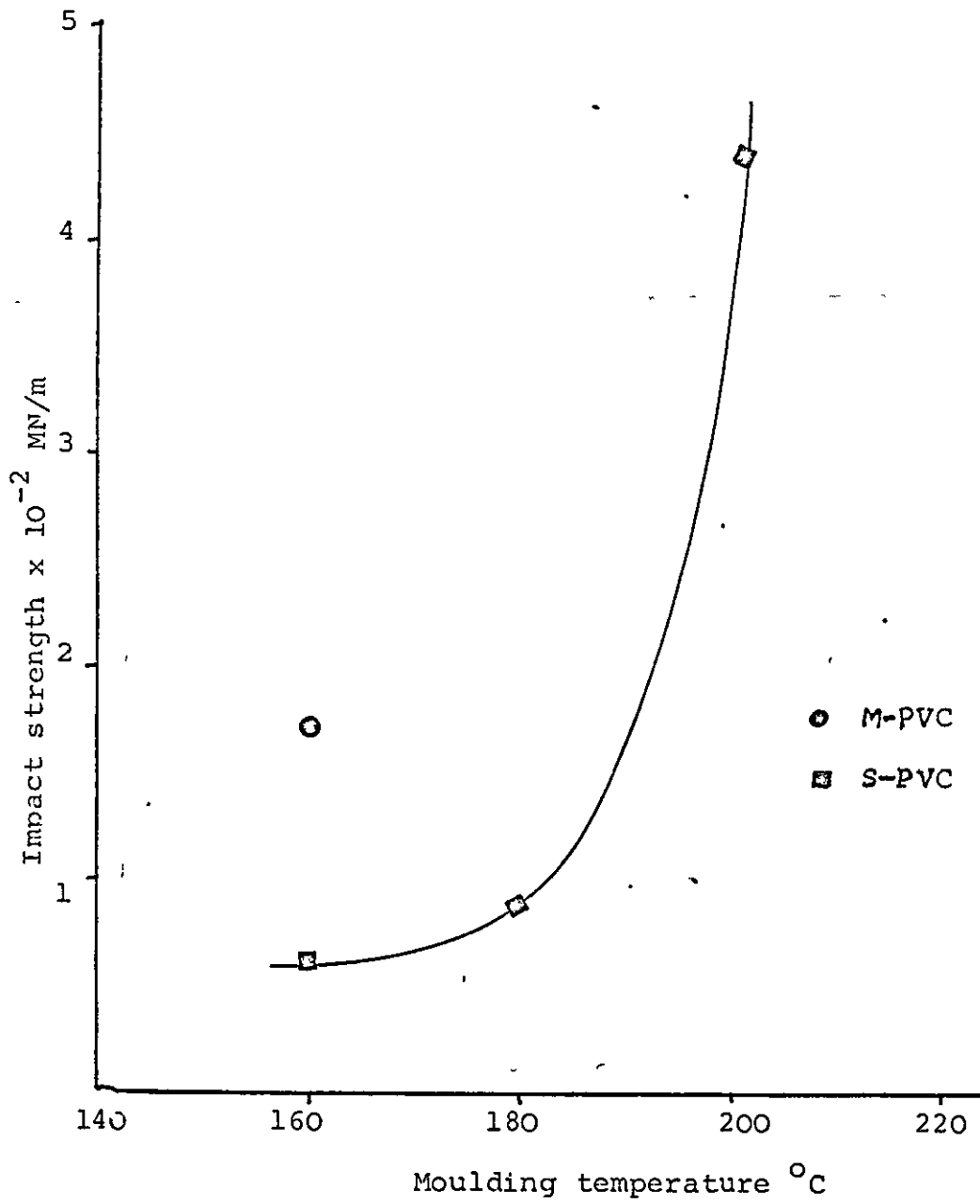


FIGURE 61 Impact strength of unnotched samples

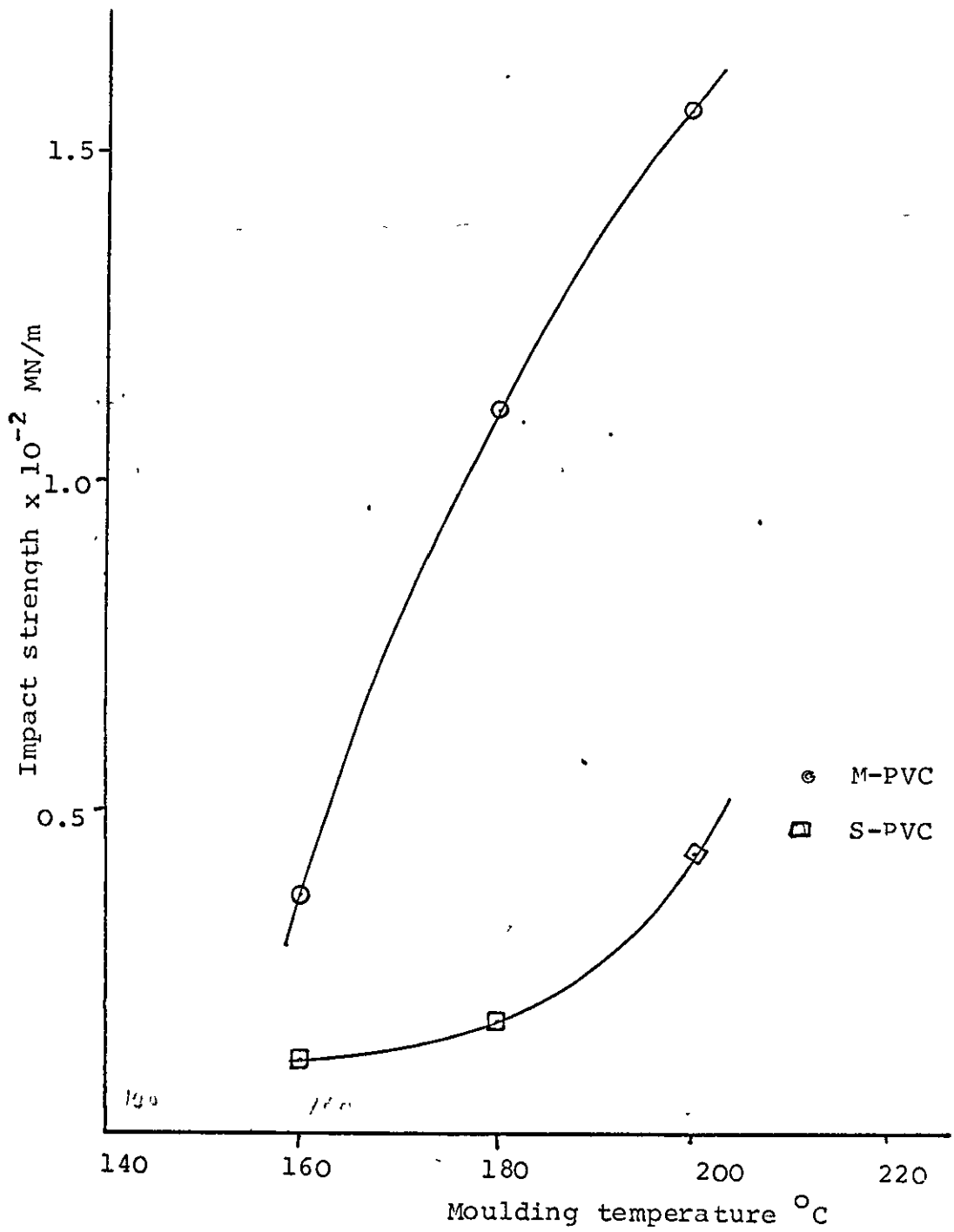


FIGURE 62 Impact strength of notched samples

CHAPTER 5

DISCUSSION5.1 Effects of Processing and Heat Treatment on Structure5.1.1 Introduction

When virgin PVC together with heat stabiliser is given heat treatment, it loses its original order and a new order is induced simultaneously. Various ideas have been put forward to explain the structural changes in PVC during heat treatment and can be divided into two groups. The first group deals with the structural changes below T_g and uses the "hole theory" of liquids as proposed by Eyring⁽⁶⁰⁾, (see Section 2.5). The other group is concerned with structural changes above T_g and the results have been explained in terms of secondary crystallinity.

In this work a mechanism will be put forward to explain the structural changes taking place in PVC during thermal treatment above T_g . The mechanism of structural changes is that of introduction of secondary crystallinity during processing and perfecting it on subsequent annealing. The results will be assessed in terms of enthalpy changes and percentage crystallinity in PVC. The schematic diagram of the mechanism is as follows.

Schematic Diagram of the Proposed Mechanism

VIRGIN POWDER

Primary
Crystallinity
(Orthorhombic
Structure)

First step
→
Processing at
high temperatures

Secondary
Crystallinity

(crystallites of
very small size
and wide range
of perfection)

Second step
→
Annealing
above T_g

Secondary
Crystallinity

(of more perfect
nature than in the
first step of its
growth)

5.1.2 Discussion of the Results

Glass transition temperature, T_g :

In thermograms of PVC powder blends from M-PVC and S-PVC, a transition is observed at about 78°C. This base line shift is attributed to the glass transition temperature, T_g , of the polymer. In moulded samples, T_g is found to decrease by 4-5°C in both the polymers. The drop in T_g can be explained as the outcome of tin stabiliser. Tin stabiliser is absorbed into the polymer particles in a manner analogous to plasticizer and hence PVC particles swell to a small amount. During blending operation the stabiliser has not been taken up enough and thus when powder blends are pressed at high temperature, PVC particles are able to imbibe the stabiliser to the maximum extent. By doing so PVC particles swell, although by small amounts, and free volume changes which results in the fall of T_g in moulded samples. Similar observations have been reported previously by Katchy⁽⁵⁷⁾, Natov and Gancheva^(101,102), and McKinney⁽¹⁰³⁾.

Structural changes:

The DTA thermogram of the PVC powder blend has a broad endotherm starting at 155°C, and extending to 200°C. This endothermic peak (transition A in

figure 19) has been ascribed to the melting of primary crystallinity introduced during polymerisation.

Thermograms obtained from moulded samples at temperatures from 160°C to 220°C both from M-PVC and S-PVC show a decrease in melting peak assigned to primary crystallinity with increasing mould temperature. This peak almost disappears for samples moulded at 200°C and above (see tables 10 and 11). This is quite reasonable because during processing we are heating the original PVC above its melting point. As we increase the moulding temperature from 160°C to 220°C, the primary crystallinity gradually melts out in the press and diminishes at temperatures 200°C and above.

The values of the percentage crystallinity measured by X-ray diffraction methods have also been found to decrease with the increasing moulding temperature. This is a clear indication that primary crystallinity is reduced in moulding cycles.

Thermograms obtained from the 160°C moulded sample and a rerun of the same sample cooled from 200°C to -40°C are shown in figure 22. In thermogram Q the peak assigned to melting of primary crystallinity is almost absent, instead there is a broad endothermic peak starting from 110°C extending to 206°C. A similar

transition was observed by Lebedev et al⁽¹⁰⁴⁾ but no explanation was given. In fact this observation has been neglected by other workers as well, although it is very important in understanding the mechanism of formation of crystallites by annealing process. In this work it has been assigned to the intermediate step for the growth of crystallites of more perfect nature on annealing. This intermediate step is suggested to be due to the melting of secondary crystallinity induced during cooling the sample from 200°C.

Similar types of endotherms are observed in the thermograms of moulded samples at 170° and above in the case of M-PVC, and 180°C and above for S-PVC, (see Figures 19 and 23, transition B). In this work this transition has been assigned to the melting of secondary crystallinity introduced during processing. The size of the endotherm 'B' increases as the moulding temperature is increased. As more and more primary crystallinity is melted out, the amount of secondary crystallinity introduced increases. This has been demonstrated by plotting the value of heat of fusion against the moulding temperature in figures 20 and 21.

The concept of secondary crystallinity has been used by Jujin et al⁽³¹⁾. According to their explana-

tion the secondary crystallinity is induced during annealing, and has a nematic structure because it starts melting at a lower temperature. In this work another explanation will be proposed. It is suggested that secondary crystallites are formed in two stages. In the first stage, during processing, secondary crystallites formed are very small in size with a wide range of perfection. In the second step, on annealing above T_g , the crystallites are perfected. Hence secondary crystallites formed during annealing are of more perfect nature than in the first step of its growth. X-ray diffraction analysis and DTA results do not give any evidence for the nematic structure of secondary crystallites. Now this will be discussed in detail.

If the thermograms of heat treated samples are examined, two transitions C and B' are detected, in addition to T_g . The thermograms are shown in figure 25. Transition B' is the left over secondary crystallinity which was introduced during processing, and unchanged by heat treatment. The transition C is assigned to the melting of crystallites of more perfect nature formed during annealing. The transition C becomes sharper, as the annealing is prolonged at the expense of transition B'. From table 16 it is noted that the magnitude of transition C is increased

with the increase in annealing time whereas the magnitude of transition B' is decreased. The melting temperature of transition C is seen to shift to a higher temperature as the time of annealing is increased. Both these phenomenon can be considered to be due to a greater extent of perfection of crystallites. Similar observations have been reported by Gray⁽⁶⁵⁾ and Illers⁽⁶⁶⁾.

In figure 29, the enthalpy changes observed for transition C in heat treated samples are plotted as a function of annealing time. The values increase steadily with time and then level off; it may, therefore, be concluded that the extent of crystallisation is approaching its maximum value at each temperature.

In table 15 enthalpy changes for transition C and B' are listed for various annealing temperatures. These values of enthalpy changes are plotted as a function of annealing temperature in figure 27. The plot of transition C passes through a maximum whereas that of transition B' passes through a minimum. The magnitude of enthalpy change for transition C is maximum at an annealing temperature of 110°C and for transition B' is minimum at the same temperature. These observations clearly indicate that the annealing effect is maximum at 110°C. Similar observations have been

reported previously by Jujin et al⁽³¹⁾, Gray⁽⁶⁵⁾ and Ohta et al⁽³⁸⁾, although the latter two authors report that the maximum occurs at 130°C.

X-ray measurements have also shown that annealing causes an increase in crystallinity both in M-PVC and S-PVC. In figures 41 and 42 the crystallinity values have been plotted as a function of annealing temperature for M-PVC and S-PVC respectively. Again, a maximum was observed at an annealing temperature of 110°C for both polymers. This is a clear indication that samples annealed at 110°C have the highest degree of crystallinity and perfection. The increase in crystallinity during annealing has been reported by several authors^(47,49,65,66).

On examination of the X-ray diffraction traces in figures 39 and 40, it is noticed that there is no significant difference in the relative intensities of reflections from all the planes, but the peaks themselves increased in annealed samples. This is again a strong evidence to believe that secondary crystallites do not have nematic structure but have a three dimensional structure as that of primary crystallites.

In the X-ray trace for annealed samples at 110°C, figure 39, a reflection has been observed at $2\theta = 28^\circ$.

This type of reflection has not been reported in the literature even for highly syndiotactic material. The Bragg spacing calculated for this reflection is 1.64 \AA . It was not possible to identify this peak from ASTM data tables. The only solid additive used is calcium stearate which has the strongest reflection at $20^\circ 2\theta$. Therefore it is assumed that a complex compound of calcium might have produced by the interaction of calcium stearate and the polymer which gives this reflection at $28^\circ 2\theta$.

Jujin⁽⁶⁴⁾ has found that the magnitude of annealing effect depends on the preheating temperature of the PVC. An unheated virgin powder does not show any effect at all. This is because primary crystallites which have orthorhombic structures prevent chain mobility in their vicinity, hence heat treatment cannot be effective unless the primary crystallites are melted out.

In the present work the annealing effect has been interpreted in terms of secondary crystallinity available, which is developed during processing, and is further perfected on subsequent annealing. It is the intermediate step which has been noted in this work.

Experimental results from X-ray and DTA also show that in the secondary crystallinity introduced during

processing, there are a wide variety of crystallites present. Certain of these crystallites can be perfected by annealing at a particular temperature and therefore various sets of perfected crystallites can be obtained in the same sample annealed at various temperatures (see figure 63). One thing is notable that the maximum number of crystallites can be perfected at about 100-115°C annealing temperature. Once they are perfected they require a higher temperature to melt and therefore melting starts at about 20°C above the annealing temperature.

The maximum annealing effect at 110°C can be considered to be due to the fact that the molecular mobility in PVC at temperatures below 100°C is poor, therefore PVC crystallites cannot be perfected to a greater extent until the temperature is raised. On the other hand, if we increase the temperature too high the crystallite will start degrading, hence maximum crystallisation will take place at an optimum annealing temperature. The optimum annealing temperature for S-PVC and M-PVC used in the present work was found to be 110°C.

Jujin et al⁽³¹⁾ have suggested that low melting temperatures of secondary crystallites, formed during annealing, is due to a nematic structure, whereas the present work suggests that this is not the case.

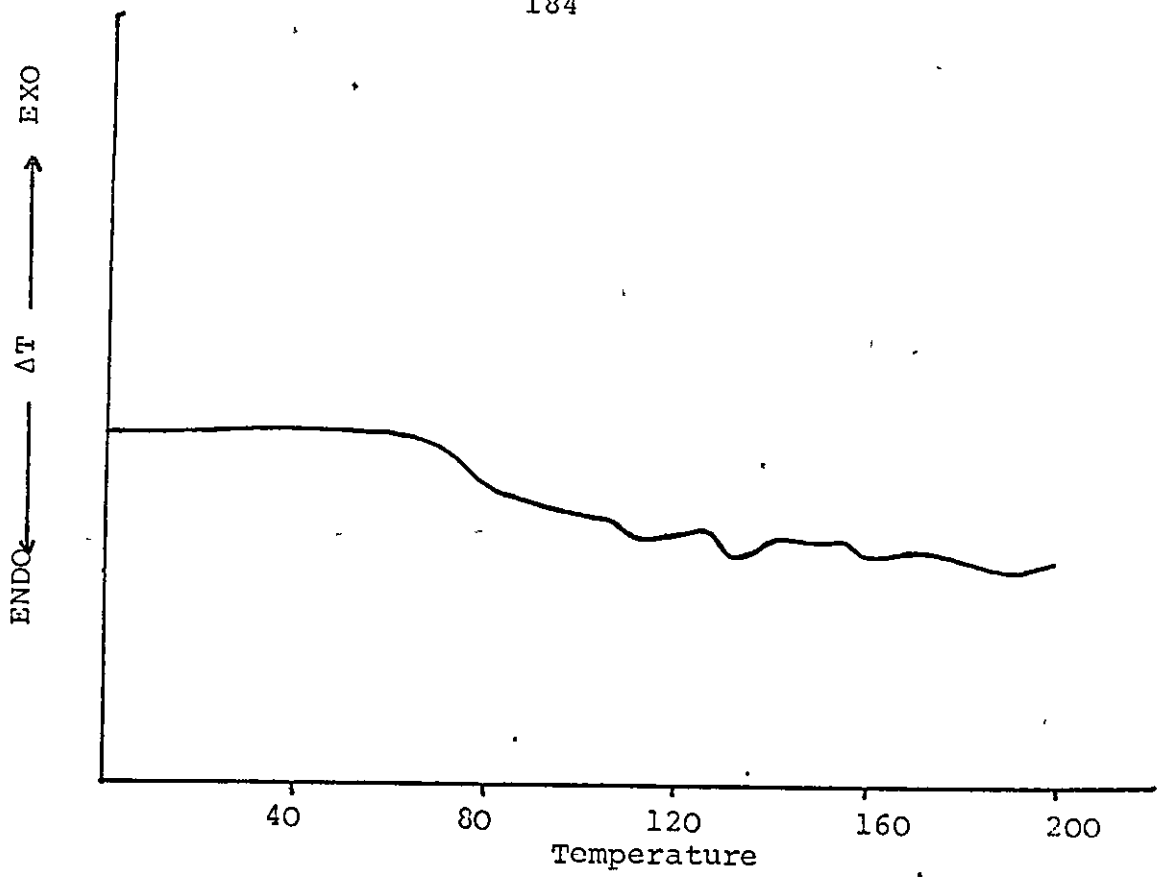


FIGURE 63 M-PVC annealed at 95°C, 110°C and 150°C for 15 minutes

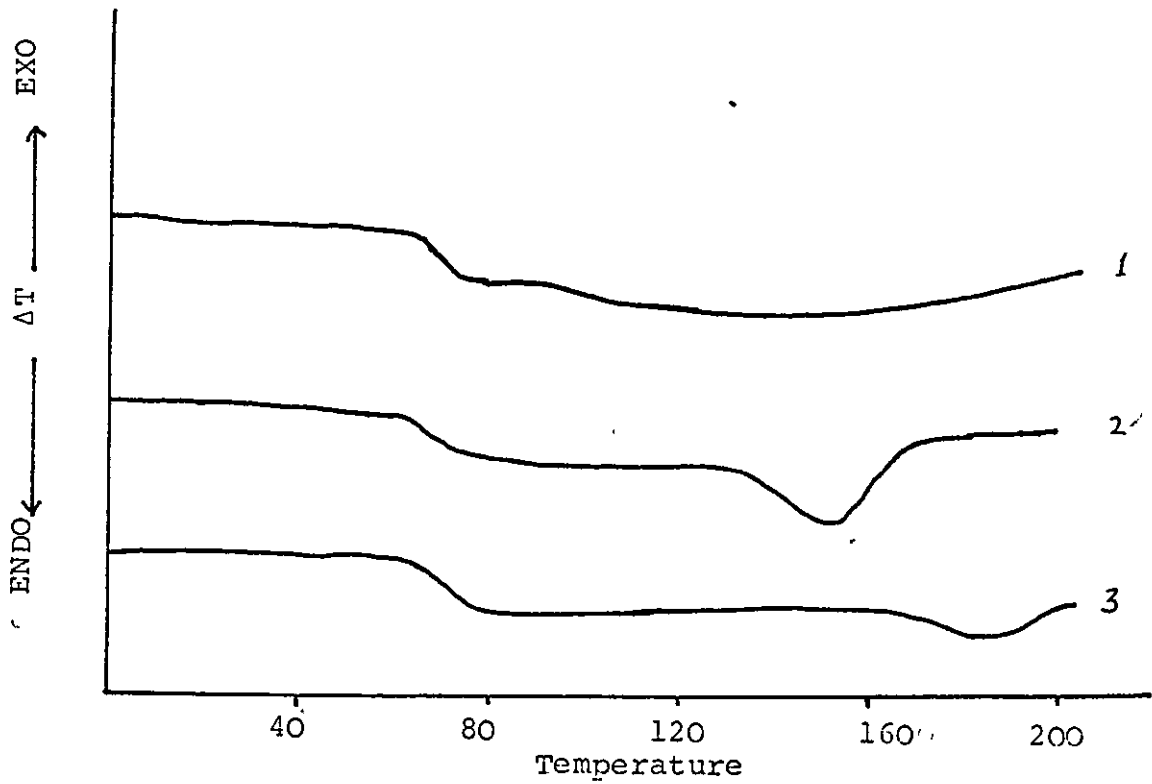


FIGURE 64 Thermograms of M-PVC annealed for 5 hours
(1) unannealed, (2) 110°C (3) 150°C

Crystallites which have melted at this low temperature in the thermogram of annealed samples, would have melted at still lower temperatures if they were not annealed (see figure 64). In this figure it has been shown that in an unannealed sample, melting starts at a lower temperature (110°C) and in the same sample after annealing at 110°C for 5 hours, melting starts at 132°C which is 22°C above its original melting temperature.. In the thermogram 3, annealed at 150°C for 5 hours, melting starts at 170°C which is even higher than the starting melting temperature of primary crystallites. The only explanation is that the crystallites are small in size and hence will melt at relatively lower temperatures, however perfect they may be, compared to the other crystallites which are larger in size.

The peaks obtained from reflections at $16-18^{\circ} 2\theta$ are assigned to the two dimensional order whereas the peaks at $24-26^{\circ} 2\theta$ range to three dimensional order⁽⁴⁷⁾. If the secondary crystallites had a nematic structure then in the X-ray diffraction of annealed samples, the relative intensities of reflections from planes (010), (200), and (110) at $16-18^{\circ} 2\theta$ would have increased and the peaks at $24-26^{\circ} 2\theta$ would have reduced, as has been observed by Gilbert and Vyvoda⁽¹⁰⁵⁾ in the stretched PVC.

Similarly Mammì and Nardi⁽⁵⁸⁾ have reported a nematic structure in a PVC stretched fibre annealed at 85-107°C. The distance between the chains in nematic structure is only slightly larger than that of orthorhombic lattice, 5.4 and 5.3 Å respectively.

Hence it is concluded that under these processing conditions, where minimum shear is used and there is no orientation in the PVC, annealing will simply help in perfecting the crystallites. The crystallites formed during annealing have orthorhombic structure. Similar conclusions were drawn by Baker et al⁽⁴⁷⁾, Gray⁽⁶⁵⁾, Illers⁽⁶⁶⁾ and Witenhafer⁽⁴⁹⁾.

Studies of the quenched sample

The thermogram obtained from a quenched sample is shown in figure 24. This consists of base line shift at approximately 72°C, followed by an exothermic peak and finally a very broad endothermic peak. The base line shift is due to the glass transition temperature. The T_g of quenched sample is about 2°C lower than that for moulded samples. This can be explained in terms of "hole theory" as proposed by Eyring⁽⁶⁰⁾ see section 2.5.

If the material is cooled rapidly through the glass transition region a non-equilibrium hole concentration may be frozen-in. In a second heating cycle at a control rate, the hole concentration approaches equilibrium and results in a lower glass transition.

The exothermic peak following the T_g is considered to be due to crystallisation.

In this work it has been checked by the X-ray diffraction method. The X-ray diffraction trace of the quenched sample shown in figure 34 is a bimodal trace. In fact the reflection at $16^\circ 2\theta$ and $18^\circ 2\theta$ have been merged into one and the reflection at $25^\circ 2\theta$ has reduced tremendously. This shows that quenching has destroyed the existing crystallinity to a considerable extent. When the quenched sample was heated up to the end of exothermic peak (100°C) for only 3 minutes, then X-rayed again, sharp reflections were observed at 16° , 18° and $25^\circ 2\theta$ which is a strong evidence that exothermic peaks in the thermogram of quenched samples is due to crystallisation. This observation is in agreement with work published by Gray and Gilbert⁽³⁵⁾ and Illers⁽⁶⁶⁾ on heat treatment of a commercial suspension PVC.

The final broad endotherm is ascribed to the melting of crystallites, if remaining, from the pre-treatment and those formed during crystallisation. All

three transitions in the DTA trace occur very close together, making calculations of the enthalpy change difficult. However, approximate values of the magnitude of the transitions have been made and are listed in table 12. The exothermic peak corresponds to 5.26 kJ/kg and the endothermic enthalpy value was found to be 8.26 kJ/kg.

The exothermic enthalpy change was equivalent to 63% which shows that more than two-thirds of the melting crystals were transformed by quenching into the amorphous state at first, and became crystals again during heating in the cell. Similar determinations have been reported by Illers and Gray and Gilbert. The value 40% of exothermic peak reported by Gray and Gilbert for a commercial suspension PVC seems to be rather low and this is due to poor quenching.

No structural changes were observed in samples cooled at different rates in the mould during processing. This may be due to the fact that cooling rate implied was not fast enough to bring about any change in the structure. Samples cooled at different rates after being annealed also did not show any significant change in structure.

5.2 Mechanical Properties

Four different types of behaviour have been observed during tensile testing which can be represented by the following figure.

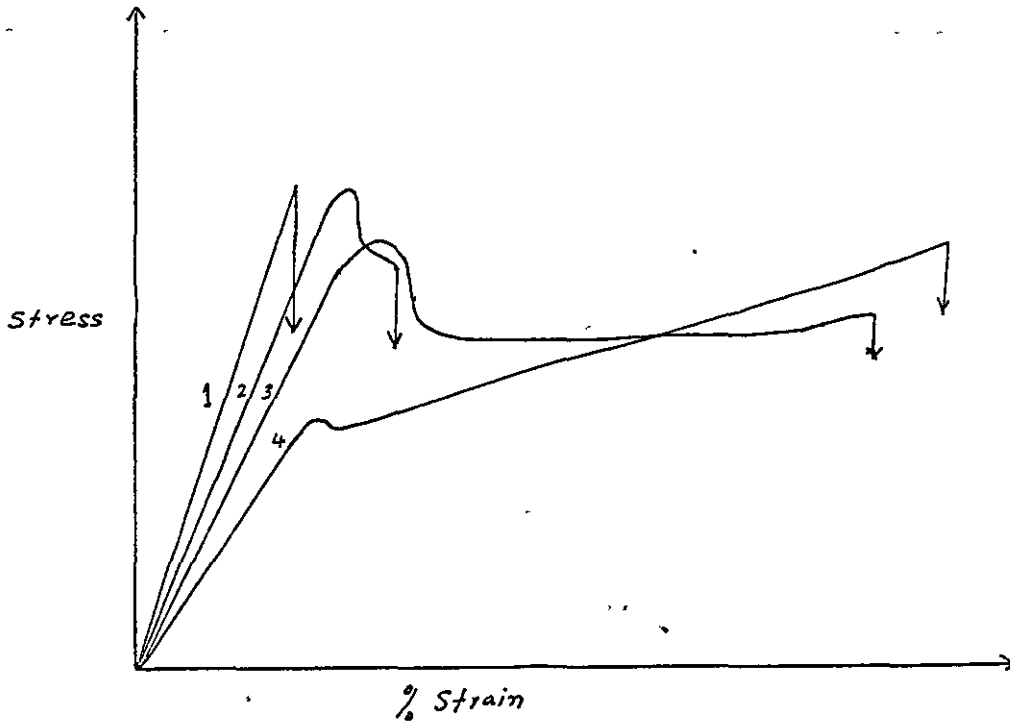


FIGURE 65

In figure 65, curve 1 shows the brittle failure, curve 2 the necking rupture, curve 3 cold drawing and the curve 4 cold drawing without necking.

Different ideas and theories, to explain the yield and cold drawing behaviour of polymers, have been discussed in section 2.5.. In this work Lazurkin-Eyring⁽⁷³⁾ concept will be used to explain the results

obtained from tensile testing.

Stress-strain curves for moulded samples from M-PVC and S-PVC are shown in figures 42-45. In the case of S-PVC the samples moulded up to 180°C underwent brittle fracture with very small elongation. On the other hand similar M-PVC moulded samples have shown ductile failure. This is due to the known morphological differences between two resins as discussed at several places in this work. The S-PVC resin particles are covered with skin around them so require a higher temperature to be processed.

Tensile testing on similar mouldings have been carried out by Katchy⁽⁵⁷⁾. He has also reported the difference in tensile behaviour of the two polymers. The brittle failure of the samples moulded at low temperatures from a commercial PVC have also been reported by Pezzin et al⁽⁸³⁾.

From literature review in section 2.5 it is clear that the complete breakdown of the network in PVC takes place at 200-210°C. In this work the brittle failure of S-PVC has been assigned to the improper melting of resin particles. As the moulding temperature is raised the boundaries of secondary particles are diffused and at about 200°C a homogeneous melt is formed. It is clear that the breakdown of particle structure is

faster in M-PVC than in S-PVC, and the mode of failure from brittle to necking rupture to cold drawing is governed by the degree of the particulate structure retained in the polymer which ultimately depends on the moulding temperature. It means that mouldings from both the polymers of similar tensile behaviour can be made by raising the moulding temperature for S-PVC to an appropriate level.

Young's modulus and yield stress values have been plotted as a function of moulding temperature in figures 46 and 47. Both modulus and yield stress increase with increasing moulding temperature. A sudden rise in the values of modulus and yield stress for S-PVC is due to the proper fusion of particles at high moulding temperatures. These parameters did not increase sharply for M-PVC as the fusion had started at a lower moulding temperature. The crystallinity measurements by X-ray diffraction show the decrease in total crystallinity with increasing moulding temperature. The possible explanation in terms of crystallinity is that the primary crystallinity which is gradually melted out in the moulding cycles does not affect the mechanical properties under these processing conditions. The development of the secondary crystallinity has a direct influence on the tensile parameters of the material.

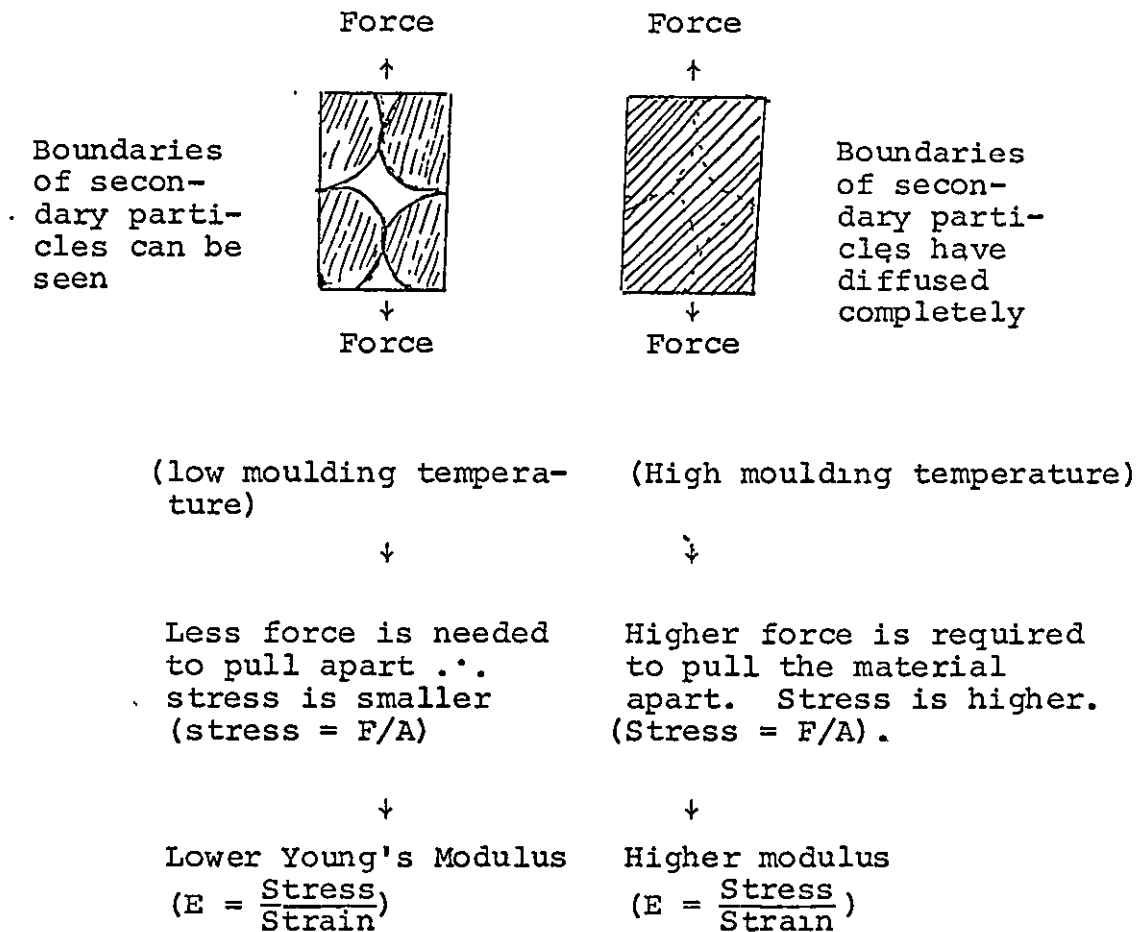
Primary crystallinity is the measure of the order of crystallisable syndiotactic segments in PVC, which is confined in a resin particle. Therefore primary crystallites can only form a crystalline network within a particle. Thus the mouldings in which the major part of primary crystallinity is retained, shows the interparticle failure which clearly indicates that primary crystallinity does not affect mechanical properties under these processing conditions.

On the other hand secondary crystallinity is introduced in PVC when the material is slowly cooled from a high moulding temperature. At high moulding temperatures (200-210°C) the particulate network of PVC breaks down and on subsequent cooling to ambient temperature secondary crystallites are formed. The secondary crystallites, though smaller in size and/or imperfect, form a stronger crystalline network throughout the material which improves the mechanical properties of PVC. Thus the secondary crystallinity in PVC causes intraparticle failure.

At low moulding temperatures the fusion of particles does not take place properly and hence less force is needed to pull the material apart. The breaking stress will be less than the yield stress under these conditions, so that no yield is observed. The stress

will be smaller which results in a lower Young's modulus. Following is the crude representation of the fusion of particles with respect to moulding temperature.

FIGURE 67



As the proper gelation and the development of secondary crystallinity in moulded samples at high temperatures reduces the segmental movement, and high

force is needed to pull the material, this results in high modulus and yield stress values. The percentage elongation of these samples also increases as the orientation hardening takes place in these cases.

Tensile tests were also performed on quenched material. On quenching from a high temperature 210°C an excess free volume is frozen-in which tends to increase the segmental mobility and at the same time voids are also trapped in. Less force will be required to pull the material and due to the presence of voids, the neck cannot be restabilised and hence necking rupture will result. This was found to be the case with quenched material from both M-PVC and S-PVC.

The Charpy impact results show that the impact strength increases with increasing moulding temperature. This is again due to the fact that proper gelling takes place at higher moulding temperatures. The values for M-PVC are higher than S-PVC which is in agreement with expectations and clearly shows the fusion behaviour of the two polymers.

The tensile tests have been performed at elevated temperatures on mouldings prepared at 180° and 200° from M-PVC and S-PVC, and on quenched samples.

The typical stress-strain curves are shown in figures 53 and 54. The mode of deformation in S-PVC changes dramatically from brittle to cold-drawing. The Young's modulus and yield stress decrease with increasing test temperatures in all the tests. A similar observation has been reported by Gonze et al⁽¹⁰⁶⁾ in PVC and they explained their results using Eyring models proposed by Roetling⁽⁷⁷⁾ and Baumen^(78,79).

Yield stress and modulus have been plotted as a function of temperature in figures 53-55. When temperature is increased the thermal motion in the material increases and results into an increase in segmental mobility. Ultimately the force to pull the material is reduced, thus decreasing the modulus. Due to the increase in segmental mobility, yield stress also decreases. Following the yield point stress decreases until it becomes constant and a neck is formed which restabilises as the molecular orientation (orientating hardening) takes place. Because of the high segmental mobility, orientation hardening is easier and the sample cold draws, the shoulder of the neck travel along the sample till it breaks. As the temperature approaching to the glass transition, the yield stress and Young's modulus for all the samples reach to a minimum value and are approximately equal. The sample does not neck because molecular orientation

takes place just at the point of yielding. The elongation of the sample increases with increasing temperature, a value of 300% elongation is observed for M-PVC tested at 70°C.

A rise in the test temperature in fact reduces the effect of the defects in the structure and lowers the yield stress of the sample. According to the principle of stress variation at a given strain, if the experimental conditions are changed (in this case temperature) in such a way that the stress is smaller at a given strain, the probability of the fracture at that strain is decreased. The ductile behaviour of S-PVC with increasing temperature is a straightforward example of this principle.

Similarly results of quenched samples at elevated temperatures can be explained.

On annealing above T_g crystallisation has been shown to occur. The crystalline network will reduce the chain mobility⁽¹⁰⁷⁾. Hence a greater force will be needed to pull the sample, thus high yield stress and drop in elongation at break will be expected. This was found to be the case with both the polymers.

Typical stress-strain curves for M-PVC annealed samples are shown in figure 58. The crystallinity was found to be maximum in the sample annealed at 110°C. The corresponding values of yield stress and elongation

are in good agreement with expectations. The sample has the highest yield stress and the lowest elongation. The value of yield stress has been plotted as a function of annealing temperature in figure 59. The yield stress value passes through a maximum at the annealing temperature of 110°C .

The annealed samples from the quenched state have also shown an increase in yield stress but there was no significant change in elongation at break. With the quenched samples, the situation becomes more complicated by the fact that on quenching from a high temperature, 210°C , an excess free volume will be frozen-in which tends to increase the segmental mobility, on the other hand annealing causes crystallisation which has the inverse effect on the chain mobility. The effect of crystalline network predominates over the free volume on segmental motion and hence high yield stresses are observed in annealed samples. The results reported here are in agreement with those published by Gray and Gilbert⁽³⁵⁾ for commercial and highly syndiotactic PVC samples.

The results for M-PVC moulded at 200°C and cooled at faster rates, did not show any significant difference in the tensile properties. Figure 60 shows the plot of yield stress for both samples, cooled at different rates, as a function of test temperature.

This may be due to the fact that the cooling rate was not fast enough to bring about any change in the structure which would have been reflected in mechanical properties.

5.3 Structure and Properties Relationships

Mechanical properties of both the polymers have large differences at low moulding temperatures (160-180°C). This can be attributed to the known difference in the particle surface morphology. The higher tensile yield stress in the case of M-PVC, suggests that the interface of this polymer is melted more easily and there is better particle adhesion than in S-PVC.

From differential thermal analysis it is noticed that the development of secondary crystallinity in the case of S-PVC starts at a higher moulding temperature, 180°C, whereas it starts at 170°C moulding temperature in the case of M-PVC. The values of enthalpy changes for secondary crystallinity are in correspondence to the tensile properties in that both increase with increased moulding temperature.

X-ray diffraction analysis of these mouldings has shown that the percentage crystallinity decreases with the increasing moulding temperature. As the moulding temperature is raised, the primary crystallinity is melted out but a new order is introduced when the melt is cooled to ambient temperature. This new order is called secondary crystallinity of PVC. The secondary crystallites are very small and have a wide range of perfection. They are not completely detected

by X-ray diffraction and hence a gradual decrease in the percentage crystallinity is observed, although the recorded crystallinity is the sum of both primary and secondary crystallinities. It has been suggested in the preceding section 5.2 that primary crystallinity does not affect the mechanical properties of PVC.

The development of secondary crystallinity seems to have direct effect on the mechanical properties.

Secondary crystallinity formed during processing in fact develops good adhesion among secondary particles and further *growth develops good adhesion among* primary particles. In other words secondary crystallinity can be associated with the fusion behaviour of PVC particles. The better the fusion, the higher the secondary crystallinity.

Higher secondary crystallinity in the PVC sample results in higher yield stress, and elongation at break, and good impact strength. A high yield stress value indicates that the crystalline network has reduced the segmental mobility and therefore higher force would be needed to yield. The higher value of elongation at break indicates the nature of the secondary crystallites. It is suggested that secondary crystallites are very small in size and their network is not strong enough to stop the molecular orientation. Soon after annealing these crystallites are perfected and hence form a stronger network which reduces the

molecular orientation which results in lower elongation at break, and higher values of yield stress are obtained. From X-ray diffraction and differential thermal analysis, it is found that on annealing the crystallinity increases and has the profound effect on mechanical properties. For example, a sample annealed at 110°C for 5 hours has the highest degree of crystallinity measured by the X-ray diffraction method and confirmed by DTA, and also has the highest value of yield stress and minimum value of elongation at break.

CHAPTER 6

CONCLUSIONS

Differential thermal analysis demonstrated the variation in structure produced by different mould temperatures. Primary crystallinity is gradually melted out with the increasing moulding temperature and secondary crystallinity is introduced on subsequent cooling the melt. The magnitude of secondary crystallinity increases whereas that of primary crystallinity decreases with the increasing moulding temperature. The traces of primary crystallinity can be seen even at the highest mould temperature, therefore the percentage crystallinity, though it decreases with increasing moulding temperature, is the sum of primary and secondary crystallinities.

Primary crystallinity has no effect on mechanical properties, but the development of secondary crystallinity has the direct influence.

The absence of secondary crystallinity causes brittle failure, whereas the complexity of ductile behaviour depends on the amount of secondary crystallinity present in the sample. The higher the secondary crystallinity, the better the mechanical properties.

At low moulding temperatures, 160-180°C, the two polymers show a great difference in mechanical properties. This is due to the difference in the surface morphology of the two polymers. The breakdown of particles is faster in M-PVC than in S-PVC. At high moulding temperature this difference is not significant and hence mouldings of similar tensile properties for both M-PVC and S-PVC can be made by increasing moulding temperature to an appropriate level for S-PVC.

A rise in temperature in tensile testing, reduces the effect of the defects in structure and hence the performance of the PVC article is bettered.

Secondary crystallinity, formed during processing, is the intermediate step for further perfection and/or increases the crystal dimension on annealing above T_g . The greater the secondary crystallinity available, the greater is the annealing effect. The effect appears to be greater for M-PVC than S-PVC.

Secondary crystallites formed during annealing have orthorhombic structure.

The exotherm in the thermogram of a quenched sample is due to crystallisation, this was checked by X-ray diffraction.

Mechanical properties correlate with the structural changes during the processing. Results obtained

from heat treated samples confirm these observations.

An attempt to see the effect of cooling rate on the structure and properties was unsuccessful. This may be because the cooling was not fast enough to bring about any structural changes.

REFERENCES

1. W PENN, PVC Technology, Applied Science Publishers, London, 1971.
2. G MATTHEWS, Vinyl and Allied Polymers, Vol. 2, Iliffe, London, 1972.
3. L I NASS, Encyclopaedia of PVC, Vol. I, 1976.
4. L I NASS, Encyclopaedia of PVC, Vol. 2, 1976.
5. D M GEZOVICH and P H GEIL, Intern. J. Polymeric Mater., Vol. 1, 1971.
6. T HATTORI, K TANAKA, M MATSUO, Polym. Eng. Sc. Vol. 12, 1972.
7. Y SHINAGAWA, Plast. Ind., News., 65, 1973.
8. C SINGLETON, J INSER, D M GEZOVICH, P K C TSOU, P H GEIL, and E A COLLINS, Pol. Eng. Sc., 14, 1974.
9. P G FAULKNER, J Makromol. Sc., Phys., B 11(2), 1975.
10. P H GEIL, J. Makromol. Sc., Chem. A11(7), 1977.
11. J LYNDAE-JORGENSEN, Polm. Eng. Sc., Vol. 14, 1974.
12. J RUDOLF and L SIEGLAFF, Polym. Eng. Sci., Vol. 18, 1978.
13. E L ZICHY, Pure and Appl. Chem., 49, 5, 1977.

14. H BEHRENS, G GRIEBEL, L MEINEL, H. REICHENBACH,
G SCHULZE, W SCHENK and K WALTER, *Plaste
Kautsch.*, 22, 414, 1975.
15. W WENIG et al, *J. Polym. Sci., Phy.*, 16, 1978.
16. G PEZZIN, *Plast. and Polym.*, 37, 294, 1967.
17. F A BOVEY, *Polym. Confor. and Config*, Academic
Press, New York, 1969.
18. J W L FORDHAM, *J. Polym. Sc.*, 39, 321, 1959.
19. H GERMER, K H HELLWEGE and U JOHNSEN, *Makromol.
Chem.*, 60, 106, 1963.
20. F A BOVEY, E P HOOD, E W ANDERSON, R L KORNEGAY,
J Phys., Chem., 71, 312, 1967.
21. G TALAMANI, G VIDOTTO, *Makromol. Chem.*, 100, 48,
1967.
22. G NATTA and P CORRADINI, *J. Polym. Sc.*, 20, 251,
1956.
23. R W SMITH and C E WILKES, *Polym. Letters*, 5, 1967.
24. A NAKAJIMA and HAYASHI, *Koll. Zeit. Polym.* 229,
12, 1969.
25. C E WILKES, V L FOLT, S KRIM, *Makromol*, 6, 235,
1973.
26. H G KILIAN and W WEING, *J. Makromol. Sc., Phys.*,
B9(3), 463, 1974.
27. R BRAMER, *Collid Polym. Sc.*, 252, 504, 1974.

28. G F NEILSON and S A JABRIM, J. Appl. Phys., 46,
1175, 1975.
29. D N BORT, V I ZEGELMAN and V A KARGIN, Polym. Sc.,
USSR- 10, 1498, 1968.
30. A KELLER, P J LEMSTRA and M CUDBY, J. Polym. Sc.,
Phys., 16, 1978.
31. J A JUJIN, J H GISOLF and W A de JONG, Koll. Zeit.
Zeit. Polym., 251, 456, 1973.
32. P J FLORY, Trans. Faraday Soc. 51, 848, 1955.
33. K H HELLWEGE, U JOHNSEN and D KOCKOTT, Kollid,
Zeit. Zeit. Polym. 194, 5, 1964.
34. K U PHOL and D O HUMMEL, Makromol. Chem. 113,
1968.
35. A GRAY and M GILBERT, Polymer 17, 1976.
36. A NAKAJIMA, H HAMAFUJI, and S HAYASHI, Makromol,
Chem., 95, 40, 1966.
37. G REHAGE and H HALBOTH, Makromol. Chem. 119, 235,
1968.
38. S OHTA, T KAJIYAMA and M TAKANAYAGI, Polym. Eng.
Sci. 16, 465, 1976.
39. E V GOUINLOCK, J. Polym. Sci. Phys. 13, 961, 1975.
40. R S STRAFF and D R UHLMANN, J. Polym. Sci. Phys.
14, 353, 1976.
41. G GERBUGLIO, A RODELLA, G C BORSIMI and E GALLINELLA,
Chim. ind. (Milan), 46, 166, 1964.

42. J A MANSON, S A IOBST, R ACOSTA, J. Polym. Sci. A(10), 179, 1972.
43. V P LEBEDEV, D Y TSVANKIN, Y V GLAZKOWSKII, Polym. Sci. USSR 14, 1123, 1972.
44. R J D'AMOTO, S STRELLA, Appl. Polym. Symp. 8, 275, 1969.
45. D M WHITE, J Amer. Chem. Soc. 82, 5678, 1960.
46. R A HORSLEY, Plastics Progress 135, 1957.
47. C BAKER, W F MADDAMS and J E PREEDY, J. Polym. Sci. Phys. 15, 1977.
48. V P LEBEDEV, L Y DERLYUKOVA, I N RAZINSKAYA, N A OKLADNOV, B P SHTARKMAN, Polym. Sci. USSR 7, 366, 1965.
49. D E WITENHAFFER, J Makromol. Sc. B4, 915, 1970.
50. H BEHRENS, Z WISS, Karl Marx Univ. Leipzig, Math. Naturw. Reihe, 15, 1966.
51. P J FLORY, J. Chem. Phys. 17, 223, 1949.
52. C E ANAGNOSTOPOULOS, A Y CORAN, H R GAMRATH, J. Appl. Polym. Sci. 4, 181, 1960.
53. F P REDING, E R WALTER, F J WELCH, J. Polym. Sci. 56, 225, 1962.
54. D KOCKOTT, Kolloid Zeit. 198, 1964.
55. H MUNSTEDT, Angewandte Makromol Chemi. 47, 229, 1975.

56. G PEZZIN, Pure and Applied Chem., 26, 241, 1971.
57. E M KATCHY, Doctoral Thesis, Loughborough University of Technology, 1979.
58. M MAMMI and V NARDI, Nature, 247, 1963.
59. V NARDI, Nature, 563, 1971.
60. H EYRING, J. Chem. Physic. 4, 283, 1936.
61. N HIRARI, H EYRING, J. Polym. Sc. 37, 51, 1959.
62. B WUNDERLICH, J. Phys. Chem. 64, 1052, 1960.
63. T G STAFFORD, RAPRA, Tech. Review 66, Part 2, 1972.
64. J A JUJIN, Doctoral Thesis.
65. A GRAY, Doctoral Thesis, Loughborough University of Technology, 1975.
66. K H ILLERS, Makromol. Chem. 127, 1969.
67. M E CARREGA, Pure and Applied Chem. 49. 569, 1977.
68. J M G COWIE, Inter. Text. Book Co. Ltd., Bucks, 1973.
69. K JACKEL, Koll. Zeit. Zeit. Polym. 137, 130, 1954.
70. I MARSHALL, A B THOMPSON, Proc. Roy. Soc. A221, 541, 1954.
71. F H MULLER, Koll. Zeit. Zeit. Polym. 126, 65, 1952.
72. P I VINCENT, Polymer I, 7, 1960.

73. J S LAZURKIN, J. Polym. Sci. 30, 595, 1958.
74. R E Robertson, J. Appl. Polym. Sci. 7, 443,
1963.
75. S S STERNSTEIN, L ONGCHIN, A SILVERMAN, Appl.
Polym. Symp. 7, 175, 1968.
76. W WHITNEY, R D ANDREWS, J. Polym. Sci. C16, 2981,
1967.
77. J A ROETLING, Appl. Polym. Symp. 5, 161-169
Interscience (N.Y) 1967.
78. J C BAUWENS, J. Polym. Sci., A-2, 5, 1145, 1967.
79. J C BAUWENS et al, J. Polym. Sci. A-2, 7, 735, 1969.
80. J MALAC, J. Appl. Polym. Sci. 13, 1767, 1969.
81. R PHILLIPS, R L COX, C A HEIBERGER, S.P.E. ANTEC,
14, 216, 1968.
82. W RETTING, Ange Makromol. Chem. 8, 87, 1969.
83. G PEZZIN et al, J. Appl. Polym. Sci. 16, 1839, 1972.
84. G BIER, Kunststoffe 55, 694, 1965.
85. M H LITT, A V TOBOLSKY, J. Makromol. Sci. Phys.
B1, 433, 1967.
86. W TRAUTVETTEV, Makromol Chem. 101, 214, 1967.
87. W AIKEN, et al, J. Polym. Sci. 2, 178, 1947.
88. R B TAYLOR, A V TOBOLSKY, J. Appl. Polym. Sci.,
8, 1563, 1964.

89. N HATTA, A V TOBOLSKY, J. Appl. Polym. Sci., 12, 2597, 1968.
90. A CRUGNOLA, M PEGARARO, F DANUSSA, J Polym. Sci., A-2, 6, 1705, 1968.
91. R SABIA, F R EIRICH, J. Polym. Sci., A-1, 2497, 1963.
92. R SABIA, F R EIRICH, J. Polym. Sci., A-1, 2511, 1963.
93. B H MADDOCK, H NALEPA, B ZURKOFF, 6th Annual Signal Corporation Wire and Cable Symp. 1957.
94. C E BERNHARDT, Tech. Paper S.P.E., 12, 2, 279, 1956.
95. J A BRYDSON, Plastics Materials, P.188, Iliffe, London, 1966.
96. J GOODING, E M KATCHY, To be published.
97. Technical Data Sheet, B P Chemicals Ltd.
98. Technical Data Sheet, C T D 125, (Vinyl Group), I.C.I. Plastics Division.
99. ASTM D-638, Standard method of test for tensile properties of plastics.
100. L S RAYNER P. A SMALL, Brit. Patent 847,676.
101. M A NATOV, T S GANECHIEVA, Vys. Soyed. A-12, (2), 273, 1970.

102. M A NATOV, T S GANCHEVA, *ibid.* A14(11), 2354,
1972.
103. P V McKINNEY, *J Appl. Polym. Sci.*, 11, 193, 1967.
104. V P LEBEDEV, N A OKLADNOV, M N SHLYKOVA, *Sov.*
Plast. 10, April 1968.
105. M GILBERT, J C VYVODA, *Polymer*. Vol. 19, 862,
July 1978.
106. A GONZE, J C CHAUFFOUVEAUX, *Report of the IUPAC*
Working Party, Butterworths, London 1972.
107. L E NEILSON, *Mechanical Properties of Polymers*,
Reinhold Publishing Corporation (N.Y), 1962.

